DISSERATION

ENVIRONMENTAL IMPACTS OF OIL AND GAS ACTIVITIES IN NORTHERN COLORADO

Submitted by

Huishu Li

Department of Civil and Environmental Engineering

In partial fulfillment of the requirements

For the Degree of Doctor of Philosophy

Colorado State University

Fort Collins, Colorado

Fall 2018

Doctoral Committee:

Advisor: Kenneth H. Carlson

Sybil Sharvelle
Pinar Omur-Ozbek
Jiangguo (James) Liu

ABSTRACT

The surge of shale oil and gas exploration and production in the United States is driven by the application of horizontal drilling and hydraulic fracturing which require and generate massive amount of water during the production of crude oil and natural gas. Since 2010, shale oil and gas production from northern Colorado (Wattenberg field) has increased rapidly due to the rich deposit of oil and natural gas in the shale formation, which also raises a lot of concerns over its potential environmental impacts on groundwater and air. To understand the contaminant transport mechanisms, identify the sources of contamination caused by oil and gas operations, and detect the contamination associated with drilling and fracturing activities will help improve the environmental and economic sustainability of shale-gas extraction.

Therefore, our research focuses on the following topics: 1, determine the contaminants due to horizontal drilling and hydraulic fracturing; 2, study on the subsurface transport and distribution of contaminants related to oil and gas activities in groundwater; 3, design and evaluate a regional groundwater monitoring network to detect the contamination events.

ACKNOWLEDGEMENTS

I would like to thank my advisor, Dr. Kenneth H. Carlson for guiding and supporting me with his patience, motivation, enthusiasm and immense knowledge during the past 7 years. None of my works could have been done without his generosity and trust that gave me enough freedom and time to do the scientific researches. Also being a mentor, he gave me tremendous insightful thoughts, suggestions and help both in academic field and in life.

I am also grateful to the members of my committee, Dr. Sybil Sharvelle, Dr. Pinar Omur-Ozbek and Dr. Jiangguo Liu, for their patience and support in overcoming numerous obstacles I have been facing through my research

I would like to thank my fellow doctoral students for their feedback, cooperation and of course friendship. In addition I would like to express my gratitude to Laurie Alburn, Linda Hinshaw, and Susheela Mallipudi as well as the stuffs in the International Programs, helping me with the school registrations.

Last but not lease, I would like to thank my family, my husband, my mother and my daughter as well as my friends from whom I gained so much supports throughout my Ph. D research and my life in general

TABLE OF CONTENTS

LIST OF TABLES

LIST OF FIGURES

Chapter 1 Introduction

Driven by the development of new drilling technologies (horizontal drilling) and hydraulic fracturing, oil and gas production from unconventional sources (tight sands, shale) has expanded in the United States while the environmental impacts of horizontal drilling and hydraulic fracturing still remains a controversial topic. To complete an unconventional oil/gas well, large amounts of water is transported and injected into the subsurface to create artificial fractures allowing oil and gas to flow to the surface in the low permeable and porous formations. Together with oil and gas, water is the major by-product in oil and gas production, known as flowback and produced water, which is normally several times higher than oil production. Flowback and produced water contains organic matter, dissolved solids, metal or other chemicals that are not commonly present in the shallow groundwater. It is a big task to handle this huge amount of the "blackish" water. Additionally, produced water or methane or other organic by-products (VOCs and BTEX) would leak from the well to the environment and contaminate water or atmosphere due to the loss of well integrity. Therefore, to identify the sources of contamination caused by oil and gas operations, and understand the contaminant transport mechanisms will help improve the environmental and economic sustainability of shale-gas extraction.

Reusing produced water can reduce the demand for fresh water and change the waste water into usable water resources. Appropriate treatment is a key factor to determine whether produced water recycling is economical or not, which will depend on the produced water quality and quantity. Therefore, it is important to know the produced water quality in order to choose the "best" treatment processes for recycling. Since the chemical constituents of produced water, such as organic matter and total dissolved solids (TDS) vary with different formations and geological locations, it is impossible to implement the same treatment design at different locations. Therefore, treatment technologies would need to be customized for each area according to the water quality and quantity.

A thorough overview of shale oil and gas (especially shale gas) development, applications of horizontal drilling and hydraulic fracture on the shale gas industry, and the potential environmental impacts

of shale oil and gas production will be presented in Chapter 2. In detail, followed by the overview of the growth of shale oil and gas, the introductions and comparisons of production and produced water quality of different major shale plays will be summarized. Environmental issues associated with shale oil/gas production, such as water stress, produced water contamination and wastewater management, methane pollution, groundwater protection and Colorado Water Watch – a regional groundwater monitoring network will be discussed in Chapter 3. Research question and hypothesis will be discussed in Chapter 4. Chapter 5 to chapter 8 will show the results of five specific studies and papers. The conclusions and the future work will be presented in Chapter 9.

Chapter 2 Literature Review

2.1 Unconventional Oil and Gas – Shale Oil and Gas

Although increasing, the use of renewable energy, hydroelectric power and nuclear energy is projected to account for half of the total energy increasing in the future 20 years but oil, natural gas and coal will still be the dominate energy sources (Figure 1)[1]. Increasing demand of oil and gas will drive and keep the growth of production of crude oil and natural gas.

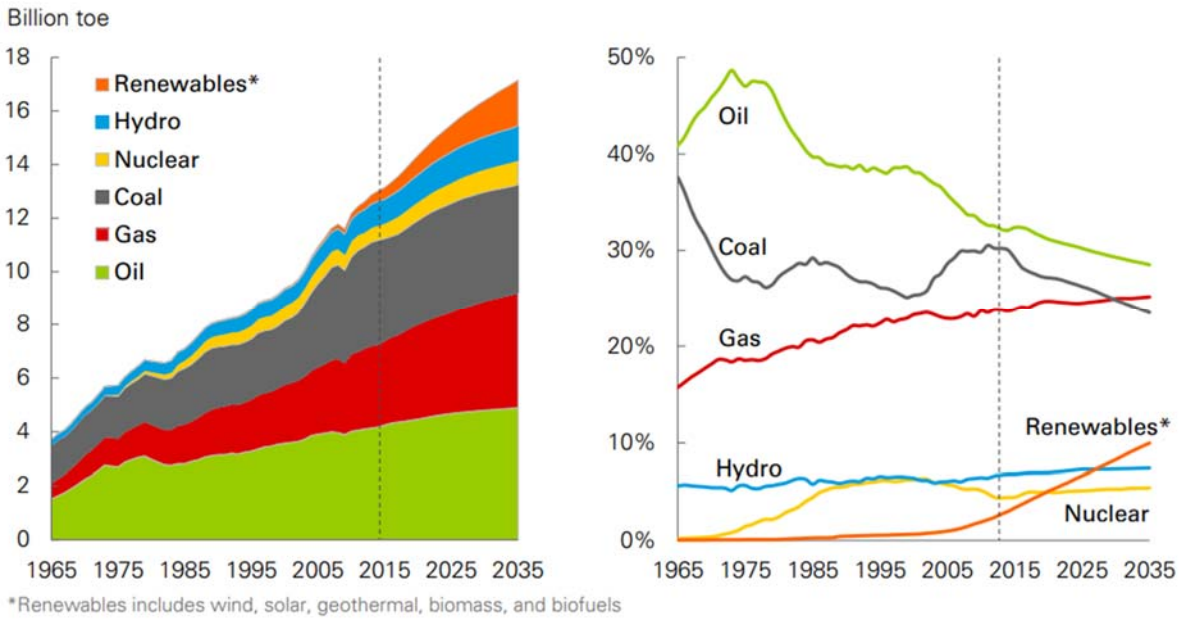

Figure 1. Energy consumption by fuel and shares of primary energy (BP)

2.1.1 Shale Oil and Gas Development

Exploration and development of new resources of oil and gas has become a hot topic in recent year. Also, horizontal drilling and multi-stage fracturing technologies have made the production of oil and gas from unconventional resources possible, with very low permeability and low porosity.[2]

Additions to natural gas production associated with shale gas activity have been instrumental in boosting overall wet gas proved reserves. Shale gas accounted for more than 90 percent of total net additions. Key shale states in 2009 include Arkansas (the Fayetteville Shale), Louisiana (the Haynesville), Oklahoma

(the Woodford), Pennsylvania (the Marcellus), and Texas (the Barnett and Haynesville/Bossier).[3] The 11 percent increase in U.S. proved natural gas reserves took place during a low-price environment that resulted in negative revisions to existing reserves. This underscores the major improvements in shale gas exploration and production technologies (horizontal drilling coupled with hydraulic fracturing) and efficiency[4].

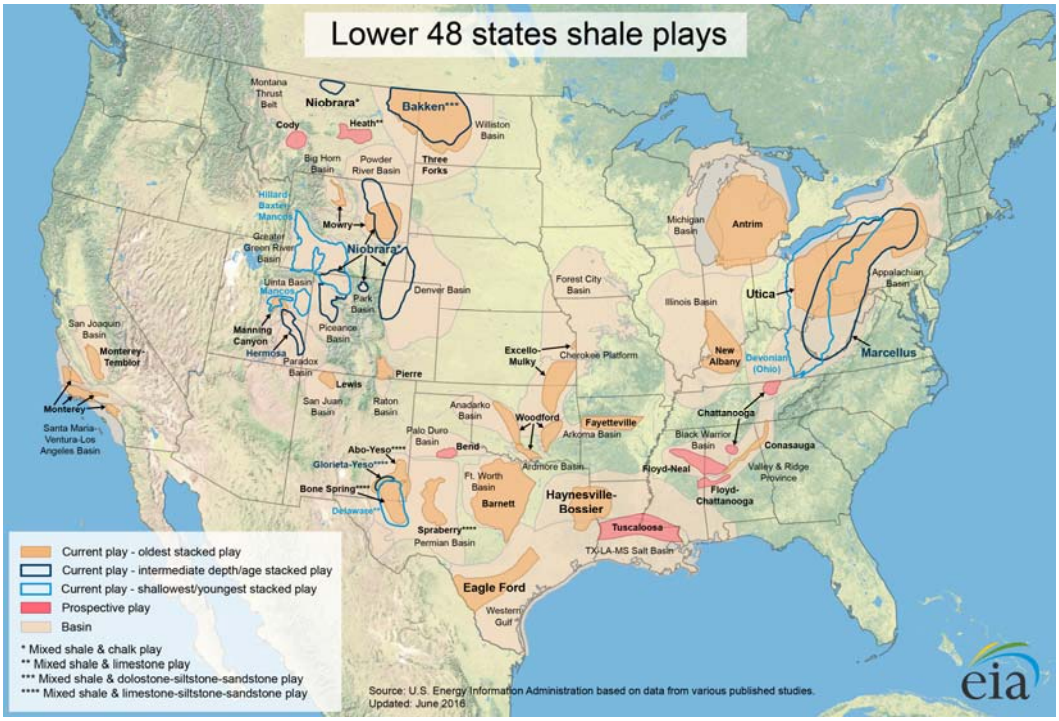

Figure 2. Major shale plays and shale basins in the U.S

North America has a large amount of shale gas, totaling about 5,146 Tcf (146 trillion cubic meters).[5] In the five major shale gas basins (Figure 2), Barnett basin, Fayetteville basin, Woodford basin, Haynesville basin and Marcellus basin, up to 3,760 trillion cubic feet of shale gas is stored underground and over 12% of the total shale gas is a recoverable resource.

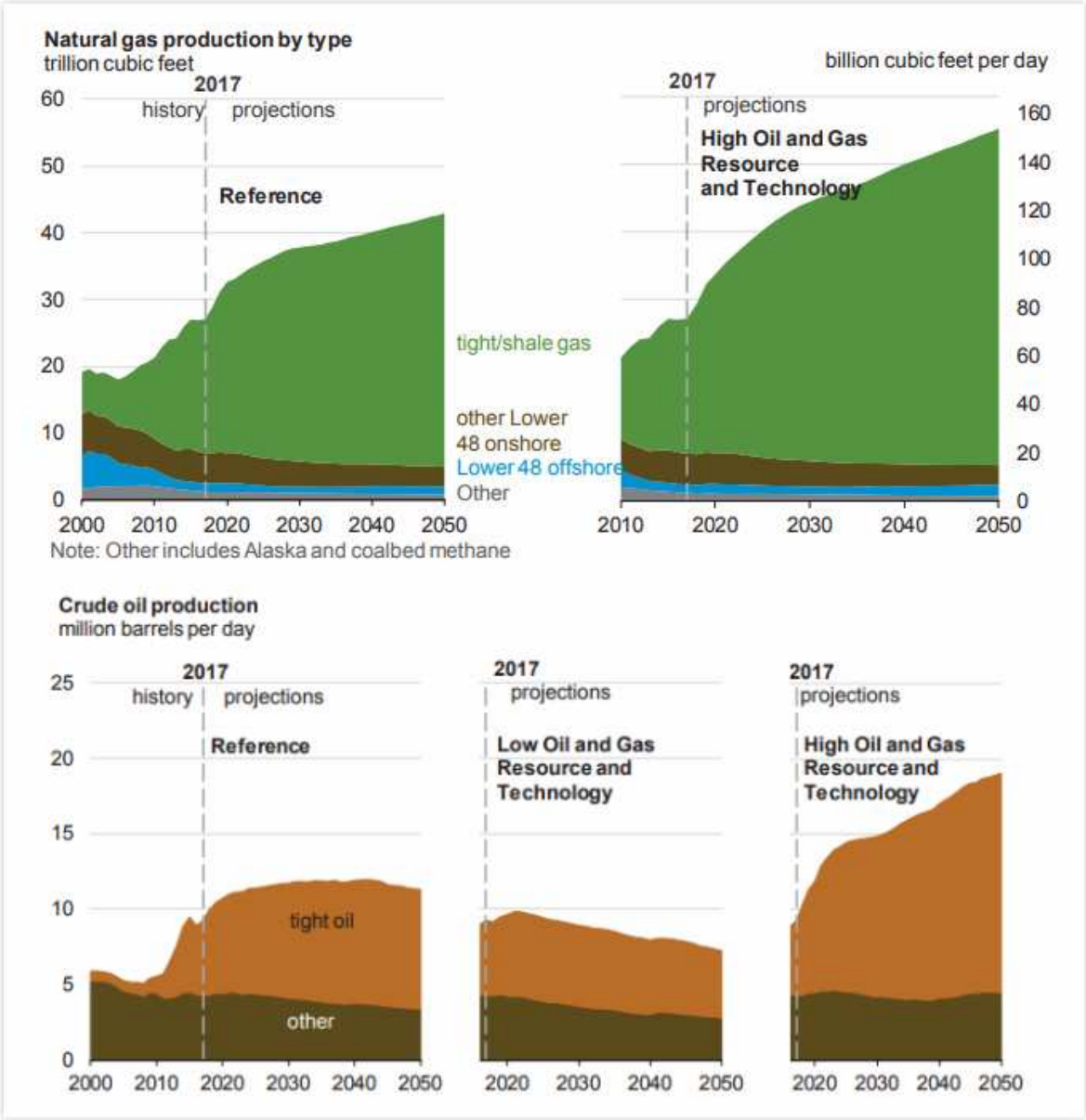

Figure 3. Crude oil production (above) and Natural gas production (below) from conventional and unconventional sources

Current and projection unconventional crude oil (tight oil) and natural gas (tight or shale gas) production are shown in Figure 3. Unconventional tight oil and shale gas will remain the leading sources of petroleum and natural gas production to 2050, projected by E.I.A[6]. Tight oil production will account for about 65% of the total crude oil production over the estimated period from 2017 to 2050. And despite the decline production from coal-bed methane and conventional natural gas production, E.I.A. projected that shale gas

production will keep growing from 2017 to 2050 and shale plays will extend to about 1,300,000 km^2 (500,000 square miles).

Commercially productive gas shale reservoirs in the United States are found at altitudes between 500 and 11,000 feet, with poor porosity and permeability. Owing to the applications of new technology and field practices, shale gas production has experienced a great expansion. Though it has long been known that natural gas was embedded in shale rocks, it was only in 2002 and 2003 that the combination of two technologies working together – hydraulic fracturing and horizontal drilling –made recovering shale gas economically feasible and desirable.[7]

2.1.2 Horizontal Drilling and Hydraulic Fracturing

Traditional drilling technology to explore oil and natural gas in the "trap" (conventional reservoir) is to drill the well vertically and stimulate the oil and gas flow from the high permeable and high porosity reservoir rocks. However, since more and more unconventional recovery reserves has been established and these unconventional oil and natural gas are usually trapped in the very low permeable and low hydraulic conducted formations, vertical drilling is not effective to extract the oil and gas from the tight formations, and therefore the application of horizontal drilling makes the oil and gas production more effectively due to more exposes and contacts with reservoir rocks, which is 2.5 to 7 times the rate and reserves of vertical drill.

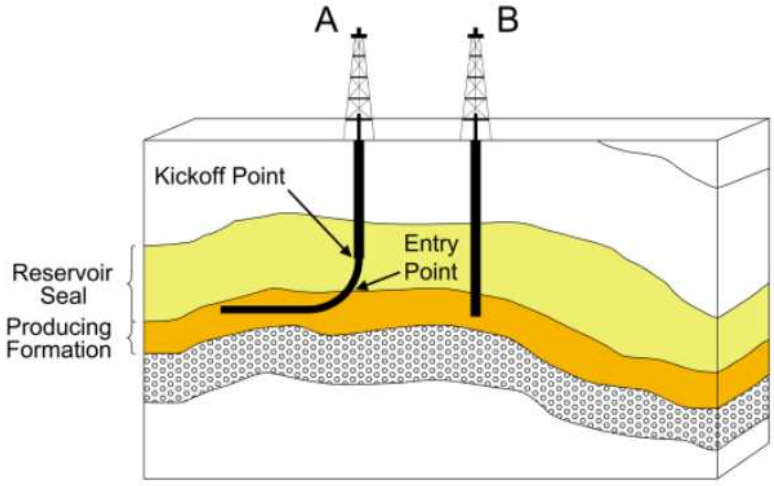

Figure 4. Horizontal and vertical drilling

Comparison of vertical drilling and horizontal drilling is shown in Figure 4. First steps for the horizontal drilling would be the same as the conventional vertical drilling and casing. The "kickoff point" is the point that vertical drilling will rotate with the normal radius of 90-150 m (300-500 ft) and then curve to horizontal drilling at the "entry point", which extends few hundred meters.

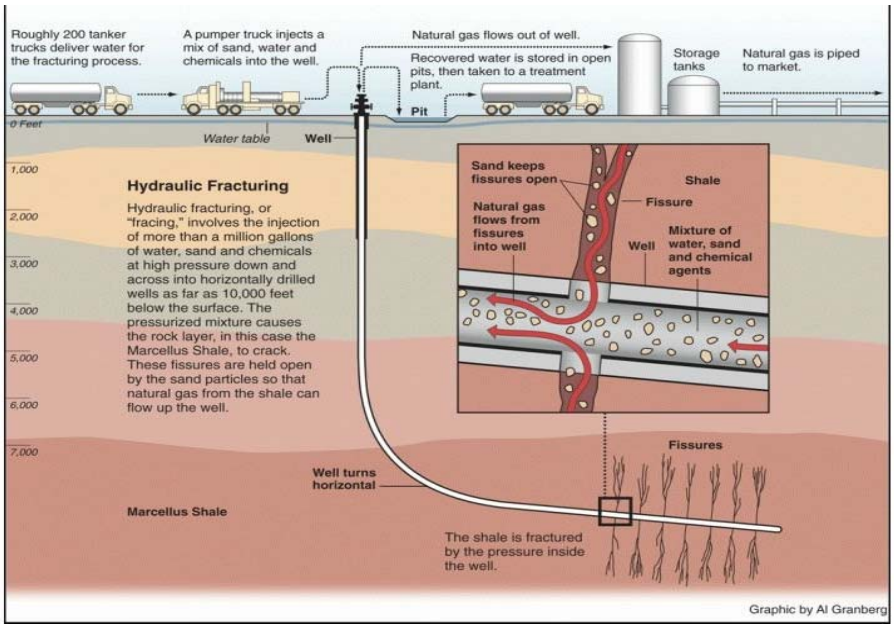

Figure 5. Hydraulic fracturing (http://www.circleofblue.org/2010/water-climate/climate-change/hydraulic-fracturing-infographic/)

Hydraulic fracturing (figure 5) has proven to be the technology key to facilitating economic recovery of natural gas from shale. Hydraulic fracturing is a formation stimulation practice used to create additional permeability in a producing formation to allow natural gas to flow more easily toward the wellbore for purposes of production. Hydraulic fracturing can be used to overcome natural barriers to the flow of fluids. Barriers may include naturally low permeability common in shale formations or reduced permeability resulting from near wellbore damage caused by drilling activities. While methods of hydraulic fracturing continually change (mostly changes in the design process and updates to additives and propping agents), this technology is utilized by the natural gas industry to increase production and to support an ever-increasing demand for energy.[8]

One of the challenges of the hydraulic fracturing process is the fact that it relies on the use of chemical additives to ensure that the fracturing functions well. Water consumed by hydraulic fracturing contains

more than 99% water and sand, with extremely low probability of fracture fluid migration from the shale up to fresh water zones.[9] Although the percentage of chemical additives in typical hydraulic fracture fluid is usually less than 0.5 percent by volume, the quantity of fluid used in these hydro-fractures is so large that the additives in a three million gallons hydro-fracture operation will be considerable.

Recent years, more and more industry companies are switching to use slick water fracturing rather than gel fracturing.[10]There are a few advantages using this aqueous-base fracturing technique, 1) there is some evidence showing that more oil and natural gas has been produced by using slick-water fracturing; 2) slick-water fracturing costs less than the gel- fracturing; 3) slick-water fracking rely less on the addictive chemicals and has high tolerance of water quality[11]. Slick water fracturing is the water-based hydraulic fracturing fluid without crosslink polymers using low viscosity fluid and pumped at high pressure to generate a complex fractures network underground. While, one big challenge applying slick-water fluid for hydraulic fracturing is that it will use much more water than gel fracturing, typically exceeding 4-8 million gallons of water which is 3-4 times of the water used in the traditional unconventional oil and gas hydraulic fracturing.[12]

2.2 Shale Oil and gas production of Wattenberg field

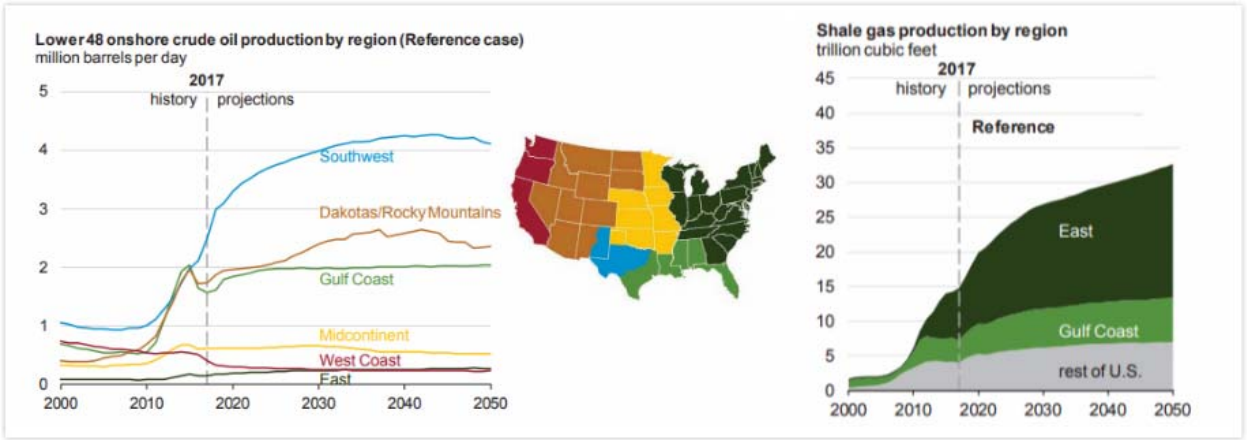

Figure 6. Historical and predicted natural gas production by region[13]

Figure 6 are the E.I.A. summarized historical and projection crude oil and natural gas production by region in the U.S. For the crude oil production, Southwest is the major contributor and Dakotas/Rocky

mountain area is the second largest oil producer. The rapid growth of crude oil production of Dakotas/Rocky mountain region is driven by increasing shale oil production from the Bakken and Niobrara shale. The large increase of gas production in the East is mainly due to the extensive oil and gas exploration from Marcellus shale and Utica play. By the year 2050, the East and Southwest regions will account for more than 60% of total U.S. natural gas production.[13]

The DJ Basin encompasses approximately 180,000 km^2 in eastern Colorado, southeastern Wyoming, and southwestern Nebraska.[14] The cross-section of the basin is that of an asymmetrical bowl that resulted from the uplift of the Rocky Mountains to the west, with the deepest sedimentary rock formation in the western flank across the axis of the basin. Currently, the Wattenberg Field is the most active oil and gas area in the DJ Basin and top 10 largest oil and gas field in the U.S., with estimated oil production of 47,259 Mbbl (thousands bbl) and gas production of 304,540 MMcf (million cubic feet) in 2013.[15]

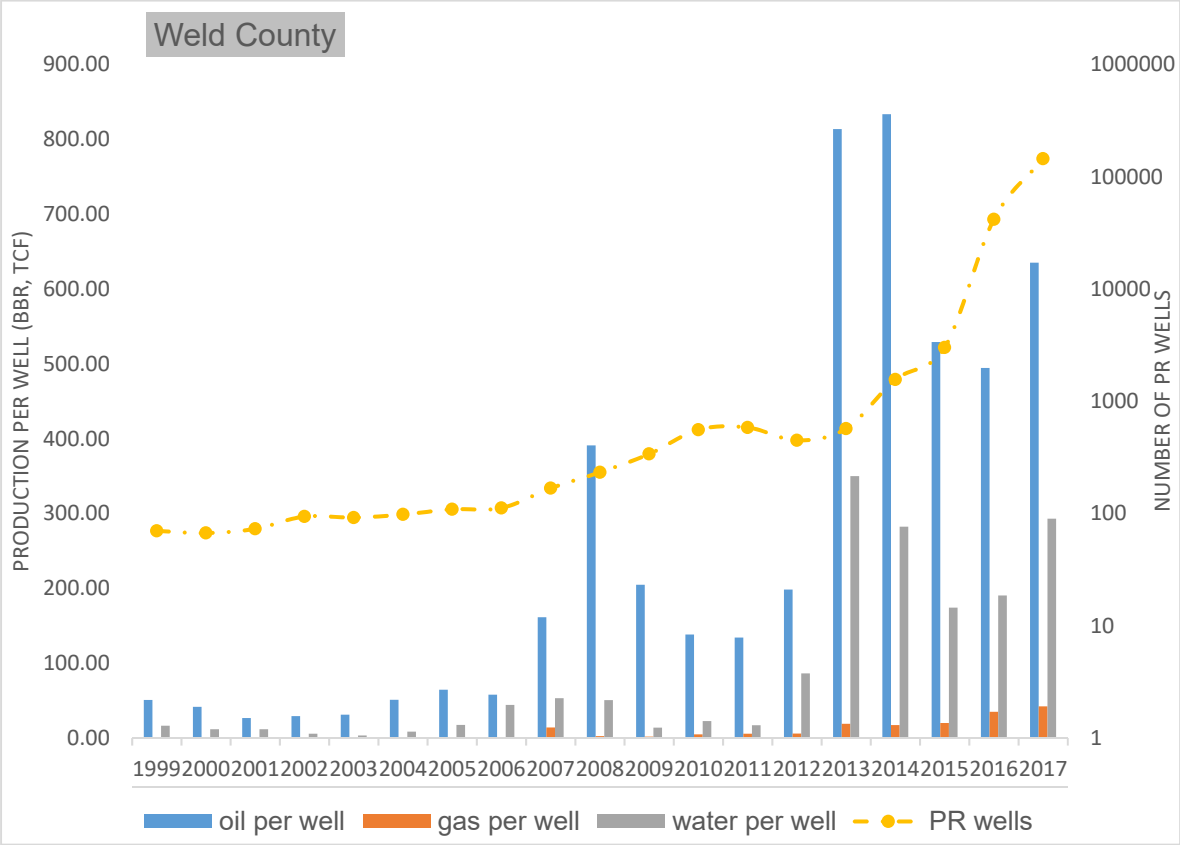

Figure 7. Oil, gas and water production per PR well and numbers of PR wells of Weld County (Wattenberg field)

Weld County is the most active oil and natural gas producing county that geologically locates in the Wattenberg field (over 80% of the total directional wells in the state of Colorado are in Weld county). Crude oil, natural gas, and water production per well together with the number of oil and gas wells of Weld Count are shown in figure 7. Codell sandstone was the main oil and gas producing formation since the discover of Wattenberg field in 1970s [14], and after the shale oil and gas surge in Northern Colorado in 2010, both Niobrara shale as well as Codell sandstone became the primary oil and natural gas producing formations. In 2017, 46% of the oil produced from Weld County was from Niobrara or Niobrara & Codell. This proportion of the oil production form Niobrara and Niobrara/Codell was as high as 82% in 2012, and kept above 74% from 2010 to 2013. The daily oil, natural gas and water production grow exponentially since 2000 in Weld County (R^2=0.8332 for natural gas, R^2=0.9390 for oil, and R^2=0.8003 for water). The lowest oil and natural production are 17,727 bbl per day and 349,282 mcf per day in 1999 and the highest is 324,914 bbl per day and 1,857,983 mcf in 2017 including the production from all the producing formations. The average water to oil ratio is 0.53, maximum ratio is 0.93 of the year 1999 and minimum ratio is 0.33 of the year 2013. Compared with total water to oil ratio of Weld County, the water to oil ratio of Niobrara/Codell is much lower that ranges from 0.18 to 0.36 since 2010, which is also lower than the national averaged water to oil ratio 9.2[16].

One factor that would impact on the number of oil and gas wells is the crude oil price according to our observation.[17] Till 2017, there are 15,476 directional wells in Weld County, 7,704 producing wells, 1,988 abandoned wells. The average true vertical depth of directional wells is 7,196 ft, and median depth is 7,273 ft. The true vertical depth of less than 5% of the directional wells is below 5,976 ft and only 5% of those is beyond 8,152 ft. The differences between measured depth and true vertical depth indicate the lateral extent of the directional wells.

Comparisons of geological settings of the five shale plays are listed in table 1. Marcellus shale formation is oldest, followed by Fayetteville shale and Barnett, Niobrara and Eagle ford shale formed latest compared with the other three shale formations. The older sediment is, more salt tends to get dissolved in the rocks leading a higher TDS in formation water because of longer contact time allowing more dissolve solids from rocks to water.

Table 1. Geology comparisons between major shale plays

Play	Marcellus	Fayetteville	Barnett	Eagle Ford	Niobrara
Area, km^2	270,000	6,500	13,000	51,200	87,515
Depth, m	1500-3000	500-2000	1500-2500	1200-3700	1500-3000
Formation age	Devonian	Mississippian	Mississippian	Cretaceous	Cretaceous
Thicknes, m		17 -180	30-150	~70	
Vitrinite reflectance, %	0.5-3.5	1.93-5.09	0.5-1.9	0.6-0.9	0.6-0.9
Location, State	Pennsylvania, West Virginia, Ohio	Arkansas	Texas	Texas	Colorado, Wyoming

Vitrinite reflectance in % is used to estimate the thermal maturity of the formation rocks. With higher vitrinite reflectance (R_0 above 1.2%), the source rock would produce more gas than oil indicating the rocks are thermally mature. The rocks having R_0 less than 1% usually suggest the formation rock is in the oil-prone stage, also known as thermally immature. Niobrara shale and eagle ford shale are not in the thermal mature stage that they produce a mixture of oil, gas and condensate, and both formations produce much less water than the national average[18].

2.3 Environmental Impacts of Unconventional Oil and Gas Drilling Activities

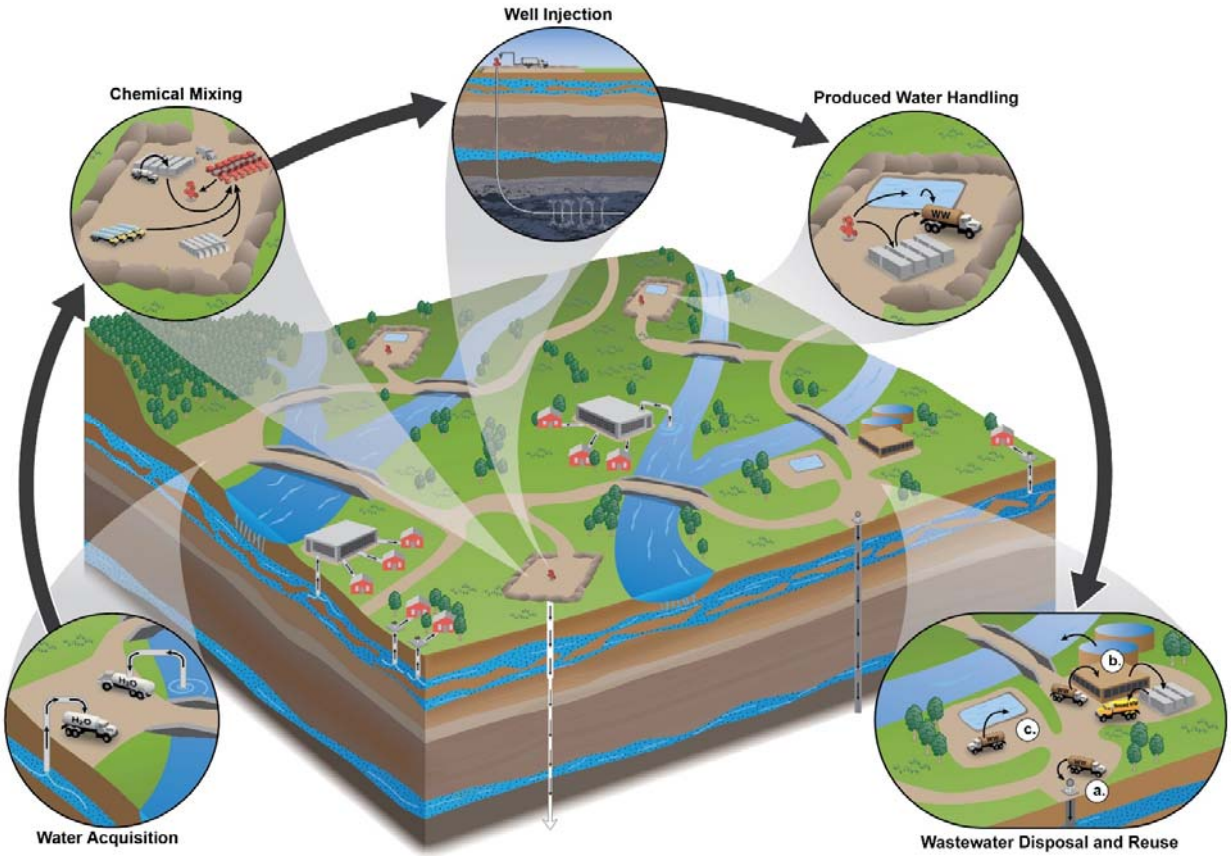

Figure 8. Typical water cycle of hydraulic fracturing (EPA)

Figure 8 is the water cycle for hydraulic fracturing by EPA[19]. Oil and gas industry get water from surface or underground, and then water is transported to the well pads where chemical additives are mixed with water and sand to make the "fracture fluid". During the unconventional oil and gas extraction and well completion, fracture fluid is injected in to subsurface a few thousands deep (usually 6000-7000 ft deep in the Wattenberg field) to create the fractures allowing oil, natural gas and water flowing back to the surface. Within the first few days after well completion, a huge amount of water will flow back to the surface called "flow back" with small amount of oil and natural gas. In the producing period, more oil and gas will be produced together with water, known as "produced water". Flow back and produced water are collected and stored in the pounds, water tanks or separation tanks. Then all the water generated during the oil and gas production could be disposed to injection wells or reused.

Some environmental issues associated with hydraulic fracturing or horizontal drilling are: 1), water stress. Since the vast amount of water is required for hydraulic fracturing, it will influence the local water supply and water allocation; 2), produced water is the biggest by-product stream of oil and gas production which is extremely high in dissolved solids, and contains oil and grease. Loss of well integrity or inappropriate disposal this water will contaminate the receiver water bodies; 3), some studies have shown that the volatile organic compounds and methane emitted from well pad were several times higher than from other sources[20]. VOCs react with other chemicals (OH and NO_2) in the atmosphere to produce ozone and longtime exposure to VOCs would increase cancer risk, respiratory distress, and endocrine disruption[21].

2.3.1 Water Stress

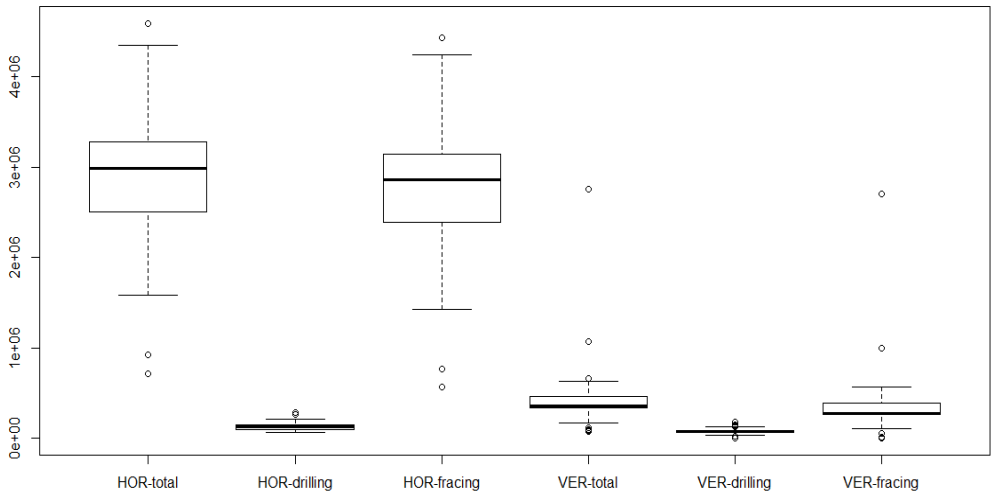

Figure 9. Total water demand for horizontal and vertical wells

Water required for drilling and fracturing depends largely upon the types of wells being drilled (vertical or horizontal) and the types of fracturing (gel-frack or slickwater frack or others). Figure 9 shows the water use for horizontal wells and vertical wells in Wattenberg field using traditional gel-fracturing (data was offered by NOBLE ENGERGY INC). To complete a horizontal oil and gas well, the total water demand is 6 times of the water required to complete a vertical well. Water for well drilling is almost the same for both vertical and horizontal wells. While, horizontal fracturing (hydraulic fracturing) uses 6 times of vertical fracturing in Wattenberg field.

Usually, more water required by horizontal wells than the vertical wells is due to the long distance of horizontal wells laterally extended for miles into the shale formation. For each stage of a hydraulic fracture, an average of 5,000 gallons (119 bbl; diluted acid stage) up to 50,000 gallons (1190 bbl; prop stages) of frac fluid is needed, which means that the entire fracture operation would require approximately 2-4 million gallons of water, 3 million gallons (71,428 bbl) being most common. [22] A typical horizontal shale well requires a maximum of approximately 600,000 gallons (14,000 bbl) for drilling and 2-4 million gallons of water for hydraulic fracturing. For vertical and directional wells, water needed for fracturing is between 100,000 and 1,000,000 gallons (2,300 – 23,000 bbl). Also, substantial amounts of water are needed for hydraulic fracturing, usually several times more than for drilling.[23]

Table 2. Estimated water needs per well for drilling and fracturing wells in the major shale plays (in gallon)

Shale play	For drilling	For fracturing	Total
Barnett shale	250,000	3,800,000	4,050,000
Fayetteville shale	65,000	4,900,000	4,965,000
Haynesville shale	600,000	5,000,000	5,600,000
Marcellus shale	85,000	5,500,000	5,585,000
Eagle Ford Shale	125,000	6,000,000	6,125,000
Niobrara shale	300,000	3,000,000	3,300,000

*volume data are approximate and may vary between wells

*data source:

https://www.epa.gov/sites/production/files/documents/09_Mantell_-_Reuse_508.pdf

Table 2 shows the estimated water needs for drilling and fracturing in the six major shale gas plays.[24] Geology of the basin, such as depth of the target formation, porosity, and permeability, is one reason that water demand varies a lot between different plays. And water requirements of various types of hydraulic fracturing technique are different in terms of water quantity and water quality. With slick water fracturing, water demand is generally 3-4 times of the water demand of gel-fracturing and water quality required by the slick water fracking is much less restricted compared with gel fracking.[11]

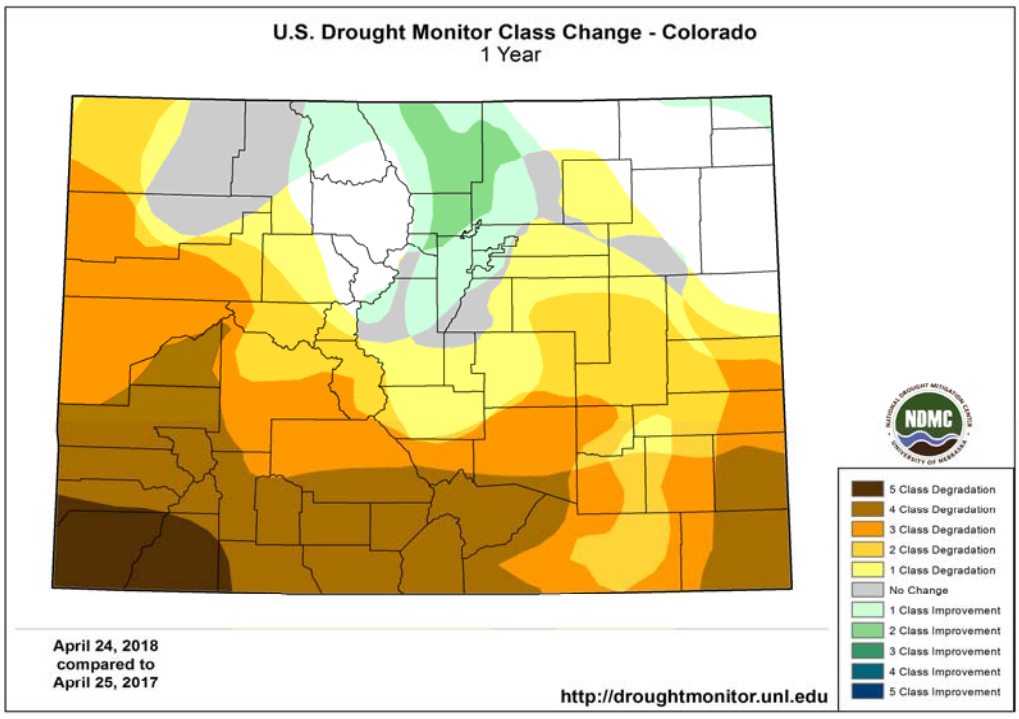

*Figure 10. Colorado drought change map from April 2017 to April 2018**

*data source: http://droughtmonitor.unl.edu/CurrentMap/StateDroughtMonitor.aspx?CO

The huge demand of water to produce oil and natural gas from shale formations will pose a potential threat to local water supply since freshwater and groundwater sources are limited and climate change might have a negative impact on the water availability due to less precipitation and rising drought. In Colorado in 2010, 86% of the total water withdraw is used by Agriculture, 8% of is for municipal use and only 1.5% is for industrial and commercial use. 2.8% of the water used in industry/commercial is consumed by hydraulic fracture, which is 4/10000 of the water consumption by agriculture. Figure 10 shows the 1-year drought change map of Colorado from April 2017 to April 2018. The drought condition of most counties in Colorado has deteriorated except in the central north where the drought has reduced compared with 2017 data. In 2018, the estimated total population in Colorado is 5,684,203 (data from U.S. drought map, http://worldpopulationreview.com/states/colorado-population/) and the estimated population in the drought area is 2,636,971, that almost 46.4% of the population of Colorado lives in the

area with potential water crisis. As new fracking technology has been applied (slick water fracking) and more unconventional oil and gas wells will be drilled in the northern Colorado (Greeley, Weld County), the water required for hydraulic fracturing will be several times more than the current water required by fracking.

Meanwhile, the major water source of Weld County is from surface water, such as rivers, lakes or reservoirs, drought will cause water deficit. Increasing water consumption of oil and gas operations will cause a water surcharge. Greeley as the county seat of Weld County, has a lot of oil and natural gas wells since 2010. The combined drinking water treatment capacity is up to 70 million gallons per day from two drinking water treatment plants, Bellvue and Boyd Lake, which is equal to drill and frack proximately 21 wells using gel fracking or 7 wells using slick water fracking. In a drilling and fracking active season, water requirement for oil and gas operation would compete with the municipal water demand.

2.3.2 Deep formation water contamination – produced water

During well drilling and completion, some water will return to the surface, known as the fracturing flowback or produced water (a water-based solution that flows back to the surface during and after the completion of hydraulic fracturing). Within the first few weeks of well completion, a great amount of water would be brought to the surface together with oil and natural gas, which is called flowback; after a month or longer production of oil and natural gas, the volume of water reduces, and this water is called produced water. Produced water and flowback is the largest wastewater stream or by-product in the oil exploration and production process.[25] There is no established way to define flowback and produced water. Sometimes they are identified according to the time of occurrence, the rate of return or the chemical composition. Most of the flowback occurs quickly in the first seven to ten days, sometimes even shorter, while the rest can occur over a three to four-week time period.

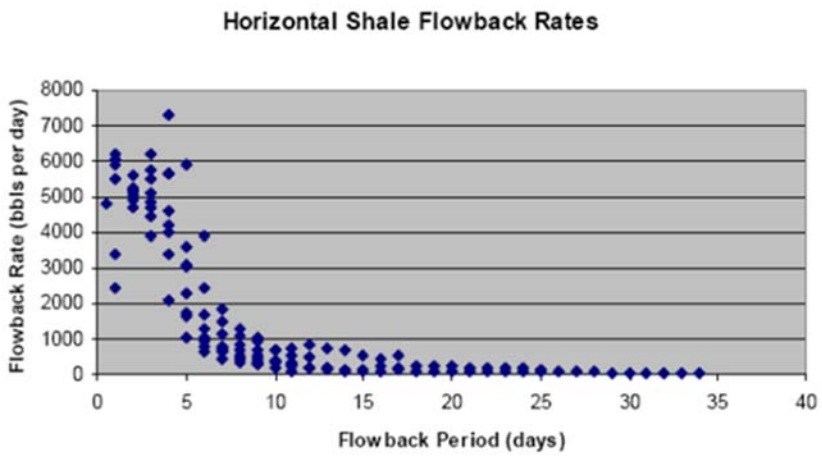

Figure 11. Flowback rate for Marcellus shale gas play

Figure 11 shows how the water decreases with the oil and gas producing in Marcellus shale play. The water decreasing follows exponential decay curve which is normally used to estimate "produced water" (including both flowback and produced water) volume.

In the year 2012, the total onshore produced water generated was about 20 billion bbl and 35% (7.4 billion bbl) of this water came from Texas, followed by California (15%), Oklahoma (11%), Wyoming (11%) and Kansas (5%) from which the volume of the produced water exceeded 1 billion bbl. [26] Texas has the two largest shale plays, Eagle Ford and Barnett. Woodford shale play locates in Oklahoma. Niobrara shale formation extends over Wyoming and Colorado, but due to different geological and geophysical settings and mutuality of the formation, the oil, gas and water production vary a lot even for the same shale formation which locates at different depth in the different places.

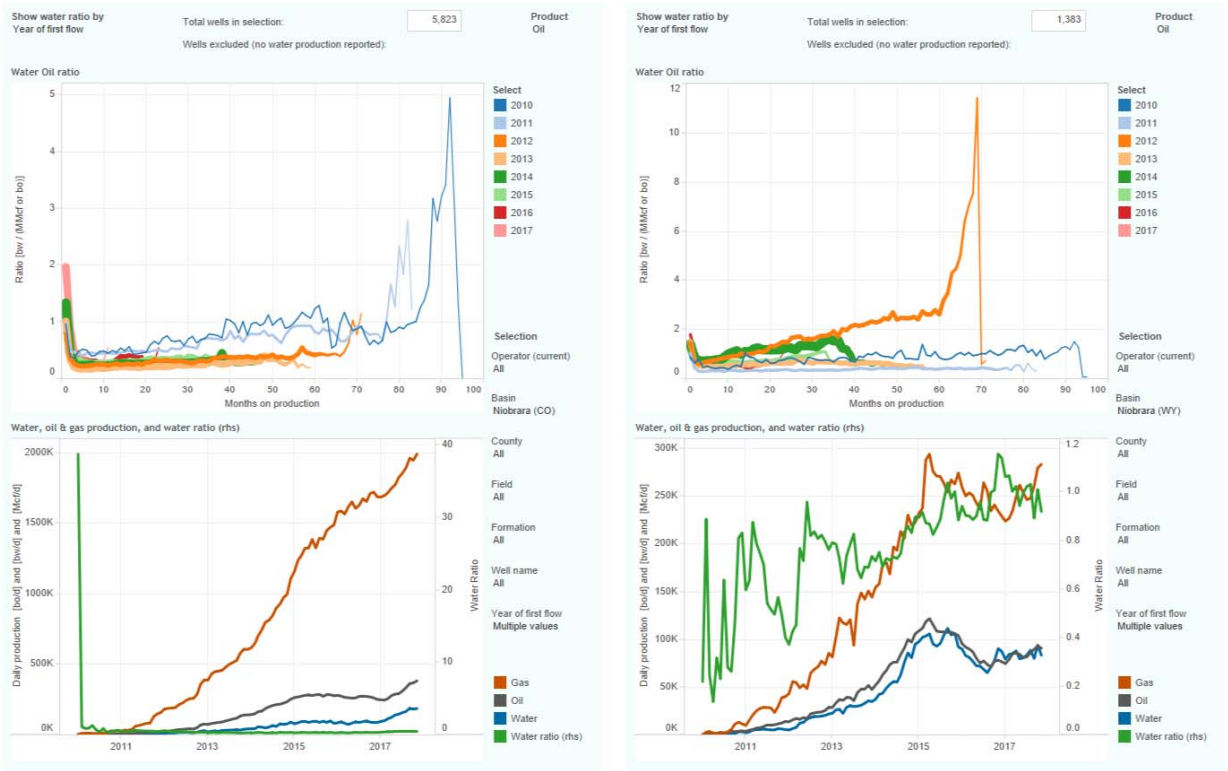

Figure 12. Water, oil and gas production comparison between Colorado and Wyoming

Productions of oil, natural gas and water and water to oil ratio of the Niobrara shale formation in different states (Colorado and Wyoming) are shown in figure 12. The left column including two plots up and down are the production of Colorado; the right column (up and down plots) is the data from Wyoming (the scale of y axis differs). Water to oil ratio does not vary a lot for Colorado and Wyoming, that water to oil ratio is around 1 for both states, while oil and gas production of these two states is quite different. The cumulative gas production of Colorado is 10 times of Wyoming and oil production of Colorado is 3-4 times of Wyoming with the similar water production. The reason might because the oil and gas activity is more intensive in Colorado since the number of producing horizontal wells in Colorado is 4.2 times of Wyoming.

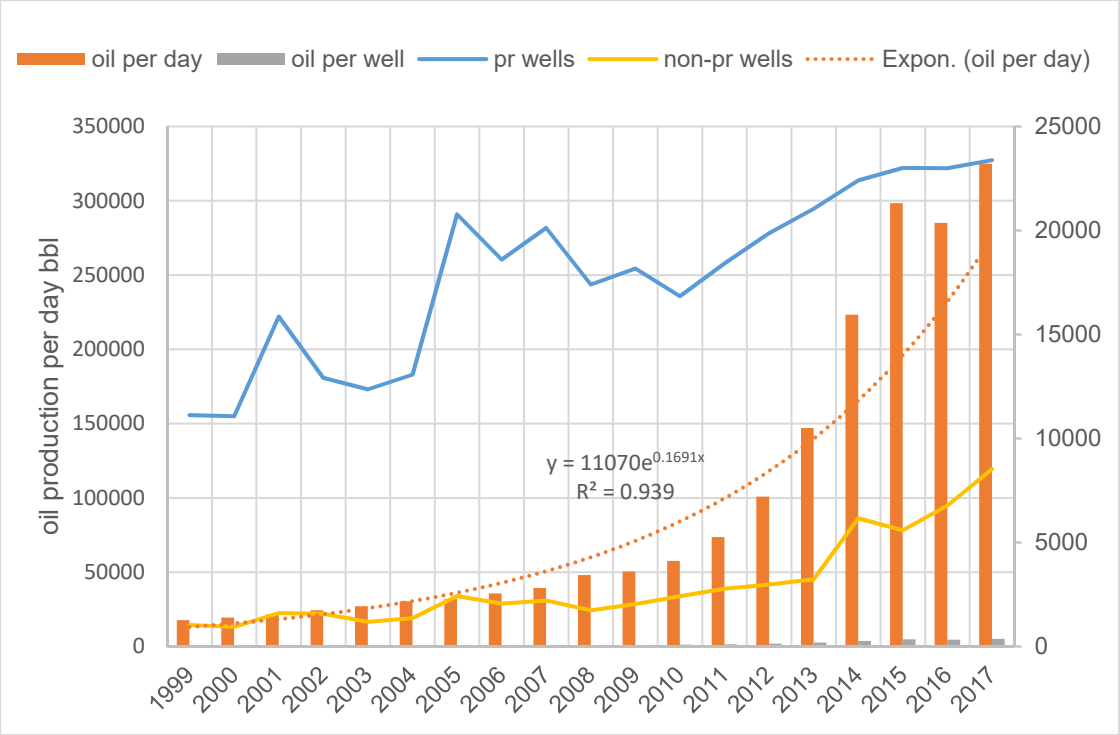

Figure 13. Total water production, water production per well and number of producing wells in Weld County (1999-2017)

Weld County is the core oil and natural gas producing county in northern Colorado. Figure 13 has summarized total water production, water production per well and number of producing wells for each year from 1999 to 2017 in Weld County. There is cumulative 2,355 million gallons of water generated in Weld County from 1999 to 2017. According to U.S.G.S water use database, in the year 2010, the total water use for public supply was 251,018 gallon, mining self-supplied was 317 million gallons, irrigation self-supplied was 152,365 million gallon, and the water produced from oil and gas wells was 529,746 gallon in Colorado. There were 45 abandoned wells, 21 drilled but not producing wells, and 54 producing wells in Weld County in the year 2010. The median water consumption for a horizontal well is around 2.9 million gallons and the average are 2.8 million gallons using gel fracking. For the year 2010, total water used for drilling and hydraulic fracturing was around 224 million gallons and water production was 357 million gallons. Water generated from oil and gas wells was much more than the water required to drill and frack a horizontal well, in addition, the remaining produced water could be enough for public supply after treatment. Currently, 99%

of the produced water is re-injected to the disposal wells. In Weld County, total 68 injection wells are put into practice in 2017. While as the continuous production of oil and natural gas, water to oil ratio become increasing over time[27], adequate produced water management, such as reuse and recycle, would reduce the water stress to a great extent.

Beside the high volume of flowback and produced water, another big problem treating produced water is its unique water quality. Having a murky appearance from high levels of suspended particles, produced water often appears weeks after production and can last for years, with high level of TDS, oil and grease. And both flowback and produced water are comprised of fracture fluid, formation water and dissolved hydrocarbons. Current produced water treatment methods involve filtration, precipitation or ozone treatment to remove suspended solids, metals and organics, reverse osmosis, distillation and crystallizer to remove excess dissolved solids and pre-treatment is often required for a successful produced water treatment which is also used to lower the extreme high TDS[28].

Unlike conventional oil and gas well, shale oil and gas wells usually would experience the production decay up to 40% in the first few years of production[29]. In the Eagle Ford shale field, the estimated well life under different oil decay curves varies between 12 years to 46 years with EUR (estimated ultimate recovery) of 126 -290 kbbl. In the Wattenberg field, a conventional oil and gas well usually serves at least 5 years to become inactive due to the rapid decline in oil production[30]. The average water to oil ratio is 0.53 agrees with our prediction that Niobrara is a relative dry oil and gas producing formation.

Produced Water Management

Currently, produced water (every water generated from an oil and gas well) management includes several methods.

1) Secondary recovery injection. Secondary Recovery injection is to re-inject water to the oil and gas bearing formation to enhance the hydrocarbon production.
2) Deep well injection. This is the most applied method to deal with produced water by transporting produced water to the class II disposal well. The cost for deep well injection is comprised of two

parts, transportation fee and disposal fee. Disposal fee ($1-$3/bbl) is much less compared with transportation fee. Long distance handling fee would be expensive as $4-$19/bbl.[31]

3) Surface discharge. There are some limitations to discharge the produced water to the surface water bodies, since produced water is high in TDS. Surface disposal of produced water is only practical when TDS drops to some certain level which is regulated by local oil and gas conservation commission or environmental department. For example, Pennsylvania's regulation forbids the surface discharge of produced water with TDS higher than 500 ppm as well as restrictions for other chemicals.
4) Beneficial reuse and recycle. As of 2012, only 0.6% of the total produced water in the U.S. has been treated and reused either in the oil and gas field (make drilling and fracking fluid) or for other purposes, such as irrigation, dust and ice control on roads. Treated produced water could be used for irrigation with specific SAR and TDS no more than 5000 ppm. If chloride concentration is lower than 1,500 ppm, this water could be used for dust and ice control on road; if treated water has more than 5,000 ppm of TDS, it could be only discharged into the type II well.

Therefore, water quality plays an important role in the produced water management as well as the availability of treatment and disposal infrastructures. Because produced water has been in contact with shale formations for a long time, some chemicals from the formation rocks would be dissolved into the water, and the salt also builds up over years, making produced water high in salinity, metals and organic compounds. Besides the large component of produced water is the ancient sea water which itself is high in salinity.

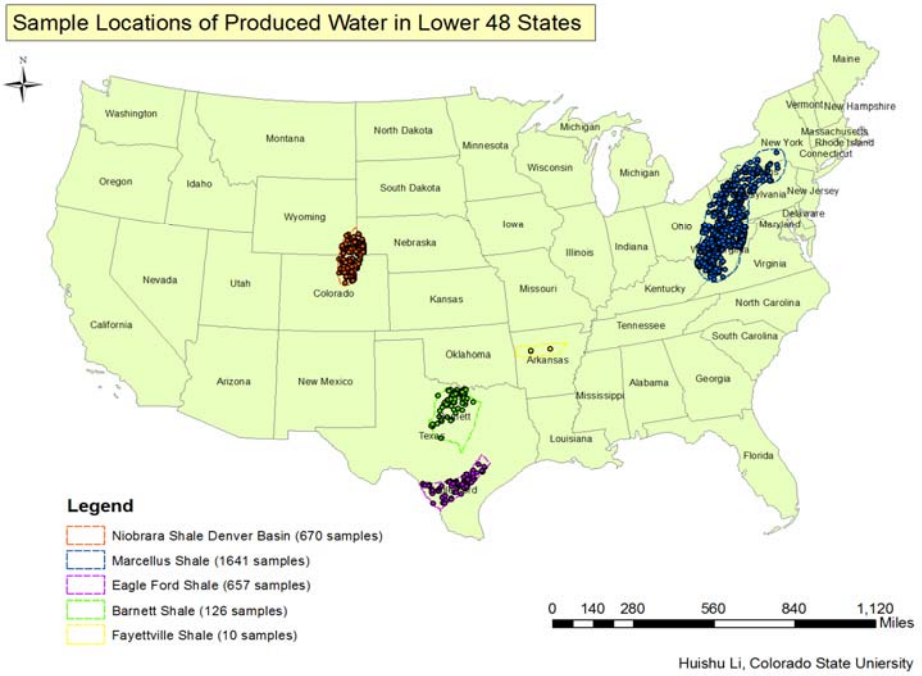

Figure 14. Map of produced water sample locations by U.S.G.S.

U.S.G.S has conducted a produced water survey from 1905 to 2014, collecting 114,943 produced water samples nation-wide (Figure 14). We have selected the water data points from five shale oil or gas plays, including the Niobrara shale (CO & WY), the Barnett shale play and Eagle shale play in TX, the Fayetteville shale play in Arkansas and the Marcellus shale play across four states. Marcellus shale, Fayetteville shale and Barnett shale are the major shale gas active producing plays. Eagle Ford shale and Niobrara shale produces mixture of oil, condensate and gas. U.S.G.S has tested 137 water parameters, including organic, inorganic and isotope signatures.

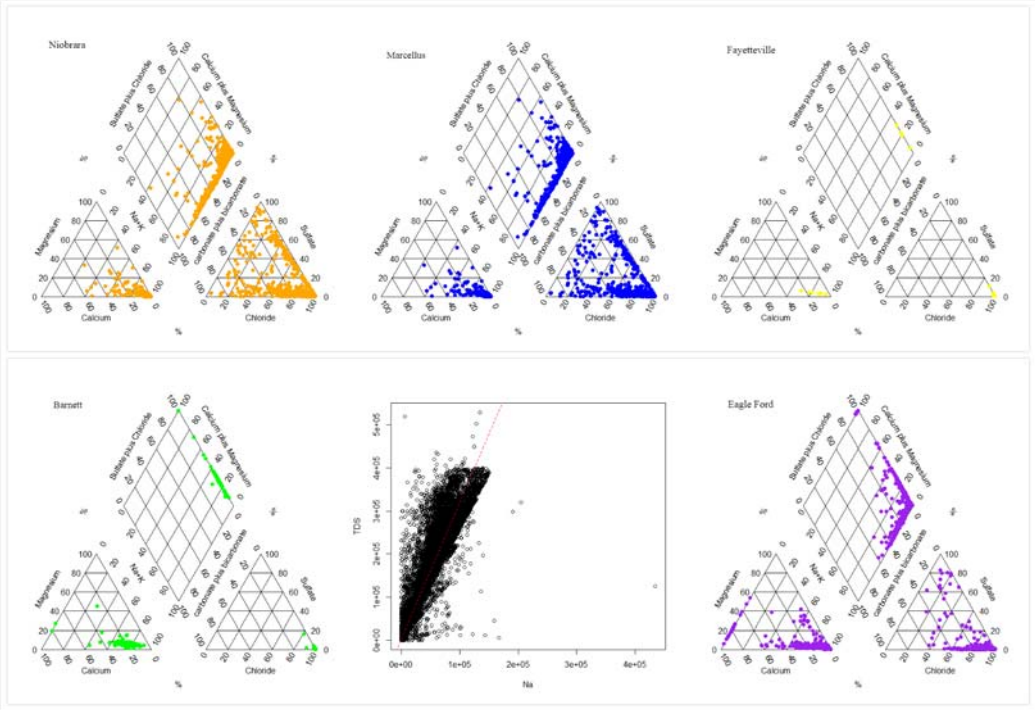

Figure 15. Piper plot of produced water from different shale plays and plot of relationship between Na and TDS (lower middle)

For all of the produced water samples, there is a liner relationship between the concentration of sodium and total dissolved solids ($R^2 = 0.9294$, p-value: < 2.2e-16, figure 15). All the produced water samples are Na-Cl type with sodium as the dominant cation, which agrees to our previous study on produced water quality characteristics. Water temperature ranges from 3ºC to 35 ºC for the four plays except for Eagle Ford play, which ranges from 3 °C to 80 °C with average water temperature of 47 °C.

2.3.2 Greenhouse gas and hazardous air pollution emission

Methane is major and core gas products from an oil and gas well but often times, natural gas extracted from the well is the mixture of methane, alkane, and other gases. Improper seal of the well or storage tank will leak the gases to the atmosphere. According to EPA's research in Weld County in 2015, methane is the major gas leaks from well pad and VOCs are the majority gases leaks from water tanks.[32] EPA estimated that total greenhouse gases emitted from oil and gas operations were 226.4 million metric tons, 14.5 million tons of NOx and 2.77 million tons of VOCs.

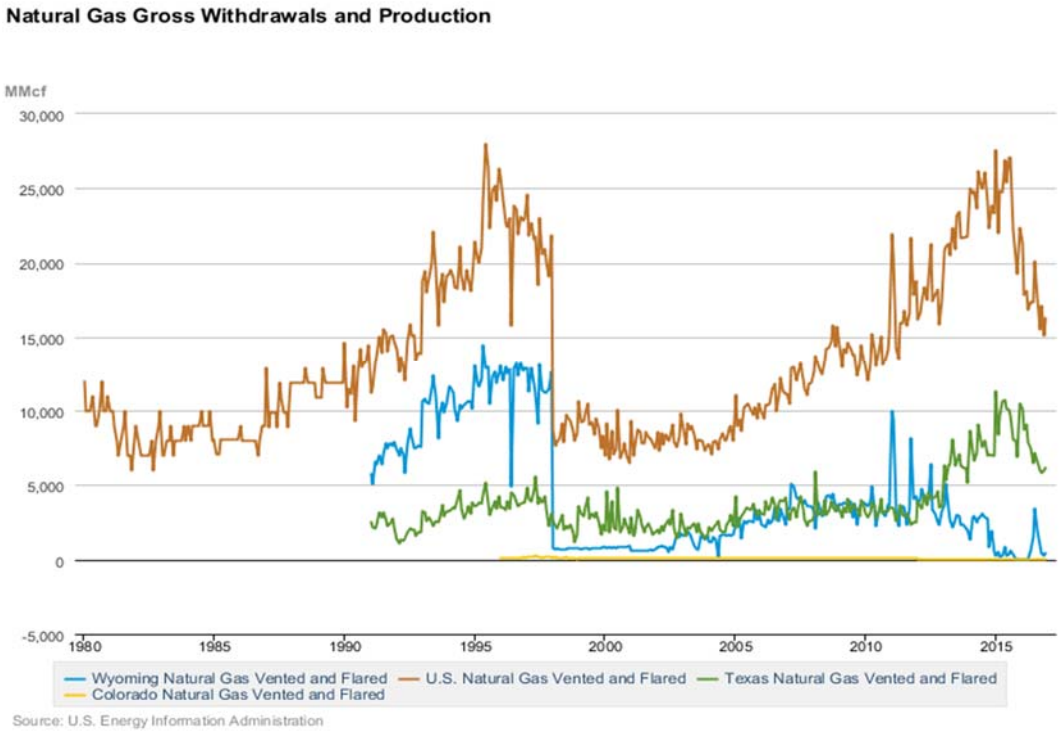

Figure 16. Vented and flared natural gas by states, E.I.A.

During the first few days of production, without efficient collection of this natural gas, it will be disposed or flared on site leading to the abundant release of methane which is known as one of the greenhouse gases. Figure 16 plots the amount of natural gas vented or flared in Colorado, Wyoming, Texas and U.S. Facilitated by the regulation of Colorado who is the first state to limit the methane emission from oil and gas operations in 2014, gases vented and flared in Colorado dropped to 0 since 2012. While, for Texas and Wyoming. According to Carnegie Mellon University's study about Measurement and Modeling to Quantify Emissions from Shale Operations, the estimated methane emissions at producing wells were approximately 1% of production levels in the Marcellus shale play. National -wide, methane emission has decreased from 2,948 Gg to 2,545 Gg from 2009 to 2011due to the regulations controlling the emission rates which might be the reason for the dropping of vented and flared natural gas for all the states except Texas in figure 16.

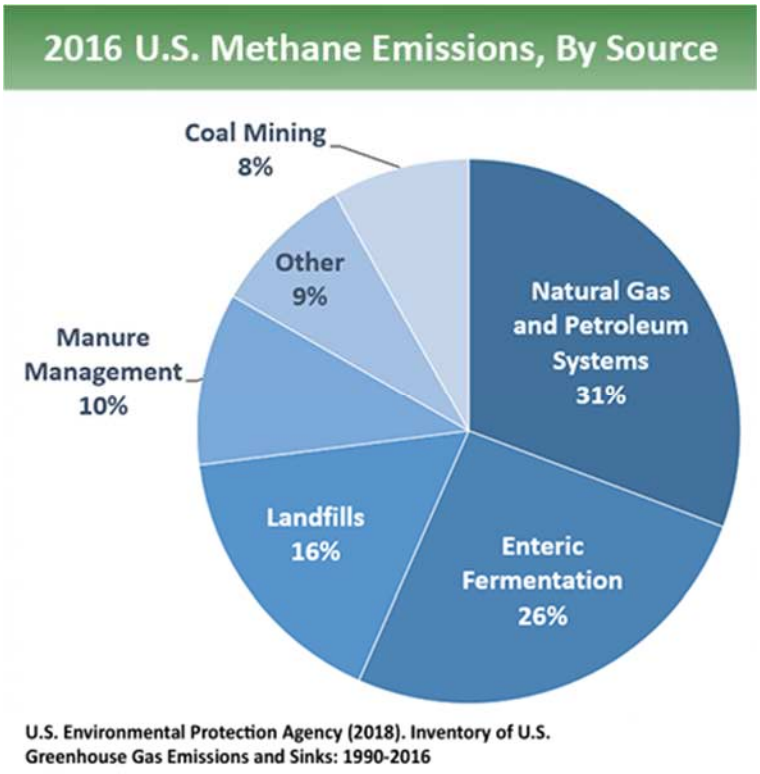

Figure 17. Methane emission by different sources in 2016

In terms of methane emission sources, 31% of the methane emission is from natural gas and oil production (31%) (Figure 17) in 2016, and within this 31%, 53% of the methane is emitted from gas production and 19% of the methane emission is from oil production.[33]

Beside methane emission, Volatile organic compounds (VOCs) are another major hazardous air pollutants from oil and gas exploration and production. Fugitive emissions from oil and gas well pads could be a significant source of VOC emissions through improper connections, seals or operations. Other sources of VOC emissions from an oil and gas pad could be during the processes of the separation of gas and liquid products, and storage.

A previous study by NOAA[34] on chemical signatures of hydrocarbon emissions (VOCs) revealed that oil and natural gas activity is the primary contributor of propane and vehicle emission accounts for majority acetylene of the ambient total volatile organic compounds (VOCs). This research focused on the oil and

gas developing areas in the state of Colorado. Isotopes of butane and propane will help with the pollutant source identification. Ratio of i-pentane and n-pentane less than 1, and ratio of i-butane to n-butane greater than 0.6 or 1 indicate an oil and gas source; i-pentane to n-pentane ratios greater than 1 and i-butane to n-butane ratio between 0.2 and 0.3 suggest a vehicular source. Wind condition will largely impact on the VOC distribution.

2.3.3 Groundwater Contamination

Groundwater in the Wattenberg field is present in two aquifers: the South Platte Aquifer and Laramie-Fox Hills Aquifer. The South Platte Aquifer is a shallow, unconfined alluvial aquifer. The aquifer has hydraulic connectivity with surface water and is recharged by infiltration of streams and the percolation of precipitation, irrigation, and canal and pond seepage.

The depth of the water from the ground surface is 0-65 m and the saturated alluvial deposit is up to 16 km wide and 60 m thick. The aquifer produces up to 11,350 lpm of water and has a transmissivity of 370-10,200 m^2/d, a hydraulic conductivity of 30-610 m/d, and a specific capacity of 140-5,200 lpm/m. The South Platte Aquifer is the largest source of water for agriculture in the area, primarily for irrigation and livestock purposes, and contains relatively high concentrations of TDS.

The Laramie-Fox Hills Aquifer is a confined bedrock aquifer, encompassing 17,000 km^2 of the Denver Julesburg Basin. The maximum depth of the water from the ground surface is 730 m, with a saturated thickness of 0-110 m. The Laramie confining unit is an impermeable layer that is between the Arapahoe Aquifer and the Laramie-Fox Hills Aquifer, obstructing water flow from the Arapahoe Aquifer to the underlying Laramie-Fox Hills Aquifer. The Laramie-Fox Hills Aquifer yields up to 1,300 lpm, with a transmissivity ranging from 12,000-87,000 lpm/m. It is a significant source of domestic and municipal water.

Some researches indicate that there is more possibility for the groundwater well to be “influenced” or “contaminated” if there was an oil and gas well within a shorter distance.

It is estimated that over 2 billion gallons of produced water (brine) are re-injected into the Class II wells (this type of well is only for liquid injection by oil and gas industry, including disposal well, enhanced

recovery well and storage well) with or without treatment[35]. There will be of a great potential environmental risk caused by the re-injection, such as earthquakes, NORM contamination and groundwater pollution.

According to our previous study, the groundwater from Laramie-fox hill aquifer is moderately alkaline and low in total dissolved solids. The major types of groundwater from Laramie-Fox hill aquifer are $NaHCO_3$, $CaSO_4$ and NaCl.

The source of methane could be from two processes, microbial (also called methanogenesis) or thermogenic. The formation of methane by bacteria occurs commonly in anaerobic subsurface environments (biogenic methane). However, there is concern that methane gas formed in the deep shale formations (thermogenic methane) can contaminate groundwater through possible connectivity between the deep shale and shallow aquifer created during drilling and hydraulic fracturing.

A previous study in Pennsylvania found higher concentrations of methane gas in groundwater near active extraction areas, while in contrast, no relationship was identified between distance from the oil and gas wells and groundwater concentrations of methane in Wattenberg field, Colorado. However, thermogenic methane was found in some aquifer wells in the Wattenberg field, implying the existence of a possible pathway from deep shale to the overlying aquifer.

Groundwater Quality Monitoring – Colorado Water Watch

To bridge the gap between fears about public health impacts caused by oil and gas development and the assumption that industry environmental and health practices are reliable,

Colorado Water Watch (CWW) designed by Colorado State University (CSU) has started to serve as a platform to support the states regulatory agency and provide real-time groundwater quality information to both industry and the public in the northern area of Wattenberg field. Wattenberg field locates north Denver Basin of Colorado and was historically one of the largest oil and gas production fields in the United States, owning more than 22,000 producing wells according to Colorado Oil and Gas Conservation Commission (COGCC), 2014.

At first decades, petroleum companies started with oil production, but recently massive hydraulic fracturing was performed for natural gas routinely on thousands of wells.

CWW adopts contaminant-surrogate sensing technology to gather and provides groundwater information at intervals of one hour. ORP is considered the surrogate of dissolved methane, which is based on the correlation between the expected close relationship between ORP and dissolved methane under certain conditions. Normally, the surrogate parameters are kept in their reasonable ranges, but sometimes will get changed dramatically due to some external reasons. Groundwater event is particularly referred to the event which leads to the significant change of water quality, with a duration one or more time steps.

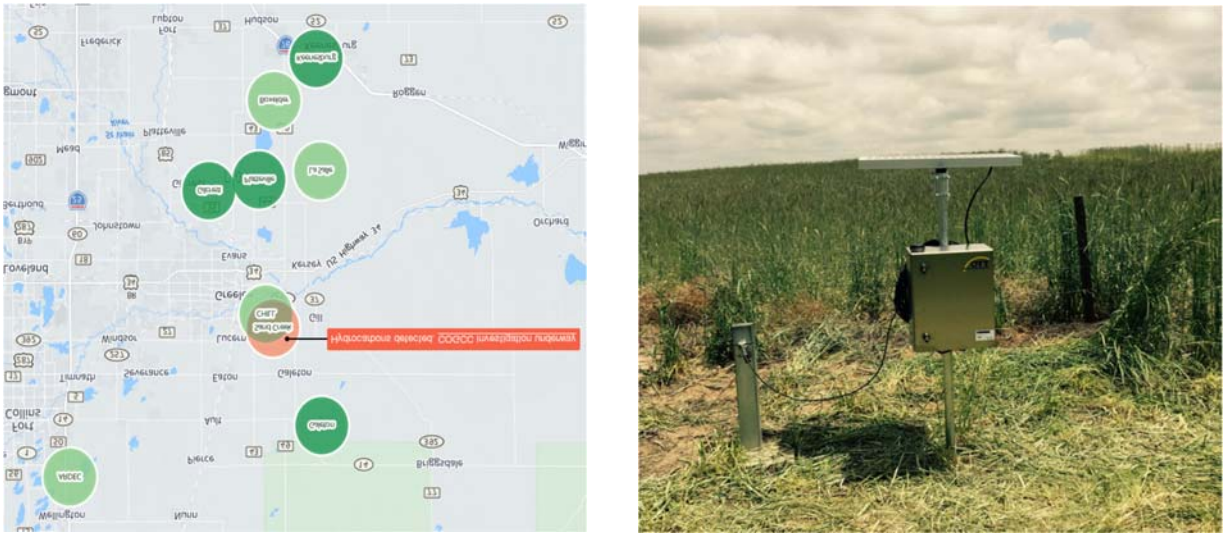

Figure 18. Left: the monitoring locations in Wattenberg field. Right: the sensor facility of one monitoring station

Locations of the monitoring stations and the photo of a sensor facility are shown in Figure 18. Multiple groundwater quality sensors are used in one monitoring station in CWW to test real time pH, water temperature, water depth, conductivity, ORP and DO.

Chapter 3 Hypotheses and Research Questions

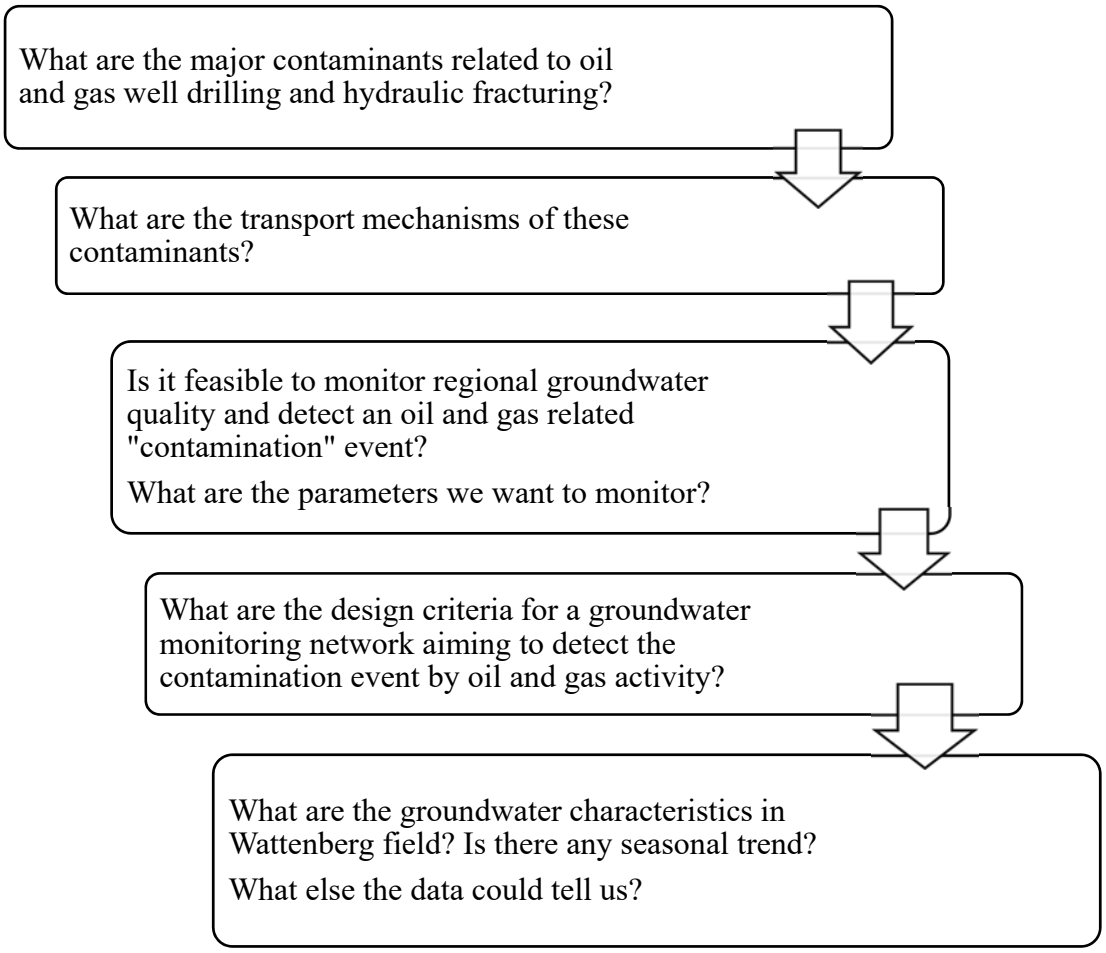

Figure 19. Study Scope

Question 1:

What are the contaminants caused by oil/gas well drilling and hydraulic fracturing?

Hypothesis: Extracting oil or natural gas from shale formations (known as unconventional oil and gas) requires pumping large amounts of water, sand and chemicals (typically 3-12 additives depending on the characteristics of the water and shale formation) into the subsurface to free the oil and gas buried in the

deep formation. A portion of that injected water, along with large quantities of existing formation water (high in salinity), (flowback and produced water) returns to the surface.

One of the public concerns over hydraulic fracturing is the potential contamination to the drinking water by unconventional gas and oil drilling and hydraulic fracturing. Methane is the major pollution reported in some water well contamination incidents which is suspected to be caused by hydraulic fracturing. Other potential contaminants include the high saline water, petroleum compounds (dark color, smelly odor and oily water). In summary, contaminants could be classified into three categories, gas phase – methane, aqueous phase – saline water or produced water, and non-aqueous phase liquids (NAPLs).

Question 2:

What are the transport mechanisms of the contaminants?

Hypothesis: Contaminants transport in different zones may have distinct transport mechanisms.

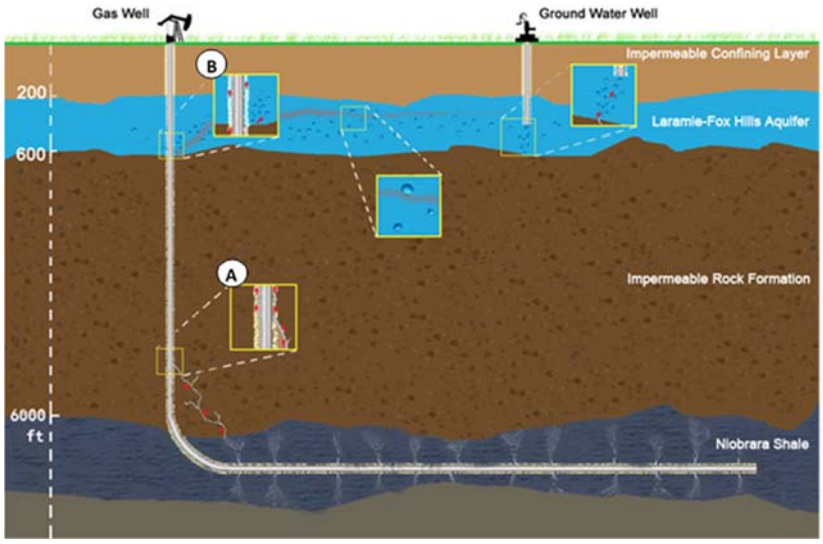

The four most probable fluid transport mechanisms from deeper hydrocarbon formations to groundwater and aquifers are: 1) vertical and lateral gas migration along natural geologic fractures and faults; 2) stray gas migration through unsealed or improperly sealed oil and gas production wellbores; 3) gas and aqueous phase migration through casing breaches and failure; and 4) percolation from surface spills of produced water—the water produced from oil and gas extraction and a mixture of shale formation water and fracture

fluids. The first two pathways are likely to be combined together and create a cross transport mechanism: gas leaked from an improperly sealed wellbore migrates through natural geological structures into groundwater or the aquifer. Although fluid migration can occur naturally along preexisting natural faults and fractures over geological time scales (e.g. millions of years), the impermeable formations overlain and underlain by the Laramie-Fox Hills aquifer in northeast Colorado make the natural migration mechanism itself less likely to occur. In addition, since the aquifer is confined, percolation from surface spills in the Wattenberg oil and gas field of the Denver-Julesburg (D-J) Basin in Colorado are not likely to contaminate the aquifer. Therefore, the most likely fluid transport mechanism to the aquifer is either produced water leaking through corrupted casing (A) or gas migration up from the producing formation along a poorly sealed wellbore (B), or both.

Question 3:

Is there any relationship between development of drilling and hydraulic fracturing and methane in groundwater?

Hypothesis: Methane exists naturally in groundwater (microbial methane) which is produced by bacteria. In some carbon rich and low redox potential environments, the biogenic methane concentration in water could be extremely high, elevated concentration of methane could be from microbial sources. There is another source of methane, called thermogenic methane, which is generated by high temperature and pressure. Methane concentration itself could not indicate a contamination related to well drilling and hydraulic fracturing, which needs to be further analyzed by isotopic signatures.

Question 4:

Is shallow groundwater water different from produced water?

Hypothesis: Ground water occurs both in loosely aggregated and unconsolidated materials, such as sand and gravel, and in consolidated rocks, such as sandstone, limestone, granite, and shale. Drinking water comes from the shallow drinking water aquifer, which is usually less than 1000 ft, while the main composition of produced water, the formation water originates from deeper formations, such as shale occurring at the depths of 6000-8000 ft. Shallow drinking water aquifer and deep shale formation are highly

variable in their degree of the composition of formation rocks, the size of mineral particles, rocks and fractures, the shape and the size of pore or open spaces between particles. Therefore, the physical and chemical properties of drinking water and produced should be different.

Question 5:

Can Real-time Monitoring of Groundwater Be Used to Detect Oil and Gas Contamination Events?

Hypothesis: Surrogate methods can be used to detect oil and gas related contaminant events including measuring ORP and DO to represent dissolved methane. Combined with pH, temperature and conductivity, anomalies in time-series can be detected using one or combined event detection methods, such as moving median, nearest neighborhood, M-set and one- class SVM.

Question 6:

How can real-time monitoring be optimized for site selection?

Hypothesis: Site selection of a monitoring network can vary due to different objectives and therefore there is no universal rule to pick the right locations for the monitoring stations. However, since the purpose of this study is to monitor groundwater quality around oil and gas wells, the most appropriate selection criteria will include 1, the proximity to oil and gas wells; 2, density of oil and gas wells; 3, groundwater flow direction; 4, density of water wells.

Question 7:

Is the event detection algorithm used by the Colorado Water Watch (CANARY) functioning properly?

Hypothesis: The event detection algorithms used by CANARY is the combination of four outlier detection methods, based on the assumption that the data follows normal distribution, which is a prerequisite of the application of CANARY. Therefore, if the data distributes normally, CANARY would be a good method. But if the data does not follow the normal distribution, the methods used by CANARY will not be suitable for this case. It is hypothesized that the monitoring data is not normal and therefore there are better approaches for event detection.

Chapter 4 Distribution and Origin of Groundwater Methane in the Oil and Gas Field of Northern Colorado Wattenberg[1]

Overview

Public concerns over potential environmental contamination associated with oil and gas well drilling and fracturing in the Wattenberg field in northeast Colorado are increasing. One of the issues of concern is the migration of oil, gas or produced water to a groundwater aquifer resulting in contamination of drinking water. Since methane is the major component of natural gas and it can be dissolved and transported with groundwater, stray gas in aquifers has elicited attention. The initial step toward understanding the environmental impacts of oil and gas activities, such as well drilling and fracturing, is to determine the occurrence, where it is and where it came from. In this study, groundwater methane data that has been collected in response to a relatively new regulation in Colorado is analyzed. Dissolved methane was detected in 78% of groundwater wells with an average concentration of 4.0 mg/L and a range of 0 to 37.1 mg/L. Greater than 95% of the methane found in groundwater wells was classified as having a microbial origin and there was minimal overlap between the C and H isotopic characterization of the produced gas and dissolved methane measured in the aquifer. Neither density of oil/gas wells nor distance to oil/gas wells had a significant impact on methane concentration suggesting other important factors were influencing methane generation and distribution. Thermogenic methane was detected in two aquifer wells indicating a potential contamination pathway from the producing formation but microbial-origin gas was by far the predominant source of dissolved methane in the Wattenberg field.

4.1 Introduction

There has been increasing atte[1]ntion directed toward the potential for environmental contamination associated with horizontal drilling and hydraulic fracturing, the key technologies employed during the extraction of unconventional oil and gas resources.[36] Hydraulic fracturing is utilized to increase formation

[1] Published in Environmental Science and Technology, January 2014, 48 (3), 1484-1491

permeability through introduction of large amounts of injection fluid under high pressure[37]. In addition to increasing the recovery of oil and gas from the producing formation, it has been suggested that hydraulic fracturing could create seepage pathways of natural gas (methane) and deep formation water (with high TDS) migrating to the shallow formation, resulting in aquifer contamination and green house gas emissions.[38] [39]

Methane is formed in nature through two primary types of processes: microbial and thermogenic. Microbial methane is produced by subsurface bacteria and is a common natural source of methane gas in groundwater aquifers, usually found in water wells, swamps and other environments with high carbon concentrations and low redox potential[40]. Microbial or biogenic methane can be produced through two pathways, acetate fermentation and CO_2 reduction. Thermogenic methane gas is produced at greater depths through high pressure and temperature processes, characteristic of deep oil and gas reservoirs that conventional and unconventional hydrocarbon wells tap.[41] Methane migration from deep underground formations to the surface can be achieved by several mechanisms including advective transport (gas migrates from areas of high pressure to areas of low pressure) through or around the protective casing that surrounds the production piping.[42]

Significant oil and gas development has occurred recently in the Denver-Julesburg (DJ) basin of northeast Colorado.[43] Intensive well drilling and fracturing in the Wattenberg field, located in the DJ basin[44], first been discovered in 1970, has resulted in greater than 19,000 producing oil and/or gas wells and 7,500 abandoned wells through August, 2013.[47] The Colorado Oil and Gas Conservation Commission (COGCC) has compiled oil and/or gas extraction and production information, and more recently, has required groundwater monitoring at a minimum of two groundwater sources before and after drilling an oil and gas well (Rule 318A.e.(4)).[45] The objective of this paper is to understand the occurrence and distribution of methane in groundwater in the Wattenberg field. In addition, the relationship between methane and oil/gas activity is studied with chemical and spatial analysis of COGCC groundwater baseline data.

4.2 Materials and Methods

The COGCC Baseline Groundwater Sampling Program requires oil and gas operators to sample two groundwater wells, springs, or seeps on opposite sides of one drilling location from the deepest aquifer within a half-mile radius of the surface location[48]. A subsequent sample needs to be taken between 12 and 18 months after the well completion or facility installation, and again between 60 and 78 months after the initial sampling event (dry holes are exempt from this requirement). Isotopic and gas compositional analysis needs to be collected if the methane concentration exceeds 1.0 mg/L.

The study area, the Wattenberg Field, is located on a 1,280,000-acre parcel in northeast Colorado[46]. Groundwater and gas composition data were collected in the area of the Wattenberg field and at COGCC groundwater well points. The components of water and gas were analyzed by standard methods (SI Table 1).[47 48 49]

A total of 223 data points from 176 drinking water wells were included in this analysis, with replicate samples collected from 45 groundwater wells that encountered a methane change, and 131 single sample wells. Within the 176 groundwater wells, 60 isotopic test results (carbon and hydrogen) from 40 wells were obtained to determine the composition of dissolved gases in water (such as methane), including 19 wells that were sampled multiple times.

4.3 Results and Discussion

The origin of methane is related to the microbial and thermal alteration of organic matter. Carbon and hydrogen isotopic compositions of methane can be used to examine the different origins due to distinct characteristics of the two types, thermogenic and biogenic.[50]

^{13}C in CH_4 is depleted in the primary microbial dissimilation reactions, acetate fermentation and carbon dioxide reduction (shown below) and is accompanied by minimal C_2 and C_3 production[51]. However, thermogenic methane production will result in the production of heavier hydrocarbons (C_2, C_3; etc.)[52] and the stable isotope ^{13}C in CH_4 is closer to the isotope of the substrate that produced methane, but more enriched via the thermogenic process than microbial mechanisms.[53]

$$Acetate\ Fermentation\ Pathway: CH_3COOH = CH_4 + CO_2$$

$$CO_2\ Reduction\ Pathway: CO_2 + 4H_2 = CH_4 + 2H_2O$$

Most microbial methane is generated in shallow aquifers while thermogenic methane is found in deep formations exceeding 3000 feet[54] due to the elevated temperature and pressure required. Therefore, the occurrence of thermogenic methane in groundwater can be indicative of upward migration of methane from deeper sections of the earth's crust. Rice and Ladwig[55] reported that Wattenberg field natural gas methane that came from greater depths (usually 6000-8000 feet deep), contained significant amounts of heavier hydrocarbons ($C_1/C_{1\text{-}5}$ values range from 0.83 to 0.87) and was isotopically heavier ($\delta\ ^{13}C\text{-}CH_4$ values range from -49 to -43 ‰). The chemical and isotopic composition of the gases indicated a thermogenic origin and were generated by thermal cracking processes during intermediate stages of thermal maturity in the deeper part of the Denver basin, consistent with the level of maturation determined by source rock studies.

Stable carbon and hydrogen isotope test results were plotted in Figure 1 to define the various sources of CH_4 and all the data points could be divided into two classifications, thermogenic and microbial, using a CD-diagram[56]. Of the 60 samples in our study, most of the samples could be classified as microbial methane and only 3 samples from 2 well sites were characterized as thermogenic-origin in the early mature stage. Average "thermogenic" methane concentration was 3.5 mg/L and average methane concentration designated microbial in origin was 3.2 mg/L. Occurrence of microbial methane is ubiquitous accounting for over one fifth of the world's gas accumulations[57] and is influenced by vegetation and soil conditions, or other anthropogenic activities.[58]

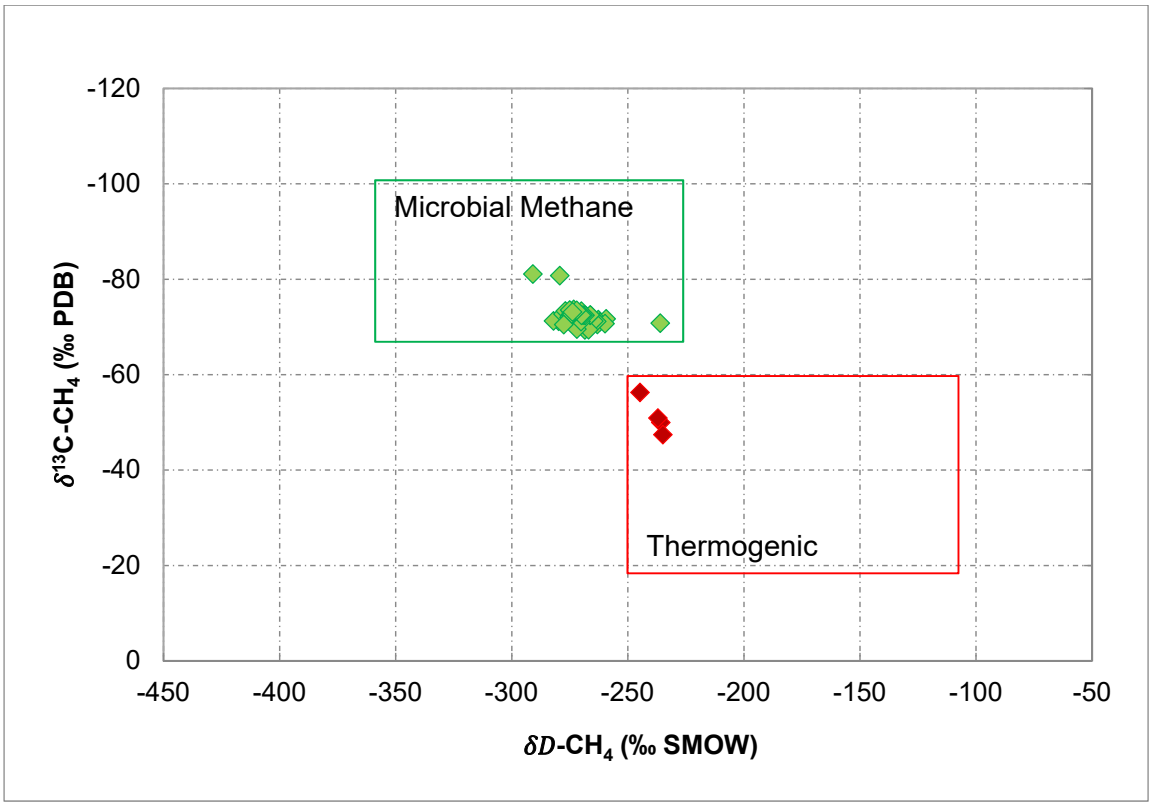

Figure 20. Carbon and hydrogen isotopic compositional ranges of methane from different sources [59]

$$*\delta^{13}C - CH_4 = \left[\frac{\left({}^{13C}/_{12C}\right)}{\left({}^{13C}/_{12C}\right)_{standard}} - 1\right] \times 10^3, \delta D - CH_4 = \left[\frac{({}^{D}/_{H})}{({}^{D}/_{H})_{standard}} - 1\right] \times 10^3$$

$*{}^{13C}/_{12C}$ is 0.0112372 for carbon standard as PDB and ${}^{D}/_{H}$ is 0.00015576 for hydrogen standard as SMOW as hydrogen standard[59]

A clear illustration of the different methane sources is shown in Figure 20, a comparison of isotopic characteristics (* listed definitions of $\delta\ {}^{13}C$ and δD) between dissolved methane found in aquifer wells (blue dots) and gas phase methane from natural gas production wells (red dots). Two distinct data point clusters are observed indicating that methane from the groundwater wells was formed with a different mechanism than methane from oil and gas wells. Samples from oil and gas wells were isotopically heavier than the samples from groundwater wells, implying thermogenic methane in origin. Oil/gas wells are much deeper than groundwater wells and produce methane by thermal cracking due to extremely high temperatures and abundant organic carbon sources during the early or intermediate thermal maturity

stages.[60] Microbial and thermogenic methane, with distinct isotopic characteristics, are separated by low-permeability formations between groundwater wells (up to 1000 feet (300 meter) deep) and oil/gas wells (average 6500 feet (1980 meter) deep).

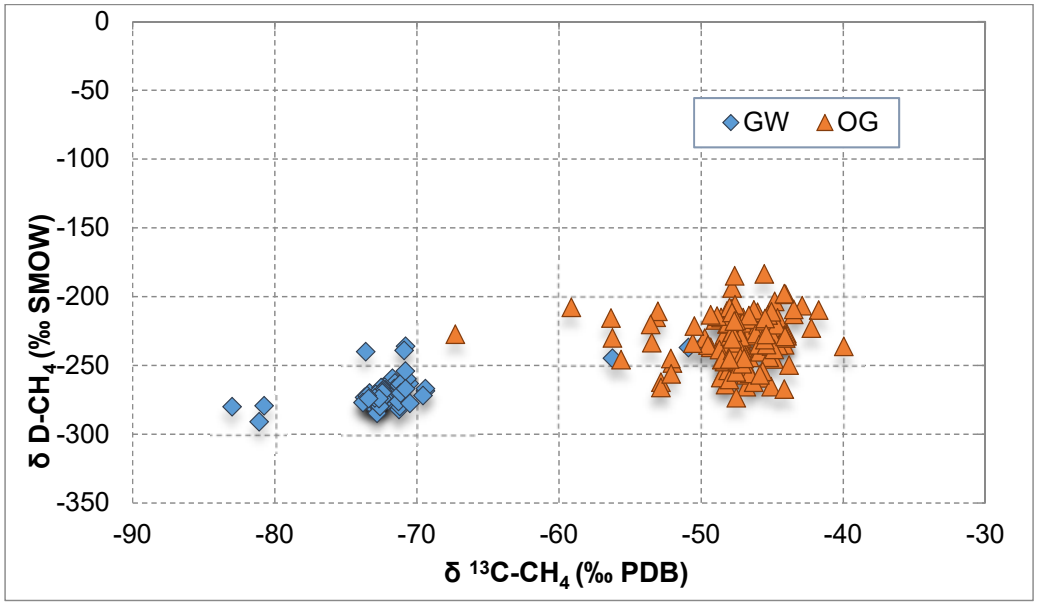

Figure 21. Plot of carbon and hydrogen isotopic results from groundwater well (blue) and gas from oil/gas well (red)

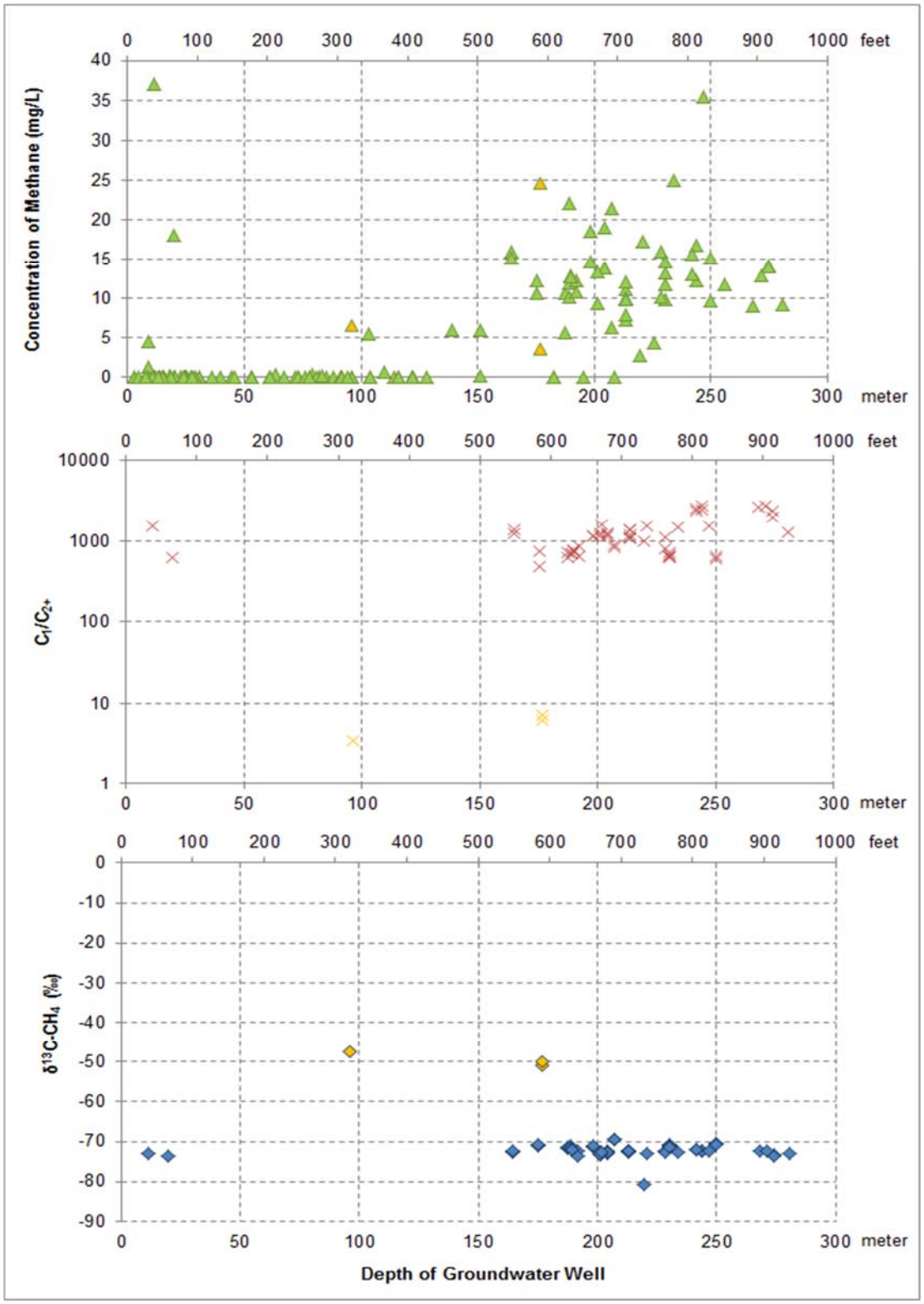

Figure 22. Plot of methane concentration, C1/C2+ and δ 13CH4 with well depth

Methane characteristics including concentration, C_1/C_{2+} and $\delta\ ^{13}CH_4$ are plotted versus groundwater well depth in Figure 21. None of the methane characteristics has a significant correlation with water well depth and concentration appears random. Figure 3b shows that most of the methane is considered "dry" or relatively devoid of C^{2+} compounds, another indication of a predominant biogenic origin[61]. In addition, most of the values of $\delta\ ^{13}CH_4$ below -60‰ (Figure 22 bottom plot) suggest a microbial methanogenesis process[62]. Figure 22 top plot shows the variation in the concentrations of dissolved methane in groundwater at different depths, that the methane concentration was low close to the surface (depth less than 150 meters) while methane began to increase in with depth. In groundwater with a low redox potential, anaerobic organisms such as *Methanogens* can produce methane. Jenden and Kaplan[62] observed that increasing depth could cause the change from fermentation to CO_2 reduction. Rich deposits of organic carbon in the shale formations not only provides large amount of hydrocarbons at greater depths but also favors anaerobic organisms to generate microbial methane in shallower formations. The presence of microbial methane coincident with deep natural gas deposits is a likely occurrence since the microorganisms could use the released energy with organic matter being oxidized to support their growth[63].

To investigate the impact of oil and gas activities in the Wattenberg field on aquifer well methane concentrations, well density was examined. The evolution of oil and gas well density was explored to understand if the increased occurrence of drilling through groundwater aquifers and shallow reservoirs of microbial methane could result in a higher occurrence of stray gas migrating around casing leading to contamination of drinking water. For water samples collected between January 2012 and August 2013, Figure 23 illustrates the distributions of methane concentration, methane of different origins (biogenic or thermogenic) and oil/gas well density. The well density was based on total wells drilled (wellbores were completed) in and before 2012 to account for potential delayed effects related to drilling activity. Because isotopic components are only measured if dissolved methane exceeded 1.0 mg/L, the number of data points with isotope results are less than shown in Figure 23-4a.

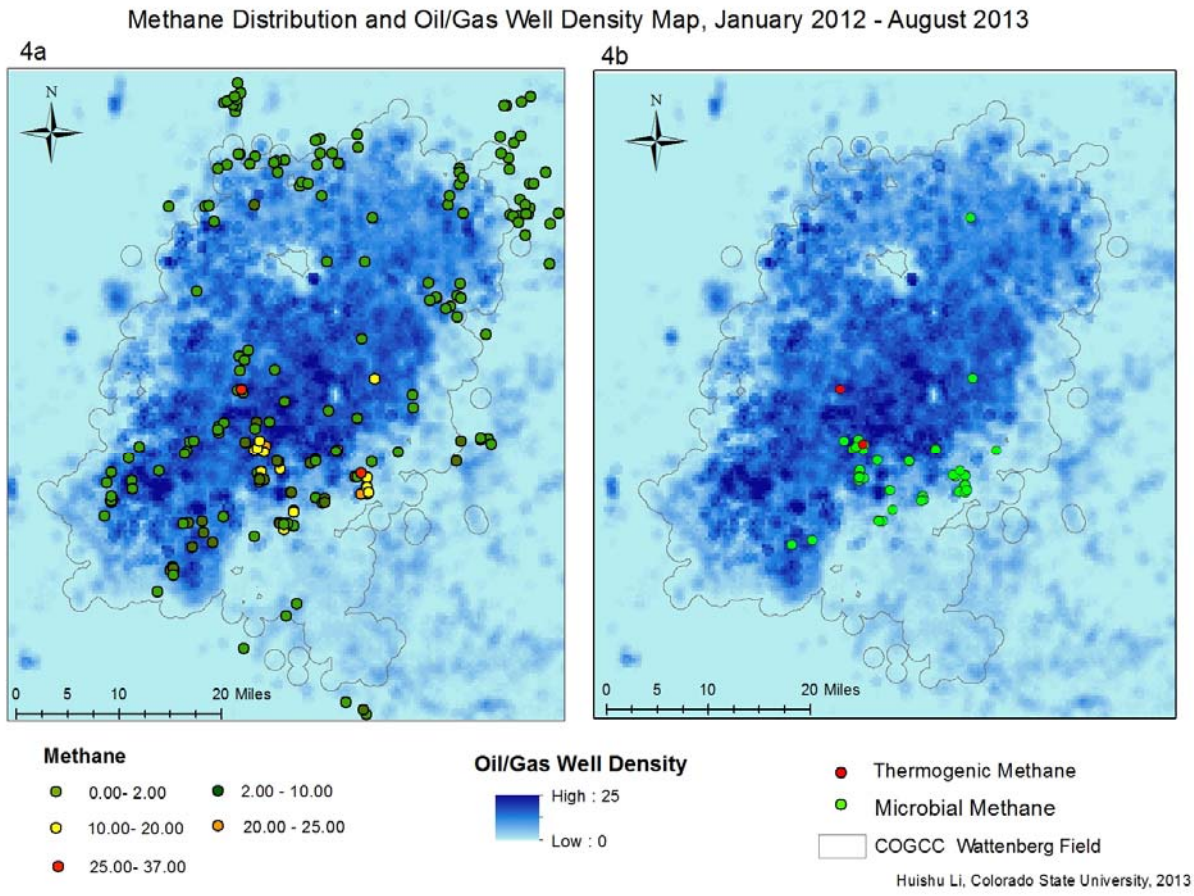

Figure 23. Location of COGCC groundwater wells in Wattenberg Field and distribution of dissolved methane in groundwater (from January 2012 to August 2013): 4a – water matrix showing methane concentrations, 4b – dissolved methane compositional analysis and isotopic results.

The average methane concentration was 4.0 mg/L ranging from 0 to 37.1 mg/L with a standard deviation of 6.6 mg/L. Over 20% of 166 samples had methane concentrations under the detection limit; 47% of the total samples had methane levels between 0 and 2 mg/L, and 2% of total sample points had methane in a range between 2 and 5 mg/L. Therefore, 70.5% of the overall samples had methane concentrations below 5 mg/L and only 2 out of 166 had values exceeding 25 mg/L (1.2%). As shown in Figure 23-4b, the two ground water wells that had "thermogenic" concentrations of methane were not located in the higher-density drilling areas.

Cumulative interpolation maps are shown in Figure 24 for both methane distribution and well density. Figure 24 shows the evolution of methane distribution and well density from 2006 to 2012 based on data provided by COGCC that included all wells drilled.

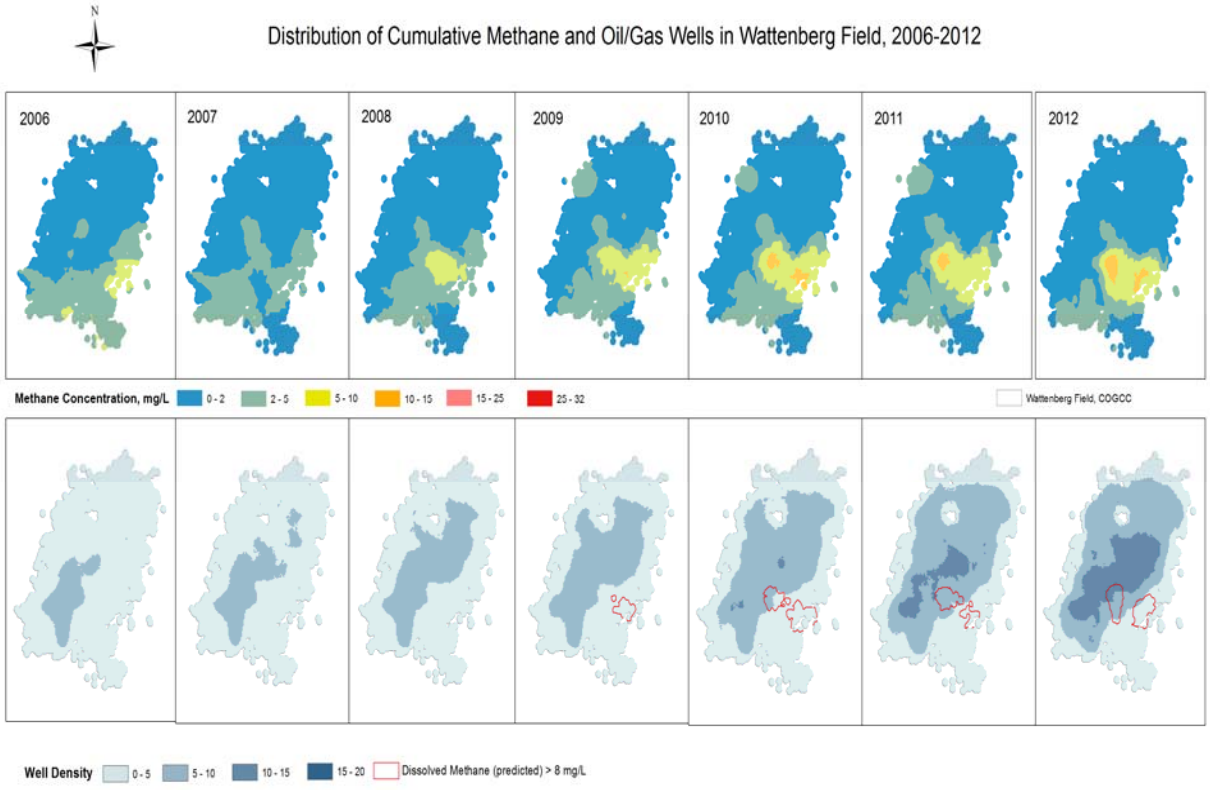

Figure 24. Distribution of methane and cumulative oil/gas well density in Wattenberg Field from 2006 to 2012 (well density was the number of oil/gas wells in a squared-kilometer)

Figure 24 shows spatial interpolation maps of methane concentration and well density incorporating all of the valid data associated with predicted areas with methane concentration exceeding 8 mg/L through the designated year into the analysis. A key assumption is that methane measured in one year will remain at that concentration in subsequent years if no more observations were available, otherwise, the mean concentration would be used. Methane in the northern Wattenberg field stayed at a low level which might be due to sufficient sulfate content in the water preventing microbial reduction of carbonate to methane.[59, 64] Figure 5 illustrates the evolution of high methane areas (concentration of methane exceeded 8 mg/L), the

growth of oil and gas activities and the overlap of the high density areas. For the year 2008, the area with methane concentrations of 2-5 mg/L expanded in the south and began to have a small region exhibiting methane above 10 mg/L in the north edge of this 2-5 mg/L methane area. Locations of relatively high methane (above 10 mg/L) remained the same after 2008 but expanded slightly from 2008 to 2012. In contrast, methane in the northern Wattenberg field remained at a low level, distinct from areas to the south. The reason for this could be explained by methane or groundwater transport and heterogeneity of geological structure.

Potential transfers of methane involved two different migration mechanisms in the unsaturated and saturated zones. In the saturated zone, most of the methane would dissolve in water and transfer with groundwater flow; while in the unsaturated zone, methane partitions into three compartments, methane gas, dissolved methane and sorbed methane on the soil surface.[65] Methane will preferentially dissolve in the water instead of partitioning to gas or solid phases when below saturation concentrations.[66]

The groundwater wells in the Wattenberg field for this analysis were located in the Laramie-Fox Hills aquifer[67] (SI figure 1 illustrates the geology and flow direction in the subsurface)[68]. Two opposite flow directions form in the north and south Wattenberg field due to an uplifting of the aquifer in the north part of the basin. This flow direction prevents the groundwater flow from south to north and along with the shallower buried depth of the aquifer contributes to the relative absence of dissolved methane in the northern section of the Wattenberg field. The lack of an available carbon source and/or the presence of higher redox conditions (higher sulfate concentrations) could also contribute to the lower incidence of elevated dissolved methane concentrations.

Table 3. Overlap between high methane areas (above 8 mg/L) and areas of different well densities for each year from 2006 to 2012

Year	Well Density (numbers of wells within 500 meter radius area)			
	0-5	5-10	10-15	15-20
2006	87%	13%	0	0
2008	97%	3%	0	0
2009	99%	1%	0	0

2010	87%	13%	0%	0
2011	45%	50%	5%	0
2012	49%	27%	24%	0

The area (km^2) and fraction (%) of the high methane areas (above 8 mg/L) in Figure 24 (bottom plot) that overlap with the different well density areas is shown Table 3. Even in the latest year for which data was analyzed (2012), there is no overlap between the highest well density areas (15-20 wells within 500 meters) and the high methane areas. The lack of overlap between the two high-density areas may indicate the absence of a correlation between oil and gas well drilling and the occurrence of microbial methane. There does appear to be an increase in the overlap of the 10-15 wells within the 500 m density and the high methane concentration, but this is accompanied by a reduction in overlap with lower density areas (111 km^2 in 2010, 91 km^2 in 2012).

Plots of methane concentration versus the number of oil/gas wells within 500 and 1000 meters are shown in Figure 25 for the water samples collected in 2012 and 2013. The figures represent the total number of oil/gas wells (since January 2012) in a circle area centered at the COGCC groundwater well with 500m and 1000m radii, respectively. Methane concentration was randomly distributed with increasing of numbers of oil/gas wells and no obvious trend was observed.

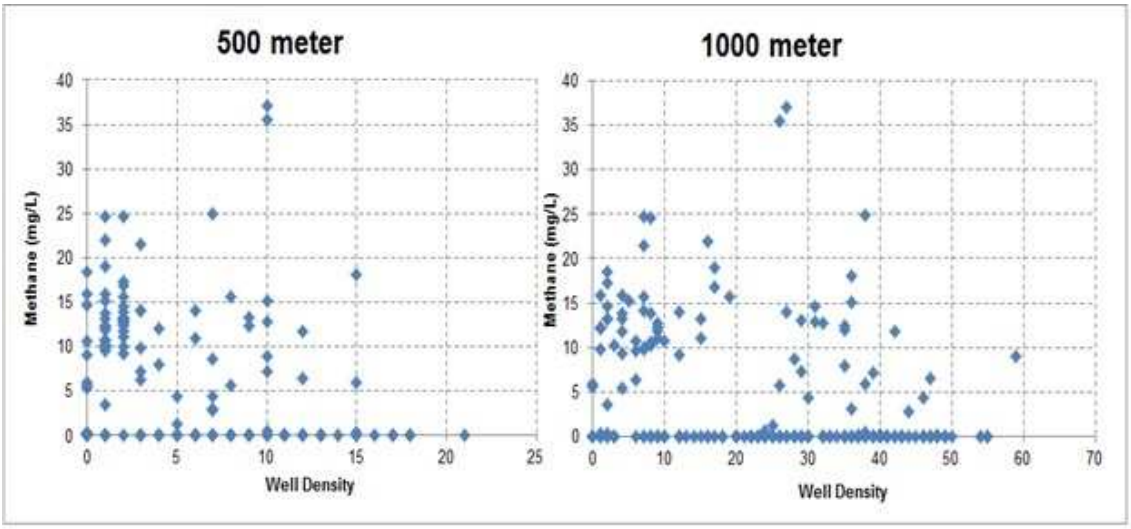

Figure 25. Histogram of methane in different well density areas for 500 meter and 1000 meter distances

For the 500-meter radius, there is an decrease of methane concentration when the number of oil/gas wells within 500 meters changed from 0-10 to 10-20 as the average methane concentration dropped from 5.8 mg/L to 2.5 mg/L (P=0.03). For a 1000-meter radius, there was no difference of methane concentration when the number of oil/gas wells changed from 0 to 40 (P=0.4483). In summary, increasing well density did not correspondingly increase the methane.

Distance from a groundwater well to the nearest oil/gas well is another factor used by Robert[69] and other studies to analyze the impact of oil and gas activities on methane. Since the Wattenberg field has been extensively developed over the past decades, there are high-density oil and gas producing areas at those distances. The majority of data points analyzed had distances to the nearest oil/gas wells less than 1,000 meters (96.59% from Table 4) and 84.66% of the total 223 data points within 500 meters. Only 6 out of 223 samples (3.4%) were greater than 1,000 meters away from an oil and/or gas well. Since 150 feet was minimum setback from an oil/gas well to a building (Rule 604)[70], few sampling wells were located within this limit.

Table 4. Frequency distribution of sample sites by distance

Distance (m)	0-100	100-200	200-300	300-400	400-500	500-1000	1000-
Frequency	8	52	42	30	17	21	6
Cumulative%	4.55%	34.09%	57.95%	75%	84.66%	96.59%	100%

Distance to the nearest oil and gas well was also used in our study to understand the contributing factors to methane occurrence in the Wattenberg field. Data were grouped by distance and average methane concentrations for each group and are shown in Figure 8. Methane concentration did not correlate with distance although the occurrence of methane levels above 5 mg/L appeared to decrease at distances greater than 700 meters. The highest mean methane concentration (6.51 mg/L) occurred in groundwater wells between 100 to 200 meters from oil and gas wells, and 42.2% of the wells in this range had methane greater

than 8 mg/L. The groundwater wells having oil/gas wells between 0-100 meters had a mean concentration of methane (4.0 mg/L) lower than within the 100-200 meters range, without a statistical difference p=0.3073. The methane concentrations did not change significantly when the distance decreased from 500 to 200 meters (t-test results shown in Table 5 by comparison of concentrations of methane grouped by distance).

Table 5. Statistical analysis results (P value) of differences of methane concentration classified by distance

P (t-test)	Distance to nearest oil/gas well (meters)					
	0-100	100-200	200-300	300-400	400-500	500-1000
100-200	0.3073					
200-300	0.5694	0.0014				
300-400	0.9485	0.0874	0.4396			
400-500	0.6667	0.0220	0.8625	0.6048		
500-1000	0.3873	0.0008	0.5571	0.2309	0.5208	
1000-	0.1077	2.81e-11	0.0045	0.0065	0.0393	0.0962

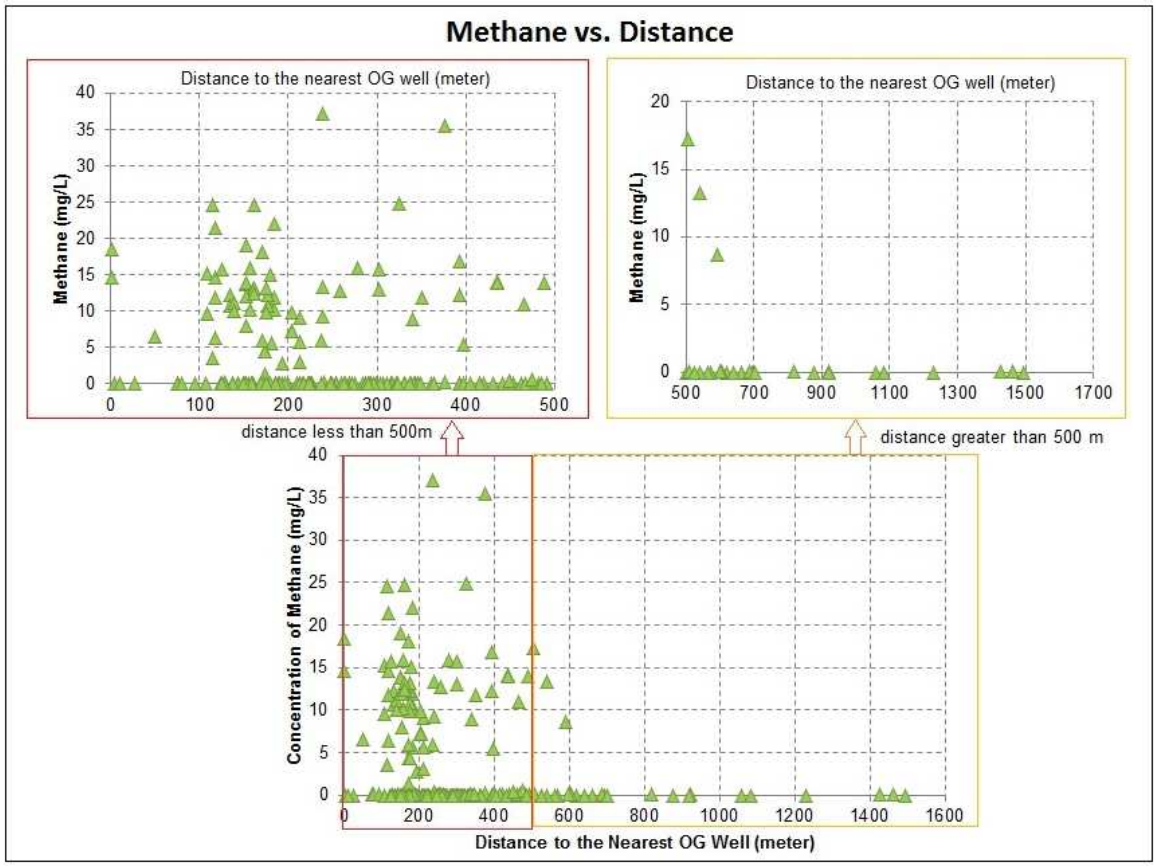

Figure 26. Plot of methane concentration versus distances to the nearest OG (oil/gas) well

Figure 26 shows $\delta^{13}C\text{-}CH_4$ and ratio of C_1 to C_{2+} plotted versus distances to the nearest oil and gas wells. Methane sources (biogenic versus thermogenic) can be estimated based on only have isotopic carbon component ($\delta^{13}C$). An isotopic signature of $\delta^{13}C\text{-}CH_4 \geq$ -40‰ (reference to Vienna Pee Dee Belemnite standard[71]) generally suggests a thermogenic origin for methane, whereas $\delta^{13}C\text{-}CH_4 \leq$ -60‰ indicates a microbial derived methane source. $\delta^{13}C\text{-}CH_4$ falling in between -40 and -60 ‰ refers to a mixed or transition status.[44]

Neither $\delta^{13}C\text{-}CH_4$ nor gas dryness (ratio of C_1 to C_{2+}) appeared to correlate with the distances to the nearest oil/gas well. These results coupled with observations from Figure 26 indicated that distance from nearest oil and gas wells does not have an obvious effect on the methane concentration or methane source. However, in both Figure 26 and 27, there are fewer data points within 100 m of an oil and gas well, potentially due to regulated setback distances. Since thermogenic methane would be expected to have a low C_1/C_{2+}, the three points with a ratio less than 10 in Figure 27-9b being closer to the water well may be an expected observation.

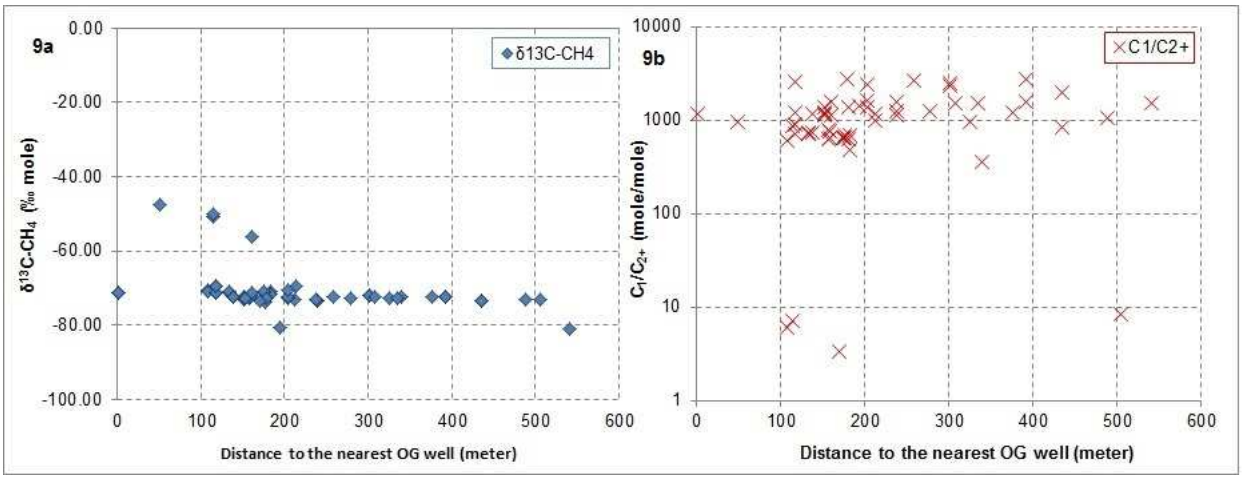

Figure 27. Plot of distances vs. δ13-CH4 and C1/C2+

Methane is pervasive in groundwater wells in the Wattenberg field with widely varying concentrations. Greater than 99% of dissolved methane measurements appear to have been generated from microbial processes and the concentration and occurrence increased with increasing water well depth. The results of

the study did not indicate systematic contamination of aquifers with methane due to oil and gas activities in the Wattenberg field and elevated methane levels do not appear to be the result of increased drilling and fracturing. More likely, increased methane occurrence is due to aquifer utilization in areas with abundant sources of naturally occurring biogenic methane.

Chapter 5 Concurrence of aqueous and gas phase contamination of groundwater in the Wattenberg oil and gas field of northern Colorado[2]

Overview

The potential impact of rapid development of unconventional oil and natural gas resources using hydraulic fracturing and horizontal drilling on regional groundwater quality has received significant attention. Major concerns are methane or hydrocarbon leaks into the aquifer due to the failure of casing and/or stray gas migration. Previously, we investigated the relationship between oil and gas activity and dissolved methane concentration in a drinking water aquifer with the major finding being the presence of thermogenic methane contamination, but did not find detectable concentrations of hydrocarbons. To understand if aqueous and gas phases from the producing formation were transported concurrently to drinking water aquifers without the presence of hydrocarbons, the ionic composition of three water groups was studied: (1) uncontaminated deep confined aquifer, (2) suspected contaminated groundwater - deep confined aquifer containing thermogenic methane, and (3) produced water from nearby oil and gas wells that would represent aqueous phase contamin[2]ants. On the basis of quantitative and spatial analysis, we identified that the "thermogenic methane contaminated" groundwater did not have similarities to produced water in terms of ionic character (e.g. Cl/TDS ratio), but rather to the "uncontaminated" groundwater. The analysis indicates that aquifer wells with demonstrated gas phase contamination have not been contacted by an aqueous phase from oil and gas operations. The results may provide insight on contamination mechanisms since improperly sealed well casing may result in stray gas but not aqueous phase transport.

5.1 Introduction

Groundwater quality can be influenced by natural conditions such as topography, aquifer lithology, and by human activities[72] such as disturbances from oil and gas drilling and production activities.[73] The four most probable fluid transport mechanisms from deeper hydrocarbon formations to groundwater and

[2] Published in Water Research, January 2016; 88, 458-466

aquifers are: 1) vertical and lateral gas migration along natural geologic fractures and faults; 2) stray gas migration through unsealed or improperly sealed oil and gas production wellbores; 3) gas and aqueous phase migration through casing breaches and failure; and 4) percolation from surface spills of produced water the water produced from oil and gas extraction and a mixture of shale formation water and fracture fluids.[74]

The first two pathways are likely to be combined together and create a cross transport mechanism: gas leaked from an improperly sealed wellbore migrates through natural geological structures into groundwater or the aquifer.[75] Although fluid migration can occur naturally along preexisting natural faults and fractures over geological time scales (e.g. millions of years), [76] [77] the impermeable formations overlain and underlain by the Laramie-Fox Hills aquifer in northeast Colorado make the natural migration mechanism itself less likely to occur. In addition, since the aquifer is confined, percolation from surface spills in the Wattenberg oil and gas field of the Denver-Julesburg (D-J) Basin in Colorado are not likely to contaminate the aquifer.

Oil and gas wells in the D-J Basin are about 1.83-2.44 kilometers deep into sandstone or Niobrara shale while the depth of Laramie-Fox Hills aquifer ranges about 0.06-0.18 km.[78] Laramie-Fox Hills aquifer is a deep confined bedrock aquifer in between Laramie confining layer (top) that is up to 0.12 kilometers thick and the Pierre confining layer (bottom) that is up to 2.44 kilometers thick.[79]

Therefore, the most likely fluid transport mechanism to the aquifer is either produced water leaking through corrupted casing or gas migration up from the producing formation along a poorly sealed wellbore, or both. In general, the lack of well integrity, primarily faulty oil and gas well casing, is considered the most conceivable path of gas fluid migration.[80] [81] [82] Casing failure can also allow aqueous (e.g. produced water) and non-aqueous phase liquids (NAPLs) to travel from the producing oil and gas wellbore into the aquifer which lays a few kilometers above the producing formation.[83]

Oil and gas production wells in the U.S. are typically constructed according to the well construction guidelines published by the American Petroleum Institute (API).[84] The casing of either vertical or horizontal oil and gas wells are structured with multiple steel pipe layers generally four layers: conductor casing, surface casing, intermediate casing, and production casing with cement sheaths around the casings in order

to isolate hydrocarbon producing formations from aquifers by preventing hydraulic connectivity between them (Supporting Information (SI), Fig. A.1).

Colorado is one of the biggest oil and gas producing states, ranked 6th in natural gas production (45.4 km3) and 7th in oil production (0.01 km3) in 2013.[85] In 2008, The Colorado Oil and Gas Conservation Commission (COGCC), the regulatory agency in Colorado, completed a series of regulations of wellbore integrity for new oil and gas wells to protect groundwater and aquifers. For instance, COGCC Rule 317 ensures that surface casing runs at least 15 meters (50 ft) below the depth of the deepest aquifer for well control and aquifer protection, and also ensures that production casing is cemented above all production zones to create a hydraulic seal.[86]

Although the COGCC regulates wellbore integrity and continuously performs intensive inspections of oil and gas production wells, there is still a risk of faulty casing strings or cementing along wellbores.

Two possible transport mechanisms for two different fluid types: gas and aqueous phases into the confined bedrock aquifers in a unique circumstance of the D-J Basin are illustrated in Figure 28.

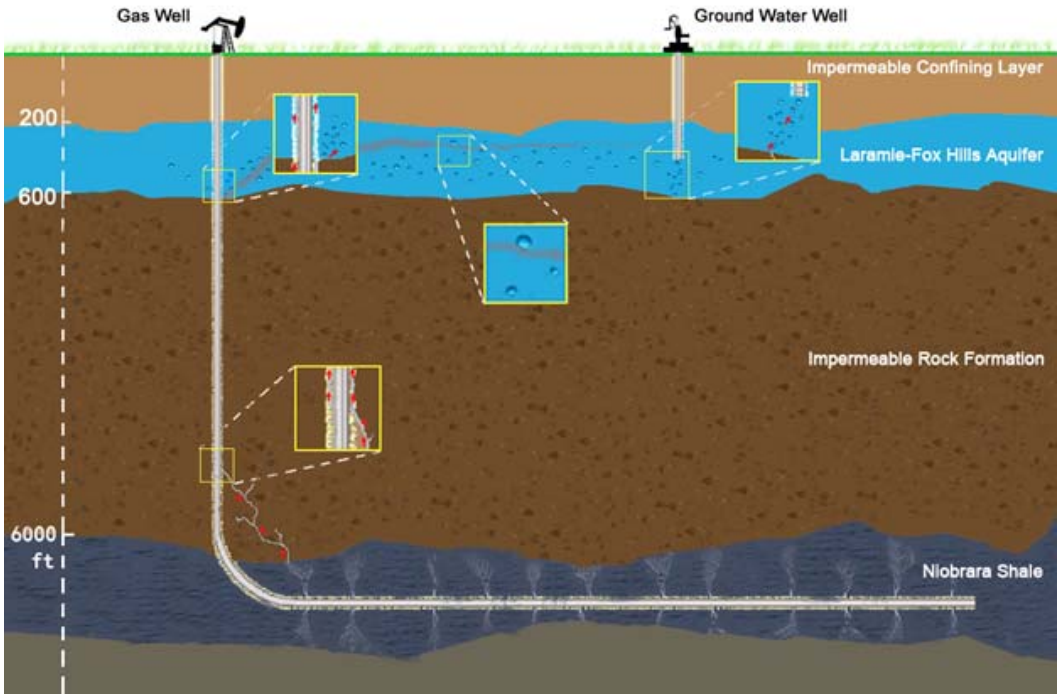

Figure 28. Simplified schematic of migration pathways of potential groundwater contaminants (aqueous and gas phase) by an adjacent oil/gas well

Gases are transported through the subsurface more efficiently and quickly compared to the aqueous phase. Stray gases including thermogenic methane gas can escape from producing wells though circumferential fractures and unsealed or improperly sealed casing strings along the wellbore (Figure 28-A)[87], leading the methane gas to leak into the aquifer.

Another pathway for fluid migration is casing breaches or leakages (Figure 28-B). Casing breaches allow gas migration as well as migration of aqueous phase contaminant of produced water into aquifer, but the risk of aqueous phase contamination varies depending on production pressure.[88] The leaked gas or aqueous phase contaminants will flow out through groundwater [89] [90]and eventually contaminate the drinking water well.

Previously, we investigated a relationship between oil and gas activity and dissolved methane concentration in the drinking water aquifer and found a relatively low level (<2% of 223 water samples) of thermogenic methane contamination in the area.[91] Although the previous study did not find detectable concentrations of hydrocarbons in the aquifer samples containing thermogenic methane, there is still a possibility that the aquifer samples containing thermogenic methane were also contaminated by the aqueous phase of produced water.

Therefore, it is important to understand the ionic composition of the aquifer containing thermogenic methane to determine if aqueous phase contaminants were transported into the aquifer concurrently with the gas phase contaminant. The ionic composition organic and inorganic characteristics of the water co-produced with oil and gas is expected to be significantly different from those of confined bedrock aquifers.[92]

Three groups of water studied here are: (1) uncontaminated deep confined aquifer (not containing thermogenic methane gas nor hydrocarbon; GW), (2) deep confined aquifer containing thermogenic methane (THGW), and (3) produced water (PW) from nearby horizontal oil and gas wells, that would represent aqueous phase contaminants.

The objective of this study is (1) to distinguish ionic compositions of three different water groups in Wattenberg Field, an area highly developed in oil and gas production activities, and (2) to identify whether the aquifer wells contaminated by thermogenic methane (2nd water group) was also influenced by aqueous

phase contaminants (3rd water group) without the presence of hydrocarbon by comparing ionic compositions of each water group.

Occurrence of produced water features in the confined bedrock aquifer might indicate that a hydraulic connectivity existed between the producing zone and aquifer, (Warner et al., 2012) which is more likely due to a casing breach. The presence of thermogenic gas without aqueous phase contaminants in the aquifer might suggest that stray gas migration along a poorly sealed wellbore is the likely mechanism.

5.2 Materials and Methods

5.2.1 Origin of Data

Detailed water quality data from 672 groundwater samples taken in Wattenberg Field of D-J Basin were obtained from the COGCC GIS-online website.[93] 514 produced water samples were collected from horizontal oil and gas production wells in the D-J Basin and measured by the Center for Energy Water Sustainability lab at Colorado State University (CSU) during the 2012-2013 period following standard water quality guidelines.[94]

Chemical parameters measured in this study included hydrogen ion concentration (pH), total dissolved solids (TDS), sodium, potassium, magnesium, calcium, barium, strontium, boron, iron, bicarbonate/carbonate, sulfate and chloride. Isotope data were used to identify the "thermogenic methane contaminated groundwater wells" from where the samples had been suspected of containing dissolved thermogenic methane. Samples considered to have thermogenic methane generally had delta ^{13}C of CH_4 greater than -50‰ and delta D of CH_4 greater than -250‰.[95] The data and analyses used for this study are shown in SI, Table B. 1.

5.2.2 Study Area: Laramie-Fox Hills Aquifer and Wattenberg Field

Water wells in our study area were completed in the sandstone and siltstone Laramie-Fox Hills aquifer. The upper Laramie-Fox Hills aquifer is comprised of sandstone from the lower Laramie formation, and the lower part of the aquifer consists of the Fox Hills formation.[96] Both the Laramie formation and Fox Hills formation in our study area contain carbonaceous shale, sandstone and lignitic coal seams.[97]

Historically, water in the Laramie-Fox Hills aquifer usually is classified as sodium-bicarbonate type water. High TDS water appeared in the northern and eastern margin of Laramie-Fox Hills aquifer since the groundwater flows toward the northeast and soluble minerals were transported by groundwater into those areas.[98] Iron, which is naturally insoluble compared with other minerals, is dissolved in water in Laramie-Fox Hills aquifer due to a reducing environment in bedrock of Laramie-Fox Hills aquifer rich in electron donating organic matter.

The Laramie-Fox Hills aquifer has three characteristic types: (1) $NaHCO_3$, groundwater influenced by limestone, (2) $CaSO_4$, groundwater influenced by gypsum formations and (3) NaCl, typical of marine or deep, ancient water.[99]

The Wattenberg Field is a highly developed oil and gas area located in the D-J Basin[100] and one of the largest natural gas deposits in the United States that has been the site of conventional production for over forty years. It recently became known for natural gas extraction and production[103] that produced 7.96 km^3 of natural gas and 0.007 km^3 of oil in 2013.[90]

Most of the oil and gas wells drilled in the Wattenberg Field before 2011 were vertical wells and horizontal well drilling dominated in 2012 and after.[101]

5.2.3 Data Treatment and Multivariate Statistical Methods

The objective of this study is to determine if eight aquifer wells with multiple measurements containing thermogenic methane gas show inorganic chemical characteristics of produced water or fall completely within the water quality distributions of the surrounding aquifer.

Graphical data plots and statistical analyses are used to depict the water quality characteristics from two different sources, Laramie-Fox Hills aquifer and produced water. Charge balances were calculated as the data quality control criteria and all sample analyses were within an acceptable limit, ±10%.

Quantitative analyses were performed on the geochemical data of the Laramie-Fox Hills aquifer and Wattenberg Field produced water using graphical representations to identify the different water chemistry.

5.3 Results and Discussion

A statistical summary of water quality of GW and PW is provided in SI, Table B. 2. In GW samples, *TDS* concentrations ranged from 36 mg/L to 13,900 mg/L with a mean concentration of 1,217 mg/L. They were statistically different from that of PW samples ($p<<0.01$) with a mean *TDS* concentration of 23,860 mg/L. The GW samples were moderately alkaline (mean pH 8.01) whereas the PW samples were mildly acidic (mean *pH* 6.77). The THGW samples were natural to mildly alkaline like GW samples and had *TDS* concentrations ranging between 370 and 3,500 mg/L.

Dissolved ion concentrations were significantly higher in PW than in GW ($p<<0.01$) except for manganese, boron, sulfate and carbonate. High concentrations of dissolved metals and ions in PW might be related to the acidic, high-temperature and high-pressure environment yielding more active cation exchange[102] and dissolution of formation rock.

Concentrations of sulfate and carbonate were low in PW and that allowed the presence of relatively high concentrations of barium and strontium. Sulfate is the most important control of barium solubility due to barite precipitation; high barium levels are usually only reported in water depleted in sulfate.[103]

Two-tailed t-tests were used in this study to compare characteristics of three water groups (GW, PW and THGW), and descriptive statistics, such as mean, median, and variance are shown in SI, Table B. 3.

The null hypothesis of the t-test was that two water groups in the comparing sets: GW—THGW and PW—THGW are from the same distribution. If the p value is greater than 0.01, the null hypothesis cannot be rejected, indicating the tested datasets are from same distributions at a significance level of $\alpha=0.01$.

The available 14 parameters: *pH, TDS,* Na^+, K^+, Ca^{2+}, Mg^{2+}, Cl^-, SO_4^{2-}, HCO_3^-, CO_3^{2-}, *Fe, Mn,* Ba^{2+}, and *B* (present in water as boric acid, $B(OH)_3$) from all three water groups were used for the test. Among the 14 parameters, 9 parameters (64%) indicated that PW and THGW were from statistically different distributions, and 12 parameters (86%) showed that GW and THGW were from the equivalent composition. Detailed t-test results are listed in SI, Table B. 3. Two parameters, *Ba* and *B*, did not reject the hypothesis that GW

and THGW were from different distributions, potentially due to the low concentration detected of *Ba* and *B* in all of the groundwater samples.

"Euclidean distance" was used to define similarities between GW and THGW, and PW and THGW. (Rajaraman and Ullman, 2012) Euclidean distances were calculated from each THGW point to all GW points and also to all PW points by the following equation,

$$d_n = \sqrt{\left(P1_n - P1_{n_{GW(PW)}}\right)^2 + \left(P2_n - P2_{nGW(PW)}\right)^2 + \left(P3_n - P3_{nGW(PW)}\right)^2 + \cdots + \left(P14_n - P14_{nGW(PW)}\right)^2}$$

n is the n^{th} datapoint of THGW ranging from 1 to 10; $n_{GW(PW)}$ is the n^{th} datapoint of GW or PW; *P1-P14* are the values of 14 parameters, *pH, TDS,* Na^+, K^+, Ca^{2+}, Mg^{2+}, Cl^-, SO_4^{2-}, HCO_3^-, CO_3^{2-}, *Fe, Mn,* Ba^{2+}, and *B.* Euclidean distances were distances between a THGW point to all GW or PW points in 14-dimensional space of the fourteen parameters. $d_{n\text{-}GW}$ is the distance from the THGW point to the closest point of GW points or PW points (detailed calculations are provided in SI, Table B. 4 - B. 5). After the minimum distance was calculated, we did the evaluation of the "closest points" to ensure they were able to represent the group which they were originally from to eliminate "outliers" by repeating the method above. If the "closest point" had the minimum distance closer to the other group than to the group it was originally from, then this point was deleted and we used the second minimum distance, and did the evaluation again until we found the "true minimum distance" which both had the closest distance to THGW point and also to the other points in its group. Because the datasets of both GW and PW vary greatly, using average values was avoided to represent Euclidean distance but the minimum values are shown in Table 1.

Table 6. Minimum Euclidean distance from THGW points to GW (GW_THGW) and to PW (PW_THGW).

THGWs	Min. Euclidean Distance		Relative Comparison
	THGW_GW	THGW_PW	(THGW_GW)/(THGW_PW)*100
THGW-1	340	751	45%
THGW-2	138	773	18%
THGW-3	81	172	47%
THGW-4	98	262	37%

THGW-5	72	371	19%
THGW-6	68	325	21%
THGW-7	154	218	72%
THGW-8	315	2099	15%
THGW-9	282	1526	18%
THGW-10	12	263	5%

A smaller minimum Euclidean distance would represent a better similarity between two tested groups. As shown in Table 1, 10 out of the ten points of THGW were closer to GW than to PW, indicating that all the THGW data points have a better similarity to GW in terms of the 6 ratios representing the major ionic components in water.

Sodium and calcium ion exchange occurs differently in saline water (PW) and fresh water (GW). Water abundant in calcium typically indicates a large proportion of fresh water, and enrichment in sodium implies more saline water than fresh water. (Appelo and Postma, 1994) Major ion concentrations of three water groups: GW, PW and THGW were plotted using piper diagrams— one of the most efficient ways to characterize and compare water quality— as separate points in each of the three zones (Fig. 2).

Within 672 GW datasets, 379 datasets had all cation and anion concentrations required for ionic characterization. In addition, 63 GW samples were classified as “high biogenic methane (GW-Bio High” since the biogenic methane concentrations for those water samples were greater than 10 mg/L, and 316 GW samples that have biogenic methane concentrations lower than 10 mg/L were classified as “low biogenic methane (GW-Bio Low)”. 15 datasets from 8 water wells showed thermogenic methane concentrations ranging from 0 (or under detection limit, 0.008mg/L) to 24.6 mg/L based on the isotopic characteristics, but only 10 samples had complete ionic composition data.

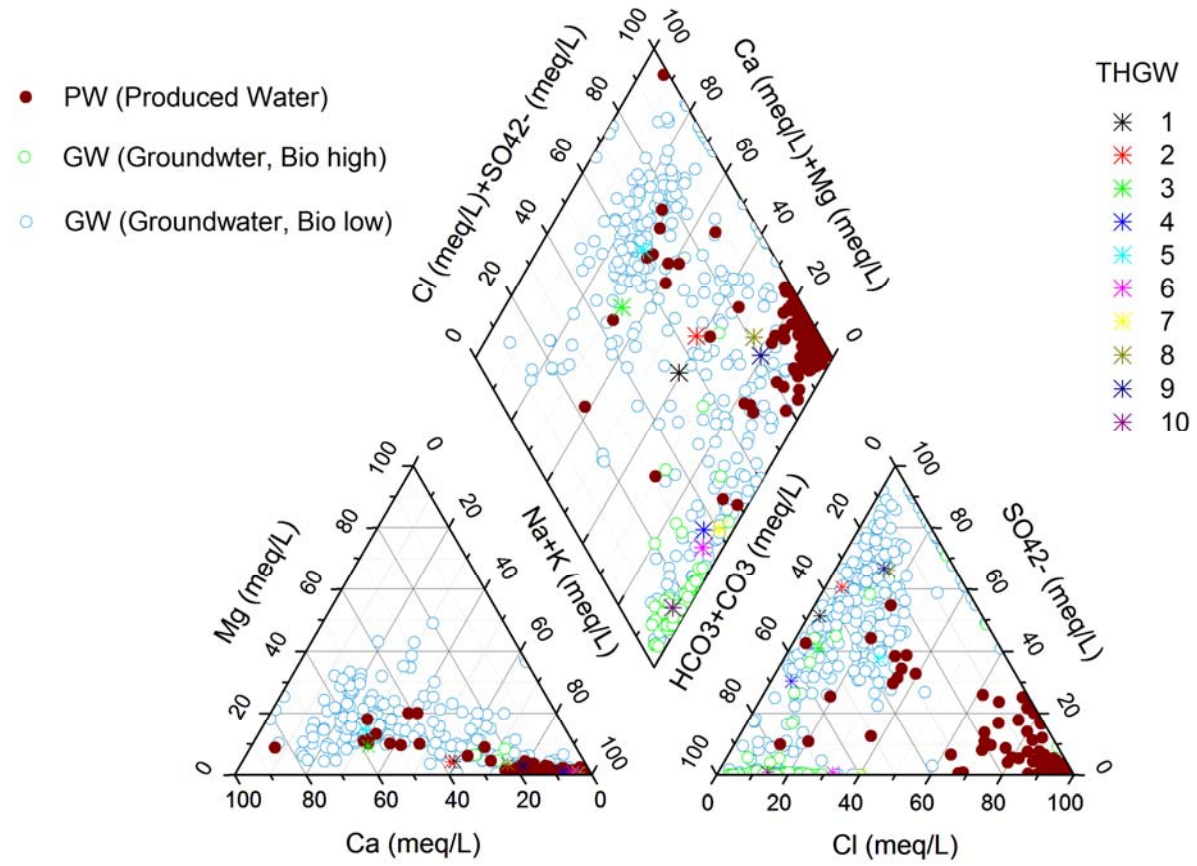

Figure 29. Piper diagram showing the chemical characteristics of uncontaminated groundwater (GW) containing high biogenic methane concentrations (Bio High) and low biogenic methane concentrations (Bio Low), produced water (PW) and groundwater containing thermogenic methane (THGW); Two trilinear diagrams represent anions (on the lower right) and cations (on the lower left) and the central quadrilateral represents the combination; Ions are expressed as percentages of total in milliequivalents per liter.[104]

PW samples from oil and gas wells showed a distinctive ionic characteristic compared to GW samples. PW samples were sodium and chloride type meaning they were dominated by sodium as the major cation and chloride as the primary anion.[105]

On the other hand, GW-Bio Low samples had significantly higher concentrations of sulfate ($p<<0.01$) and proportions of multivalent cations (percentage of $([Ca]+[Mg])/(\sum[major\ cations])$) ($p<<0.01$) and lower chloride concentrations. GW-Bio Low samples did not show any typical type of ionic characteristic

but tend to be calcium and sulfate type. GW-Bio High samples, however, appeared as a sodium and bicarbonate type and had lower sulfate and multivalent cation concentrations.

THGW samples were generally higher in sodium concentrations—a sodium type like PW and GW-High Bio samples—and lower in chloride concentration but did not show any type of anion characteristic.

Similar to Figure 29, the inorganic chemistry of GW and PW is characterized in Fig. 3 by introducing two perpendicular axes to offer a more concise and visual description of different types of water. The x-axis represents the relative significance of monovalent (Na^+ and K^+) versus divalent (Ca^{2+} and Mg^{2+}) major cations and the y-axis represents the majority of anions, either strong bases (SO_4^{2-} and Cl^-) or weak bases (HCO_3^-)[106] calculated by the equations below.

$$x = \frac{Ca^{2+}+Mg^{2+}-(Na^{+}+K^{+})}{Ca^{2+}+Mg^{2+}+(Na^{+}+K^{+})} \text{ in meq/L; } y = \frac{HCO_3^{-}+CO_3^{2-}-(SO_4^{2-}+Cl^{-})}{HCO_3^{-}+CO_3^{2-}+(SO_4^{2-}+Cl^{-})} \text{ in meq/L}$$

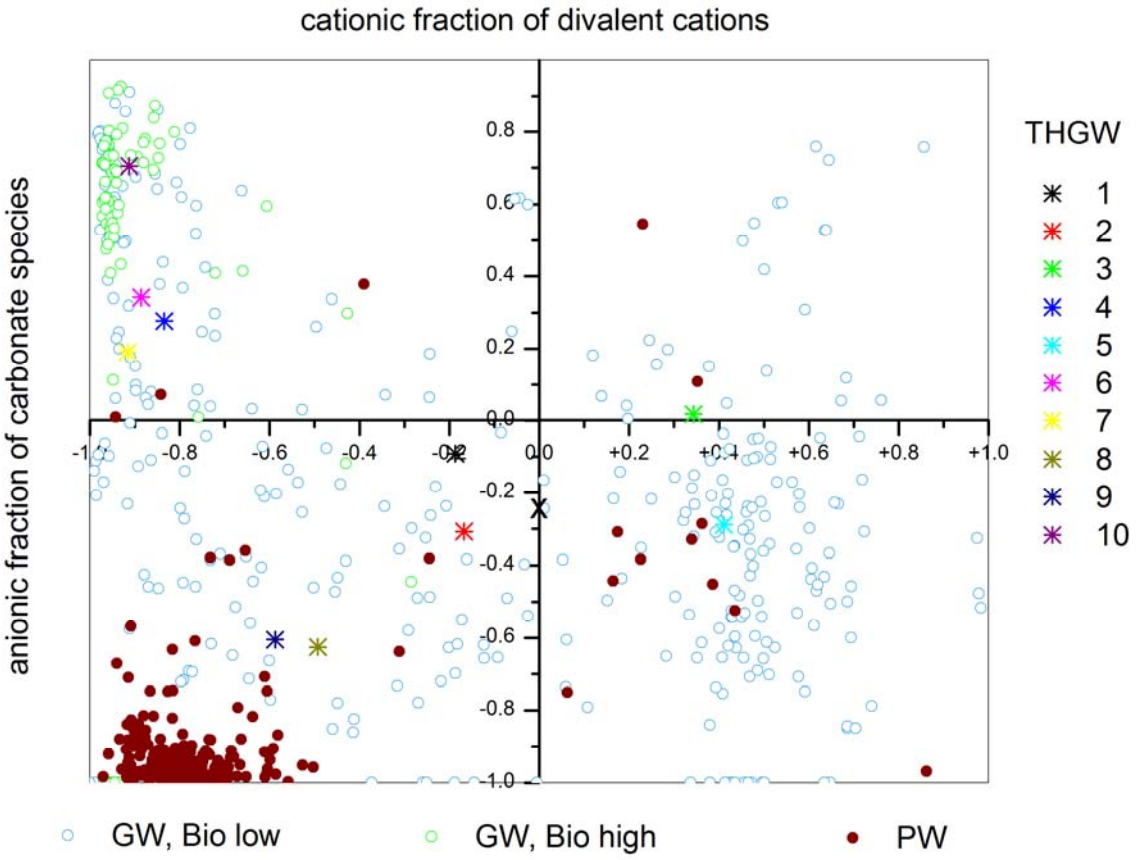

Figure 30. Inorganic characterization of GW-Bio high, GW-Bio low, THGW, and PW; X-axis is relative concentration of divalent versus monovalent cations and Y-axis is relative concentration of weak and strong conjugate bases.

As shown in Figure 30, PW was located completely in the lower left zone ($x<0$ and $y<0$) indicating low concentrations of divalent cations and weak bases, (Robson and Andrew, 1981) but high levels of monovalent cations and strong bases. PW has a distinct ionic "signature" because produced water had a large proportion of deep formation water[107] that is depleted in sulfate, likely due to the precipitation of barium sulfate.[108]

GW-Low Bio samples showed a large variation in ionic characteristics dispersed in all four zones divided by $x=0$ and $y=0$, and ten THGW samples were distributed among the GW sample points and did not indicate the same patterns of ionic character in PW.

However, the GW-High Bio samples had a higher fraction of monovalent cations and weak bases as shown above. Among the GW-High Bio data points, the ratios of HCO_3^-/CO_3^{2-} were all above 10, indicating bicarbonate as the major anion component. Because methanogens convert organic compounds to methane and carbon dioxide the presence of biogenic methane can cause increases in total carbonate concentration and thus higher concentrations of bicarbonate and carbonate in GW-High Bio samples.

$(Ca+Mg)/HCO_3^-$ approximately equaled to 1 indicating the source of *Ca, Mg* and HCO_3^- is mainly due to the dissolution of carbonate minerals. High ratio of $(Ca+Mg)/HCO_3^-$ represents additional sources of *Ca* and *Mg*; and low ratio suggests ion exchanges from *Ca* and *Mg* to *Na* or HCO_3^- origins from silicate weathering.[109] Therefore, the higher concentration of carbonate species could result in the balance of cations being tipped toward monovalent sodium and potassium.[110] Since the section of Laramie-Fox Hills aquifer in the study area comprises biogenic sedimentary rocks such as coal in reducing conditions, the oxidation of iron can reduce the pH resulting in a higher fraction of bicarbonate relative to carbonate.

Subsurface water from different sources, shallow aquifer (GW) or deep formation (PW), could also be characterized by distinguishable chemistry or isotopic characteristics because of different rock-water

interactions and oxidation-reduction reactions.[111] Absolute concentrations would vary widely but constituent ratios might only vary within a small range.

In our study, ionic ratios, such as *Na/Cl,* and $(HCO_3^- + CO_3^{2-})/SO_4^{2-}$, were used to explain the geochemical characteristics (Figure 31). The reason for using these constituents in order to identify possible water contamination by deep formation saline was because they were generally measured simultaneously.[112]

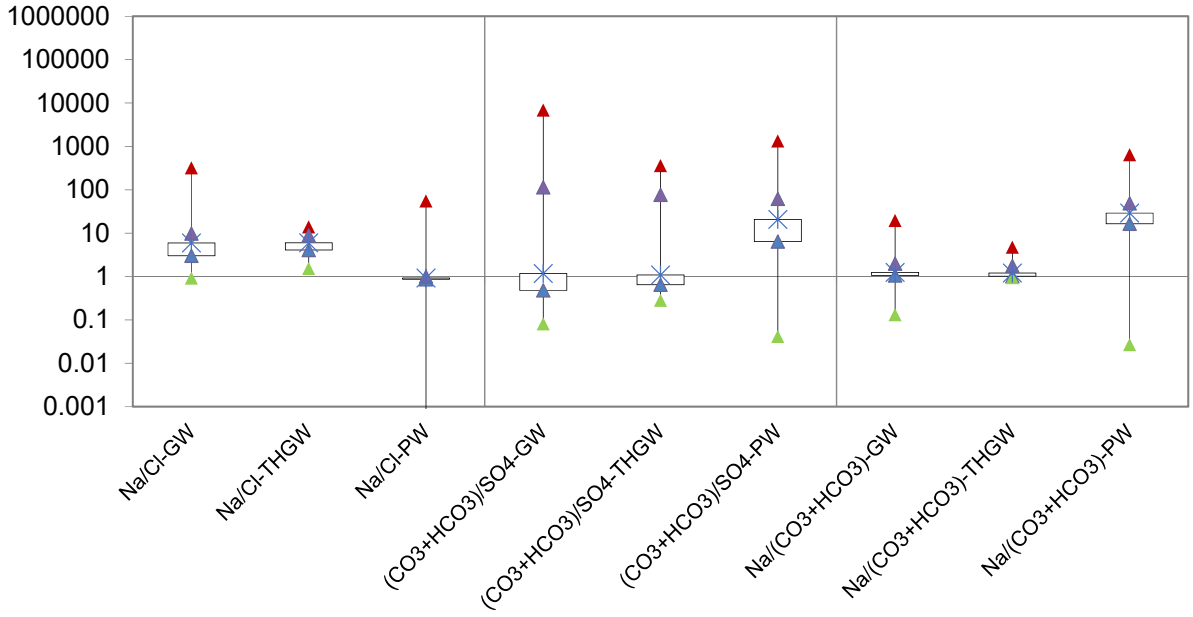

Figure 31. Summary of major ionic components and heavy metals for GW, PW and THGW using box plots on a logarithmic scale.

A higher proportion of dissolved sodium was observed in PW compared to GW. The majority of Na/Cl ratios in PW are equal to one indicating the dominant source of Na is halite dissolution. In contrast, the *Na/Cl* for most of the GW samples and THGW exceeds 1 indicating silicate weathering and anthropogenic activities might contribute to the excess of *Na*.[113]

A result of sulfate depletion in PW, represented by the lower ratio of $(HCO_3^- + CO_3^{2-})/SO_4^{2-}$, was consistent with the conclusions from the previous analyses. Of all the 10 THGW samples, 3 samples showed higher Na/SO_4, *Na/Cl* and $(HCO_3^- + CO_3^{2-})/SO_4^{2-}$ which were similar to that of PW. But none of the THGW

samples had $Na/(HCO_3^- + CO_3^{2-})$ higher than 5 which was much less than that in PW—the ratio in 90% of the PW samples was greater than 8.

Ratios of *Na/Cl* and $(HCO_3^- + CO_3^{2-})/SO_4^{2-}$ between PW and THGW samples were significantly different ($p<0.01$) but other tested ratios in Figure 31 were not statistically different. Mostly, the averaged major ionic composition of THGW samples was comparable to that of the GW samples.

If only a small amount of deep formation water transports to the shallow drinking water aquifer, the absolute concentrations in groundwater will not be affected and therefore could not be used to differentiate the sources of water. In our study, utilization of ionic ratios is evaluated as the aqueous signatures of different sources of water.

Due to its conservative nature in solution, chloride is the commonly used parameter to identify fresh water contaminated by saline water under the assumption that mixture of fresh water and formation water is the predominant pollution trend. Unlike chloride which is the conservative tracer from limited sources in groundwater[114] sodium and potassium can enter groundwater from the decomposition of sodium and potassium bearing rocks.

Among the ionic ratios we tested to differentiate GW and PW, the ratio of *Cl/TDS* was considered the best indicator, successfully separating GW from PW at a confidence level of 95%. A cumulative distribution plot of *Cl/TDS* is shown in figure 32.

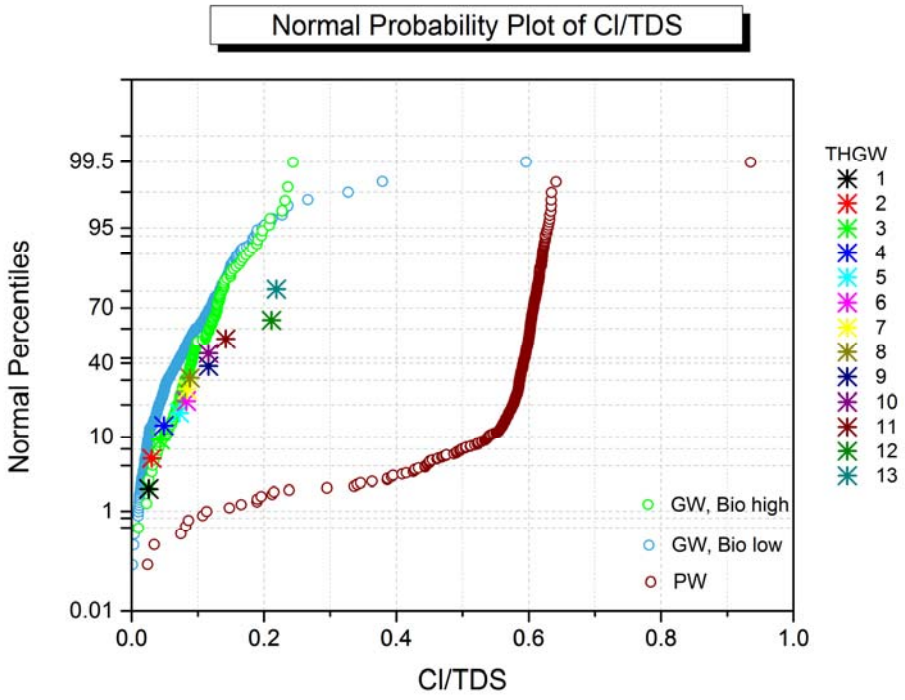

Figure 32. Normal Probability Plot of Cl/TDS measured in GW, PW, and THGW

Comparison of *Cl/TDS* distribution between three water groups was plotted in Figure 32. The *Cl/TDS* ratio in 99% of the GW samples was less than 0.25, while *Cl/TDS* ratios for 99% of the PW were between 0.29 and 0.84, significantly different from that of GW samples. All the *Cl/TDS* ratios of THGW samples fell into the region that was classified as GW and separated from the PW zone.

The *Cl/TDS* ratio spatial interpolation map was created based on the water quality data from groundwater wells excluding the thermogenic methane groundwater samples using an empirical Bayes Kriging approach.[115] The ratios of *Cl/TDS* were extracted to points that correspond to the locations of the thermogenic methane groundwater well and oil and gas wells and referred to as predicted Cl/TDS values for THGW and PW, separately. Comparison and correlation between the predicted Cl/TDS values and the actual Cl/TDS values for PW and THGW are shown in Figure 33.

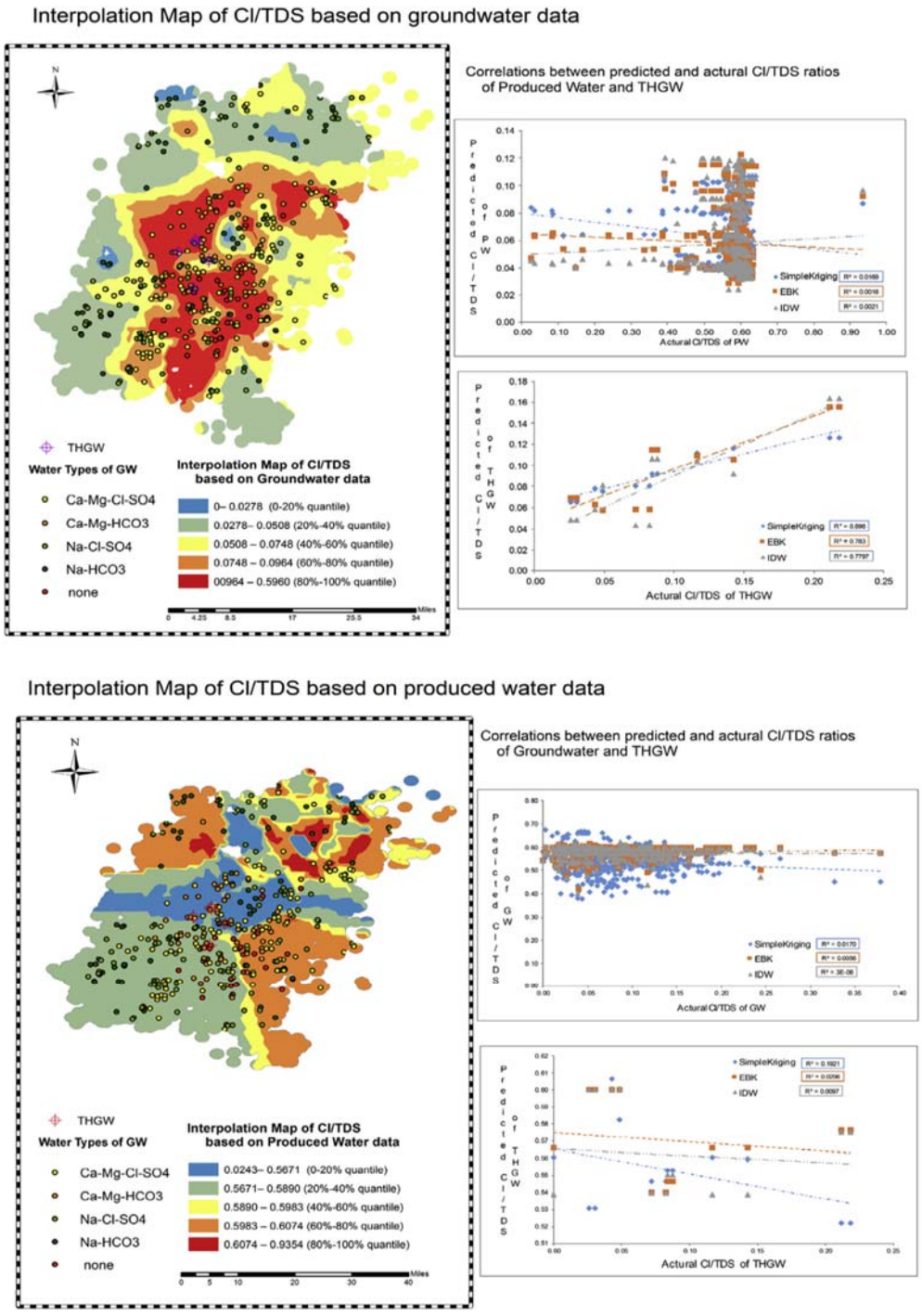

Figure 33. Ratio of Cl/TDS interpolation results for produced water and water samples from water wells containing thermogenic methane

A linear correlation (R^2=*0.83*) was observed between the predicted values and the actual values of *Cl/TDS* in THGW, but no correlation was found between those in PW. A similarity between THGW and

surrounding GW was identified in terms of *Cl/TDS* ratio, but GW and PW were significantly different as seen in the previous analyses.

5.4 Conclusion

Based on multiple analyses of inorganic water quality performed in this study, ionic signatures of THGW were statistically consistent with that of surrounding GW, but no significant similarity in ionic characteristics between THGW and PW were found. This result showed no evidence of aqueous phase contamination in THGW even in the presence of gas phase contamination from oil and gas operations.

The groundwater contamination only by gas phase constituents may be due to different subsurface transport rates of gas and aqueous phases or a contamination mechanism that occurs only with the gas phase contaminants (e.g. stray gas from producing zone).

Chapter 6 Colorado Water Watch: Real-Time Groundwater Monitoring for Possible Contamination from Oil and Gas Activity[3]

Overview

Currently, o[3]nly a few states in the U.S. (e.g., Colorado and Ohio) require mandatory baseline groundwater sampling from nearby groundwater wells prior to drilling a new oil or gas well. Colorado is the first state to regulate groundwater testing before and after drilling, which requires one pre-drilling sample and two additional post-drilling samples within 6-12 months and 5-6 years of drilling. However, the monitoring method is limited to the state's regulatory agency and to ex-situ sampling, which offers only a snapshot in time. To overcome the limitations and increase monitoring performance, a new groundwater monitoring system, Colorado Water Watch (CWW), was introduced as a decision-making tool to support the state's regulatory agency and also to provide real-time groundwater quality data to both industry and the public. The CWW uses simple in-situ water quality sensors based on the surrogate sensing technology that employs an event detection system to screen the incoming data in near real-time.

6.1 Introduction

With increasing energy requirements, economical and cleaner renewable energy resources are in great demand; over the past several decades, this has led to global growth in natural gas production.

In 2002-2003, the combination of advanced horizontal drilling and hydraulic fracturing technologies was developed and employed in the exploration and production stages, allowing economically feasible extraction of natural gas from unconventional sources, primarily shale, throughout the U.S. Since then, shale gas has been the primary energy source in the U.S., delivering 63% of the total energy in 2011, with a growth rate in production of 48% between 2006 and 2010.[116] [117] The production of shale gas is expected to increase by a further 113% from 2011 through 2040.[118]

[3] Published in Journal of Water Resource and Protection, December 2017; 9, 1660-1687

Hydraulic fracturing fluid, a mixture of 7,000-18,000 m^3 volume of water and sand (99.5%) with chemical additives (0.5%), including acid, friction reducer (polyacrylamide, mineral oil), surfactant (isopropanol), salt (potassium chloride), scale inhibitor (ethylene glycol), pH adjusting agent (sodium, potassium carbonate), corrosion inhibitor (n,n-dimethyl formamide), and biocide (glutaraldehyde), was designed specifically to create a well-flow path to the targeted shale formation, which has very low permeability ($k < 0.01$ md).[119]

During the hydraulic fracturing process, the fracturing fluid is injected into multiple layers of horizontal pipes at high pressure to exert enough force on the shale formation—at depths of 5,000-16,000 km and lateral distances up to 8,000 km—to open fractures within the formation to create paths for the gas held in pores in the shale to flow to the well, while the proppant (sand) keeps the fractures open.[120] [121] [122]

In the first two weeks after the completion of hydraulic fracturing, pressure is released at the well bore, and 10-50% of the fracturing fluid that was deposited in the shale (flowback water), returns to the surface carrying chemical additives, total dissolved solids (TDS), gas and oil compounds, naturally-occurring metal ions and radioactive materials, while the rest of the fluid returns to the surface and produces oil and gas over the lifetime of the well (produced water). The returning flow (flowback water and produced water) is collected on the surface, and sent to the treatment process to be recycled or disposed of. When the wells reach their lifespan, they are abandoned, filled with cement, sealed, and buried.[123]

Recently, dramatic increases in the number of oil and gas extraction wells in the U.S. have also raised environmental concerns about the potential effects of oil and gas activities, with intense debates about groundwater pollution and safety issues related to hydraulic fracturing.[124] [125] [126] [127] The two most furious debates related to potential groundwater contamination are possible methane gas migration and groundwater contamination by flowback and produced water.[128]

The formation of methane by bacteria occurs commonly in anaerobic subsurface environments (biogenic methane). However, there is concern that methane gas formed in the deep shale formations (thermogenic methane) can contaminate groundwater through possible connectivity between the deep shale and shallow aquifer created during drilling and hydraulic fracturing.

A previous study in Pennsylvania found higher concentrations of methane gas in groundwater near active extraction areas[129], while in contrast, no relationship was identified between distance from the oil and gas wells and groundwater concentrations of methane in Wattenberg field, Colorado. However, thermogenic methane was found in two aquifer wells in the Wattenberg field, implying the existence of a possible pathway from deep shale to the overlying aquifer.[130]

The potential paths of groundwater contamination with flowback and produced water are: improper disposal of saline water produced during oil and gas exploration and production activities; surface spills and leaks; poorly constructed wells, and well casing failure.[131] However, no evidence of systemic groundwater contamination due to oil and gas activities has been found in the U.S., possibly because of a lack of data.[132]

The importance of monitoring water quality before, during, and after drilling has been emphasized by federal agencies such as the U.S. EPA, and a few states have adopted regular monitoring practices. In February, 2013, Colorado was the first state to pass groundwater sampling and monitoring regulations (Rule 609).

The Rule of the Colorado Oil and Gas Conservation Commission (COGCC) requires up to four baseline samples collected within a 0.8 km radius of a proposed oil and gas well within 12 months prior to drilling, and post-completion sampling between 6 and 12 months after drilling, followed by additional sampling between 5 and 6 years after the last sampling event at the initial sample locations. The list of water quality parameters required for groundwater quality testing includes: pH; specific electrical conductivity (EC); TDS; dissolved gases, such as methane, ethane and propane; alkalinity; anions; cations; bacteria; benzene; toluene; ethylbenzene; xylenes, and total petroleum hydrocarbons (TPH).[133] These data are available on the COGCC website.

The most important goal of monitoring groundwater quality in the oil and gas industry is to determine the effects of oil and gas production activities on groundwater quality by monitoring changes in groundwater quality before, during, and after the construction of oil and gas wells in the area. Sufficient consecutive water quality data are required to understand trends in groundwater quality (e.g., seasonal) for

a period of time before it is possible to determine the significance of changes in the water quality by comparison to normal conditions.

However, the limitations of field sampling (ex-situ) methods have been acknowledged by regulatory agencies and scientists, not only due to the insufficient acquisition of the temporal and spatial data necessary for evaluation, but also due to the resources and time-intensiveness, as well as the high cost, of such methods. For these reasons, wireless real-time technology, which is capable of continuous monitoring of groundwater quality on-site using remote in-situ sensors, has been proposed in recent years. Despite growing needs for real-time in-situ monitoring methods, there are technical difficulties and economic challenges associated with building contaminant-specific sensors and wireless telemetry systems.

6.1.1 A Real-Time Groundwater Monitoring System: Colorado Water Watch

In response to perceived industry and community needs, the Colorado Water Watch (CWW) real-time groundwater monitoring system was developed in a cost-effective manner based on lab-qualified surrogate technologies; it uses equipment currently available to bridge the gap between the two monitoring methods: ex-situ and in-situ, and to increase the performance efficiency of monitoring (Figure 34).

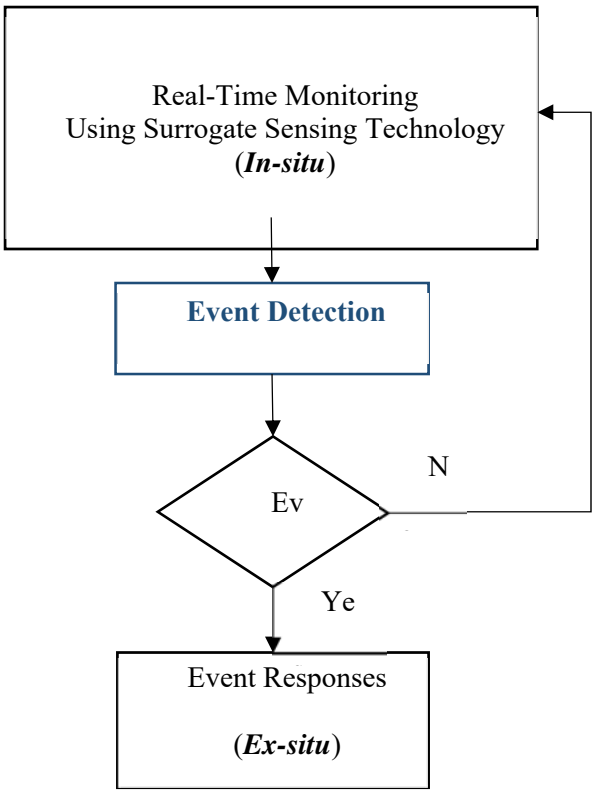

Figure 34. The CWW System Workflow, event: a time period of anomalous water quality

Using a simple in-situ water quality multi-parameter probe, the CWW system monitors groundwater in real-time and collects enough historical data to understand normal water quality conditions (e.g., pH, EC, DO, etc.). After establishing an initial acceptable baseline, if the groundwater is contaminated by oil and gas activities, the surrogate water quality parameters will indicate a change using the anomaly detection algorithms. The CWW system's anomaly detection algorithms can decide whether ex-situ monitoring is necessary to determine whether or not the groundwater disturbance is due to oil and gas activities.

The main purpose of the CWW is to enhance the effectiveness of the regulatory agency's monitoring practices—not only through long-term data acquisition, but also through screening massive amounts of data from large segments of oil and gas operations—by incorporating an event detection system (EDS) in the CWW system. The key aspect of the CWW system is that it generates information through data evaluation (qualitative monitoring), not just data collection (quantitative monitoring), which makes the system

different from existing monitoring. Information generated by the system will help the industry understand normal background conditions and anomalies of groundwater quality and provide the time needed to sample groundwater for in-depth lab analysis. The differences between the existing COGCC groundwater monitoring rule and the CWW system are well described in Supporting Information (SI) Table S1.

The objectives of the CWW real-time groundwater monitoring system are to: 1) establish a wireless data network and automate multiple steps of data flow; 2) develop a real-time groundwater monitoring network in the Denver-Julesburg (DJ) Basin; 3) collect and evaluate long-term water quality data as a decision-making tool for regulatory agencies, and 4) expand the conversation with local communities by establishing a public web-based information resource on groundwater quality associated with oil and gas production activities.

6.1.2 Basin Description

The DJ Basin encompasses approximately 180,000 km2 in eastern Colorado, southeastern Wyoming, and southwestern Nebraska. The cross-section of the basin is that of an asymmetrical bowl that resulted from the uplift of the Rocky Mountains to the west, with the deepest sedimentary rock formation in the western flank across the axis of the basin.[134]

The first oil and natural gas wells in the DJ Basin were completed in 1881 in the Florence Field, but the Wattenberg field, where the deepest shale formation crosses, has only been developed in the past 40 years after its discovery in 1970. Petroleum source rocks in the gas field date mostly from the Cretaceous period, with six potential reservoirs: J Sandstone, Codell, Dakota, Niobrara, Sussex, and Shannon, that range in age from 68 to over 100 million years and are buried at depths between 1.2 and 2.7 km.[135] Currently, the Wattenberg Field is the most active oil and gas area in the DJ Basin, having over 22,000 wells that produced 0.02 km3 of gas and 1,400 kL of oil per day in 2013 (SI, Fig. S1).[136]

Groundwater in the area is present in two forms: the South Platte Aquifer and Laramie-Fox Hills Aquifer. The South Platte Aquifer is a shallow, unconfined alluvial aquifer. The aquifer has hydraulic connectivity with surface water and is recharged by infiltration of streams and the percolation of precipitation, irrigation, and canal and pond seepage.

The depth of the water from the ground surface is 0-65 m and the saturated alluvial deposit is up to 16 km wide and 60 m thick. The aquifer produces up to 11,350 Lpm of water and has a transmissivity of 370-10,200 m2/d, a hydraulic conductivity of 30-610 m/d, and a specific capacity of 140-5,200 Lpm/m. The South Platte Aquifer is the largest source of water for agriculture in the area, primarily for irrigation and livestock purposes, and contains relatively high concentrations of TDS.

The Laramie-Fox Hills Aquifer is a confined bedrock aquifer, encompassing 17,000 km2 of the Denver Basin. The maximum depth of the water from the ground surface is 730 m, with a saturated thickness of 0-110 m. The Laramie confining unit is an impermeable layer that is between the Arapahoe Aquifer and the Laramie-Fox Hills Aquifer, obstructing water flow from the Arapahoe Aquifer to the underlying Laramie-Fox Hills Aquifer. The Laramie-Fox Hills Aquifer yields up to 1,300 Lpm, with a transmissivity ranging from 12,000-87,000 Lpm/m. It is a significant source of domestic and municipal water.[137]

In an effort to monitor potential groundwater contamination from oil and gas activities, mainly in the form of surface spills and/or well casing failures, both deep, confined aquifers and shallow alluvial aquifers were targeted for monitoring. Contamination caused by casing and cementing failures of oil and gas wells can be detected through monitoring the deep, confined aquifer (mechanisms 1 and 2 in Figure 35), and contaminants from surface spills are detected by sensors that monitor the shallow alluvial aquifer (mechanism 3 in Figure 35).

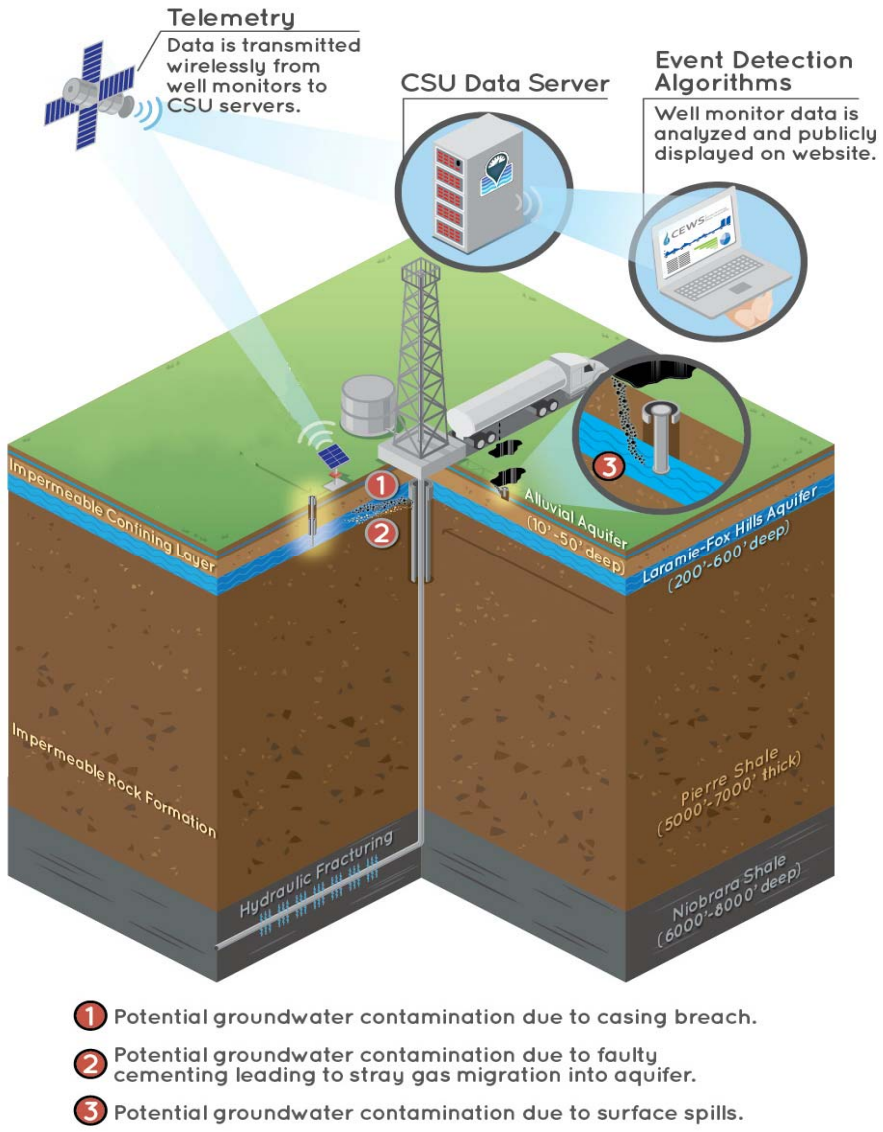

Figure 35. System design of the CWW

6.1.3 Site Description and Monitor Installation

Groundwater monitors were installed in four shallow alluvial aquifer wells and a deep, confined aquifer well. The monitoring stations in the shallow alluvial aquifer wells are: ARDEC (control), CHILL, LaSalle and Gilcrest, and the deep, confined aquifer well is Galeton (Table 7)

Table 7. CWW site locations and descriptions

Well type	Monitoring aquifer	Site name	Installed date	Well depth (m)	Location	Site description
Shallow well	South Platte Alluvial Aquifer	ARDEC (control)	2/12/2014	7.62	Northern Fort Collins, CO	Surrounded by agricultural area with no active oil and gas wells
		CHILL	2/03/2014	9.14	Northeastern Greeley, CO	Surrounded by agricultural area with active oil and gas wells
		Gilcrest	6/07/2014	7.62	Southwestern La Salle, CO	
		La Salle	10/31/2014	18.3	Southeastern La Salle, CO	
Deep well	Laramie Fox Hill	Galeton	3/27/2014	114.3	Northeastern Eaton, CO	Surrounded by active oil and gas wells

Prior to installation of the monitor, all existing and newly-drilled groundwater wells were cleaned, and in-depth baseline water quality tests were performed at each site, according to COGCC Rule 609. No oil and gas-related issues were discovered.

A multi-parameter in-situ probe was installed at the screened level of each monitoring well to measure fresh groundwater and avoid measuring stagnant water in the well. The self-charging cellular data-logger was placed in an enclosed box immediately next to the monitored well (SI, Fig. S3).

6.1.4 Surrogate Sensing Technology

Sensors that measure specific parameters of TDS (e.g., chloride) or dissolved gases (e.g., methane) related to oil and gas activity were considered for use with the CWW. However, contaminant-specific sensing has a relatively high cost in addition to being less durable and requiring more maintenance.

To resolve these issues, a contaminant-surrogate sensing approach was evaluated in the laboratory at Colorado State University.[138] The contaminant-surrogate sensing technology chosen is a cost-effective, low

maintenance, long-term monitoring method that was developed based on the well-known correlation between EC and TDS, and the expected close relationship between oxidation-reduction potential (ORP), dissolved oxygen (DO) and dissolved methane gas in water (SI, Table S2).

In general, groundwater contamination by oil and gas production activities occurs in two forms: liquid and gas. Liquid contamination occurs through contact of groundwater with produced or flowback water, both of which have significantly higher TDS concentrations than even the highest drinkable groundwater TDS concentration of approximately 2,000 mg/L. Thus, a small amount of produced and/or flowback water can disturb groundwater and be detected easily by measuring the EC of groundwater, which has a high correlation with TDS.

Gas contamination can be caused by a similar mechanism to liquid and in addition, natural gas can migrate upward along the annulus of an improperly sealed casing and wellbore. Using surrogates of methane—ORP and DO—increased concentrations of methane in groundwater can be detected and the origin of the methane can be determined by subsequent isotopic lab analysis.

The EC, ORP, and DO sensors are relatively inexpensive and adequate for deployment in the field for long-term monitoring. A multi-parameter in-situ probe (Hach Hydrolab, USA) was selected subject to three requirements: cost-efficiency; durability, and low maintenance, in order to measure six preferred water quality parameters: temperature; pH; EC; ORP; DO, and water depth in the selected groundwater wells.

6.2 Event Detection System

An EDS was adopted in the CWW system to look for changes in monitoring parameters when compared to historical data. The EDS chosen was CANARY, a set of algorithms that have been developed by the U.S. EPA for the purpose of detecting contaminants in drinking water resources.[139]

The CWW establishes a real-time connection between the database and the EDS, which runs constantly on the server; the EDS flow diagram is shown in SI, Fig. S4. An “outlier” is defined by the system as an immediate anomaly in the water quality data caused by an incident or a false operation, and an “event” is an occurrence of multiple outliers for a given duration.

To detect outliers in time series data, CANARY uses statistical and mathematical event detection algorithms, such as the linear prediction coefficient filter (LPCF), multivariate near neighbor (MVNN), and set-point proximity (SPP) algorithms.

The LPCF algorithm predicts the next value based on the historical data at each time step and calculates a residual by measuring the distance between the incoming and predicted data. The MVNN calculates a residual by measuring the distance of multiple parameters in a three-dimensional space and comparing these to the historical distances of the parameters. The SPP algorithm is the simplest; it estimates a residual by measuring the distance between the new data and the pre-defined minimum or maximum limit of the parameter.

The algorithms then classify the new data as either normal background or an outlier. The new datum is an outlier if the estimated residual exceeds a pre-determined outlier threshold, which means that the new datum is significantly different from the historical data. The data then go through the binomial event discriminator step. In this step, the system recognizes an event if the occurrence of outliers exceeds a pre-defined event probability threshold in a moving time frame (history window). A consensus algorithm, CMAX, was employed to report the maximum event probability from all event detection algorithms applied. An event is considered to indicate that "something happened," and therefore it requires a follow-up study to determine the cause, as mentioned above in the purpose of the CWW system.

More details about the algorithms and the EDS can be found in the CANARY user's manual.[139] A study on the EDS performance optimization for the CWW system was conducted to determine event detection algorithm inputs required based on the CANARY Testing and Sensitivity Analysis.[142]

Three sets of the first two months of data, acquired hourly from the CWW monitoring sites, were used in the study. The consecutive two-month data were assumed to be background data containing no oil and gas-related events. This assumption was supported by the laboratory groundwater quality data analysis from the monthly sampling performed in the first stage to understand groundwater quality at the CWW monitoring sites.

The window size in LPCF and MVNN algorithms are defined as the number of previous time steps used to predict the next value and to compare water quality values at each time step, respectively. To determine the appropriate window size, outlier and event probability thresholds were pre-set to infinite to have neither outliers nor events. Window sizes between 168 (one week) and 672 (four weeks) were tested with one half week (84) increments to find the optimal window size, which has the lowest average and standard deviations of residuals of all measuring parameters calculated by each algorithm (SI, Fig. S5). A window size of 588 (3.5 weeks) was selected because the standard deviation of the residuals of the window size was similar to their minimum for both LPCF and MVNN algorithms.[143]

6.2.1 Event Responses

When an event is detected by the EDS, the system alerts the registered CWW group to initiate a detailed inspection at the site. The systematic flow of the event responses is shown in SI, Fig. S6. An event can be operational, such as sensor failure, or seasonal, caused, for example, by water table fluctuations due to irrigation; thus, a primary event analysis is required to classify the type of event based on the practical data and previous experiences. If the event was operational or seasonal, it can be stored in the historical pattern library to prevent future false positives.

In the case of non-operational or non-seasonal events, the CWW team is deployed to the site within 24 hours of the event alarm to sample groundwater according to COGCC Rule 609; they also conduct a brief site inspection. The samples are then transported to an EPA-certified laboratory, where they undergo a comprehensive lab analysis for 7-10 days.

From the results of the lab analysis, combined with the sensor data acquired at the same time that the samples were collected, researchers in the CWW team can identify what triggered the event and whether the event is related to oil and gas residuals.

If the event is related to oil and gas operations, the COGCC is notified and begins an extensive inspection with respect to the type of contamination, source, extent, and other characteristics; the results are posted subsequently on the CWW website (http://waterwatch.colostate.edu), as well as on the COGCC website (http://cogcc.state.co.us). The overall systematic monitoring scheme is described in SI, Fig. S7.

6.2.2 Real-Time Data and Monitoring Network

A wireless, real-time groundwater monitoring network was designed, in general, to have four steps: 1) wireless data acquisition and transfer; 2) data management and storage; 3) data processing and analysis, and 4) data interpretation and display of results.

Wireless data acquisition and transfer are achieved by employing a cellular data logger (Hach Hydromet, USA) with a multi-parameter probe through an SDI-12 interface. The cellular data logger is capable of general packet radio service (GPRS) that enables hourly remote data transfer from the probe in the field to the CWW data server. Power is supplied by a self-charging solar battery. The data are transmitted to a cloud server, and then stored automatically in the database, where they go through the real-time event detection system. The results from the data analysis are then posted in the database and displayed on the CWW website in simplified form to show the public whether the recent groundwater quality data for each site are normal or not.

When an event is detected in the data analysis step, the system alerts the CWW team for further inspection of the groundwater quality, including the COGCC baseline testing as described above.

The end-user interface was constructed using ASP.NET. ASP.NET is an easy-to-use, comprehensive tool for building powerful websites and interfaces that incorporate component-based development. The data from the aforementioned data logger are transmitted to the server in the form of XMLs. These XMLs are decoded to populate the database, which is located securely in the local SQL Server.

The data acquisition infrastructure is primarily an automated process of the telemetry system that sends data to a host address in real-time. The host address is set up inside the data-processing infrastructure in the server, which organizes the raw data to its corresponding entries in the database. The workflow shown in SI, Fig. 8 explains the structure of our current system.

6.3 Results/Discussion

The CWW described in this paper was put together at a proof-of-concept scale consisting of only 5 monitoring sites. It is one of the first real-time groundwater monitoring systems in an active oil and gas production field. The CWW is intended to be an early warning system that can provide risk management

and decision-making tools utilizing advanced monitoring and information technologies. It has the ability to enhance other groundwater monitoring networks and approaches for oil and gas regulatory agencies, industry, and communities as well.

Over a one-year monitoring period, real-time groundwater data were collected hourly, transmitted into the CWW database, and analyzed through the event detection software.

6.3.1 Statistic summary of the real-time monitoring data

Real-time monitoring data for this analysis started from the installation date and ended in January 2017, which represents a one-hour frequency, and two-year long period of groundwater quality observation.

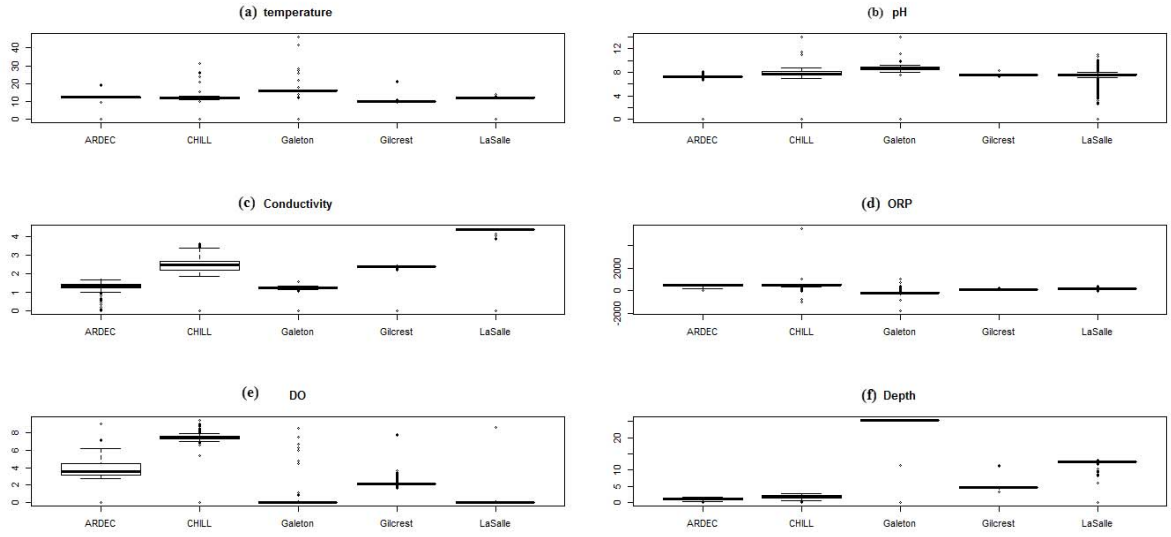

Figure 36. Comparison of six quality variables between five monitoring wells(from the installation date to June 23th, 2015) (temperature – groundwater temperature, ORP –oxidation-reduction potential, depth – water level in the well)

Normality tests show that none of the water quality variables exhibits the same form of normal distribution. As shown in Figure 36, all five monitoring wells have distinguishing groundwater ($p < 0.01$, t-test) except dissolved oxygen between Galeton and LaSalle ($p = 0.1618$).

All the monitoring wells had a relatively stable background signal. 90% of the temperature readings are between 10.39˚C and 16.16˚C. Galeton had the highest water temperature, with a mean of 16.05˚C and Gilcrest had the lowest water temperature with mean of 10.77˚C. pH ranges from 5.47 to 8.88 for 90% of

the readings, which vary a lot for the individual wells. Shallower groundwater wells have lower pH values than the deep groundwater well, because water would react with carbonate minerals during the downward migration of water and correspond to the exchange of sodium in the clay with calcium in water[140].

High ORP level in water indicates an oxygen-rich water that is capable of oxidizing metals such as manganese and iron. The more electron-donating organic compounds in the water, the lower ORP level. Also, according to our surrogate study[141], low ORP values could indicate the presence of dissolved methane in water. Over 94% of the measurements showed negative ORP in Galeton, while less than 0.1% of the ORP readings are negative for the other four monitoring wells. Meanwhile, most of the dissolved oxygen of the four shallow wells is greater than zero and most of the DO readings (99%) of Galeton are less than zero indicating a more reduced environment in this well. Higher water temperature, higher pH, lower ORP and lower dissolved oxygen are observed in Galeton because it is the only deep monitoring well with a depth of 114 m while the depth of the deepest shallow well is 20 m. The appearance of the water becoming reducing with the increasing depth underground would be caused by the absence of dissolved oxygen. The conductivity of groundwater in Galeton is lower than the conductivity of groundwater in shallow wells. Dissolved solids which have a positive linear correlation to conductivity in groundwater come from several sources, 1) mineral-dissolution in the subsoil, 2) surface runoff infiltration, 3) saline leakage from other formations[142]. Since rainfall is low in TDS and cross-formation transport of salts is limited due to the underlying confined aquifer, the main factors that would affect the TDS are surface runoff infiltration and mineral dissolution in the subsurface.

The real-time monitoring data shows that ORP was not linearly correlated to dissolved oxygen, and it might be due to the combination effect of water temperature, pH, dissolved oxygen and conductivity.

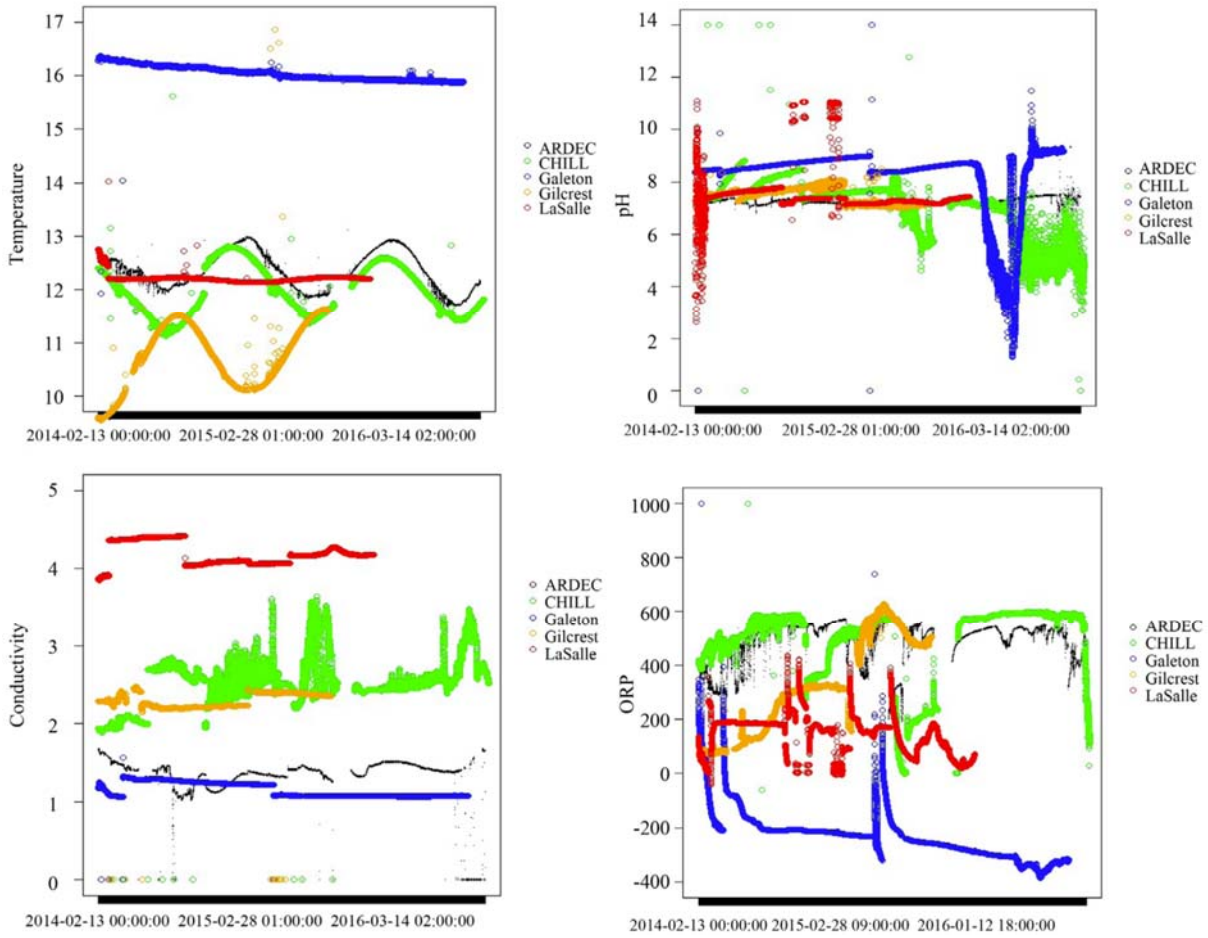

Figure 37. Real time monitoring data comparison 2014-2016 (x-axis of the plots represents the data observation date from Feb

Since the oldest monitoring well in this study was installed in Feb 2014 and the latest one was in Nov 2014, we can compare the changing trends of all the water quality parameters in 2014, 2015 and 2016 (Figure 37). The unit is ˚C for temperature, 100 µS/cm for conductivity, mV for ORP in Figure 4 above. The trend of water temperature of CHILL and ARDEC are the same that water temperature drops to the lowest level in the summer time and rises to the highest level in the winter, while Gilcrest has the opposite trend. Water temperature in LaSalle and Galeton was stable. The highest overall water temperature occurs at Galeton (over 20˚C) among the five monitoring wells due to its deepest well depth. Most of the "events" detected by CANARY (detection probability greater or equal to 0.9) occurred in June-September (summer),

and there are a few events detected in Feb and March. Most of the "events" occurred during the irrigation season, which lasts from late April to early Oct, with the lowest water depth during the year.

Galeton has the most stable water since it is in a confined aquifer and is likely not affected by surface activities. Dissolved oxygen in water either rises in the summer (ARDEC and Gilcrest) or is stable during the whole year. Most data for the same month (2014 & 2015) at the same monitoring well are nonidentical except the water depth at Galeton, which remains the same ($p > 0.05$, Mann-Whitney-Wilcoxon Test), indicating the water table of this deep monitoring well has not been changed and not affected by surface activities. ORP ranges from 0 to 600 mV for the four shallow wells and 0 - 150 mV for Galeton.

6.3.2 Trend analysis and Outlier detection

Since the background knowledge of groundwater quality in Wattenberg field is not available, learning process to understand the quality-changing trend is required and necessary. For an individual monitoring well, the behavior of a groundwater quality variable on the time scale was fitted into the moving median[143]. Equations are shown below:

$$y = runmed(x, k)$$

$$y[j] = median(x[(j - k_2) : (j + k_2)]) \quad (k = 2 * k_2 + 1)$$

$y = \text{movmedian}(x, k)$ returns an array of local *k-point median values, where* each median is calculated over a sliding window *of length k across neighboring* elements of x . When k is odd, the window is ce*ntered about the element in the* current position. When k is even, the window is *centered about the current and* previous elements. The window size is automatic*ally truncated at the endpoints* when there are not enough elements to fill *the window. When the window is* truncated, the median is taken over the element*s that fill the window. Optimal* window size of five is selected and the Goodness of fit for the simple moving median results are shown in Table 8. Moving median method gives a good estimation *and prediction of temperature,* pH, conductivity and ORP. Using the movi*ng median method, we can filter* out the outliers that fell beyond the range of $[mean + 4 * standard\ deviation, \text{mean} - 4 * \text{standard deviation}]$ (99% confidence interval) for each single water quality variable.

Table 8. Goodness of fit (R-square) by moving median mode (n=5) by monitored value for each site

	ARDEC	CHILL	GALETON	GILCREST	LASALLE
TEMPERATURE	0.9404	0.7589	0.9909	0.9057	0.9659
PH	0.9273	0.9703	0.9954	0.9937	0.973
CONDUCTIVITY	0.9901	0.9337	0.9993	0.7842	0.9553
ORP	−4.8e−05	0.9417	0.9941	0.9999	0.9959
DO	0.9904	0.9907	0.611	0.9997	−2.9e−05

6.3.3 Event detection

"Events" may be the result of natural processes (such as surface runoff that infiltrated to the subsurface and flow towards a point of discharge (monitoring site) or anthropogenic activities. The human related activities that are particularly relevant to the groundwater "anomalies" include:

Non-oil/gas related activities

1) Irrigation—large quantity of the irrigation water that recharges the subsurface can raise the groundwater table accompanied by significant changes in groundwater quality, especially nutrient level. Irrigation is an important source of surface and groundwater non-point source contamination, due to the high concentration of nutrients, pesticides, salinity and trace elements. Nitrate is a significant soluble nutrient that can contribute to the change of redox potential, which would affect ORP. The Wattenberg field has over 1100 irrigation wells, an indicator of the extent of agricultural activity in the area[144].

2) Fertilizer pollution—the use of fertilizer would result in increasing nutrient loading, such as NO_3-, which could increase the EC or TDS[145].

3) Pumping—extracting groundwater through a pumping well near a monitoring site could lower the regional water table and draw water from other sources[146].

4) Instrument malfunctions and sampling disturbance—pH and water temperature signals respond to an instrument malfunction almost without any lags, including monitoring instruments installation, sensor calibration and recalibration, and groundwater sampling (when an event occurred). An abrupt increase or decrease in water temperature usually suggests an instrument malfunction.

Oil/gas related activities, such as surface spills, well leakage or well construction failure, would cause contaminants, such as methane and deep formation water, dissolving and mixing with groundwater leading

to a change in ORP and/or conductivity. Deep formation water usually contains high concentrations of dissolved solids, and has a high proportion of chloride with respect to TDS[147].

For the only deep monitoring well, 85% of the "events" detected from Galeton are due to the ORP change both for MOVING MEDIAN and for CANARY, indicating that the groundwater from the deep monitoring well is largely impacted by the redox reactions rather than the physical exchanges, such as the tempera ture and water depth. In addition, the occurrence of the outliers at the Galeton site is not the most among all the five monitoring wells even though it is surrounded by highest density of OG wells, suggesting that oil/gas activity might not be the major influence that could change the groundwater quality in a short time period. Increasing water temperature corresponded to instrument malfunctions and sampling.

Table 8 shows the when and how many of outliers detected by CANARY and moving median. There are some outliers clustered in months, such as March, July and August, even though different wells perform differently. The two methods do not agree with each other in terms of the numbers of outliers or the months that have the most outliers.

The moving median is used to give additional information about outliers and anomalies, to compare with CANARY's result. PCA, (principal components analysis) is applied as a tool to organize the chemical variable matrix and differentiate different groups (outlier predictions by MOVING MEDIAN and CANARY). Six chemical variables including water temperature, pH, conductivity, ORP, DO and water depth were analyzed. PCA reduces the high-dimension data (6 in our study) and transforms the multi-dimension to two principle components (PCA1 and PCA2), which are the subsets of the attributes. The first two principle components, PCA1 (x axis) and PCA2 (y axis), spanned the two-dimensional plot space (PCA1 and PCA2 explained over 75% of the variance which could be used to analyze the inter-relations between each chemical variable and their impacts).

Table 9. Comparison of numbers of outliers detected by CANARY and moving median

ARDEC				CHILL				Galeton			
Canary		Moving Median		Canary		Moving Median		CANARY		Moving Median	
Month	Freq.	Month	Freq.	Month	Freq.	Month	Freq.	Month	Freq.	Month	Freq.
July 2014	13	Mar 2014	1	Mar 2014	19	Mar 2014	2	Mar 2015	22	Apr 2014	2
Aug 2014	30	May 2014	2	Feb 2016	22	Apr 2014	1	Sep 2015	34	May 2014	3
Feb 2015	22	Jul 2014	1	Mar 2016	48	Jun 2014	1	Mar 2016	22	Feb 2015	2
Mar 2015	10	Aug 2014	2	Aug 2016	35	Jul 2014	1	Aug 2016	22	May 2015	3
May 2015	13	Nov 2015	2			Aug 2014	3			Jun 2015	21
Aug 2015	22	Jun 2016	1			Sep 2014	1			Oct 2015	2
Jul 2016	7	Aug 2016	17			Oct 2014	139			Nov 2015	7
		Sep 2016	6			Jun 2015	3			Dec 2015	11
						Jul 2015	1			Jan 2016	28
						Sep 2015	1			Feb 2016	26
						Oct 2015	11			Apr 2016	3
						Sep 2016	110			May 2016	201
										Jun 2016	30
										Jul 2016	5
										Aug 2016	4
										Sep 2016	11
Total	117	Total	32	Total	124	Total	276	Total	100	Total	361

Gilcrest				LaSalle			
CANARY		Moving Median		CANARY		Moving Median	
Month	Freq.	Month	Freq.	Month	Freq.	Month	Freq.
Jul 2014	9	Jul 2014	1	Mar 2015	22	Nov 2014	287
Jun 2015	23	Aug 2014	1			Dec 2014	85
		Sep 2014	1			Jun 2015	5
		Jun 2015	325			Jul 2015	114
		Jul 2015	64			Aug 2015	68
		Aug 2015	7			Oct 2015	279
		Sep 2015	3			Nov 2015	66
Total	32	Total	402	Total	22	Total	904

Real time data includes the number of outliers detected by CANARY & MOVING MEDIAN (on the left) and PCA plot (on the right) are shown in Figures 38 (a)-(e). Red and green dots represent the outliers

detected by moving median and CANARY. According to COGCC inspection, there were four surface spills including three that occurred at tank batteries and one at a well less than 2 miles upstream of CHILL on Oct 10th, Oct 13th, Dec 8th, and Dec 15th in the year of 2014. There were 139 "events" detected by moving median for CHILL, in Oct 2014. This event might be a reflection of these four surface spills since E&P wastes usually have a high BOD concentration. The event detected on Feb 15th 2015 for LaSalle might be a delayed impact of surface spill occurred on Dec 23th 2014 within 2 miles of the monitoring site. The surface spill occurred on May 28th 2014 near the Galeton site did not influence the water quality because the monitoring well is in a confined aquifer that is usually not affected by surface activities.

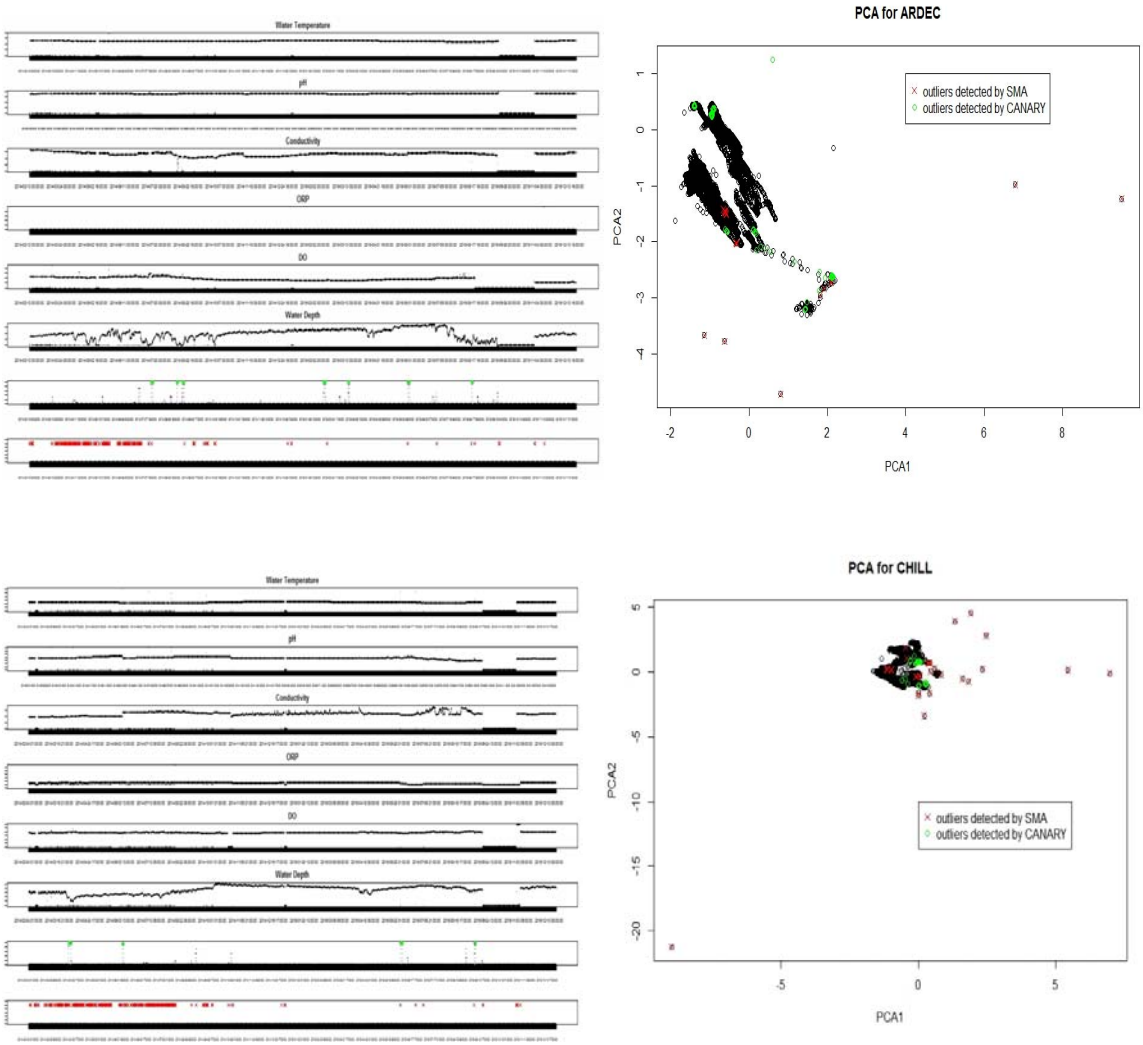

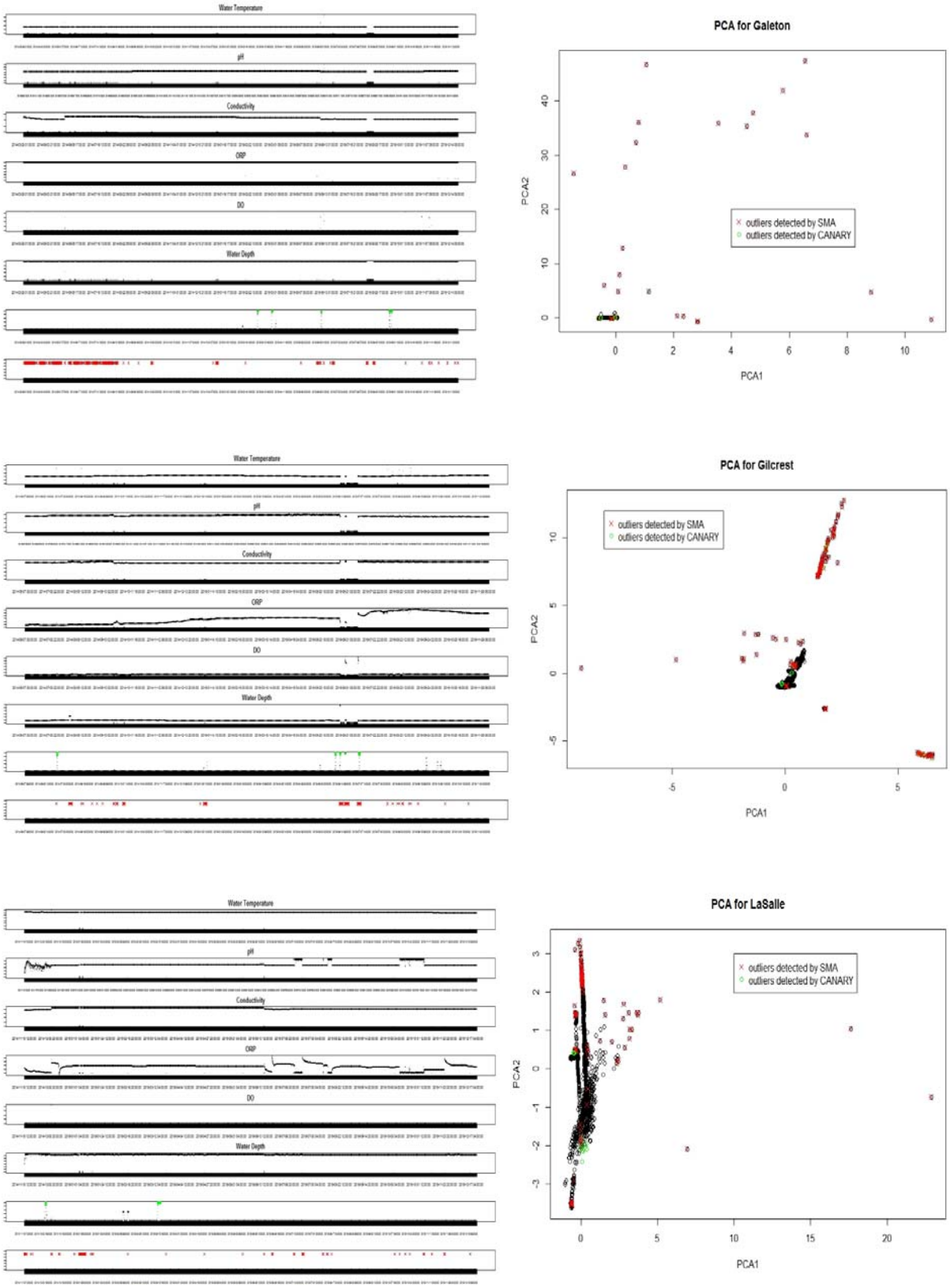

Figure 38. Real-time data and outliers detected by CANARY and SMA (simple moving average)

As shown in Figures 38 (a)-(e), moving median is more sensitive to data changes compared to the CANARY EDS. Different clusters plotted in the PCA diagrams represent various data types. All the data points are drawn as black in the PCA diagrams, if the data was considered to be an “abnormal” or an outlier by Moving Median, it would be crossed by red; if the data was considered to be an outlier by CANARY, it would be circled out by green. As a result, the numbers of outliers detected by MOVING MEDIAN is more than those detected by CANARY and also the outliers detected by MOVING MEDIAN agrees with the PCA analysis, outliers shown by PCA analysis are the data points that separate with the group of “normal” data. The reason might be the real-time data was not normally distributed, a key assumption made by the CANARY algorithms by default. According to our comparisons, CANARY has not detected most of the abrupt changes as MOVING MEDIAN does, but MOVING MEDIIAN still has some drawbacks. Advantages and disadvantages for CANARY and MOVING MEDIAN are listed below:

1) The window size needs to be selected for both MOVING MEDIAN and CANARY, but during the first window size, MOVING MEDIAN can do the calculation but CANARY cannot.

2) Background information, such as the normal groundwater quality data, is required for both methods. For CANARY, the algorithm could be trained by using normal water quality data to optimize the settings, such as the window size, the occurrence of the abnormal events, and etc. For MOVING MEDIAN, it is a good option to select the unusual event if the data is stable for most of the time.

3) There are multiple algorithms to calculate outliers and events in CANARY that could largely reduce the noise while MOVING MEDIAN is only based on one calculation that is good for data analysis but its performance in real-time

6.4 Conclusion

Although a seamless integration of real-time data flow, data analysis (event detection) application, event response protocols, and results visualization on a user-friendly website were established, additional monitoring stations are required to provide a network with greater resolution and coverage. The CWW is currently being expanded with support from both the oil and gas industry and the Colorado Department of

Natural Resources. Additional partnerships are expected as the system becomes more accepted by the primary stakeholders, communities and industry.

Chapter 7 Groundwater Flow and Transport Simulation in an Oil & Gas Field of Northern Colorado[4]

Overview

Monitoring of regional groundw[4]ater quality is in high demand since the increasing public concerns about the potential environmental risks of the application of two novel techniques, horizontal drilling and hydraulic fracturing in the development of unconventional natural gas production. One challenge and also the main purpose of real-time ground water monitoring is to establish an event detection algorithm or system to identify "outlier" data points related to contamination events. In our study, multivariate state estimation technique (MSET) and one-class support vector machine (1-SVM) methods are utilized and improved for real-time groundwater anomaly detection. The effectiveness of the two methods are validated based on different data patterns obtained from the Colorado Water Watch (CWW) project conducted from 2014 to 2016. An event was also simulated by means of finite difference methods (FDMs) to test the reliability of the two methods.

7.1 Introduction

Public concerns about groundwater quality have increased in areas that have shale oil and gas extraction activities in the United States. Shale oil and gas extraction activities, including drilling and hydraulic fracturing, have grown exponentially since 2008[148]. The increased activity is a result of technology advances in horizontal drilling, fracturing of shale formations hydraulically and 3d seismic analyses. Hydraulic fracturing involves drilling into oil and gas rich shale formations and then with horizontal drilling, exposing wellbores of up to two miles in length. Frac fluid (mixture of water, sand and chemicals) is injected

---

[4] Authors: Jianli Gu, Huishu Li, Ken Carlson, Jiangguo Liu*

Department of Mathematics, Colorado State University, USA

Email: liu@math.colostate.edu

at high pressures to create cracks in the shale-rock formations through which the oil and gas flow back to the surface for collection (Figure 28).

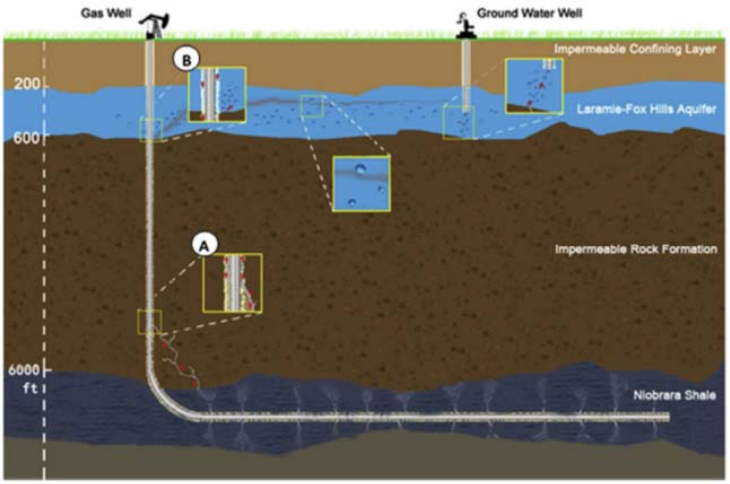

Figure 28. Horizontal drilling and fracking, and illustration of potential pathways for groundwater contamination (A: stray gas; B: fracking fluid and produced water)

However, the application of hydraulic fracturing and horizontal drilling is controversial due to its uncertain environmental impacts. As shown in Figure 28 above, the potential environmental risks related to oil/gas activities include the natural gas escaping from producing wells through circumferential fractures and/or from improperly sealed casing strings along the wellbore, and fracking fluid leakage along casing breaches into the groundwater aquifer[149]. Natural gas can become explosive and flammable when the methane concentration in water is greater than its solubility, and the produced fluids are full of hazardous compounds. Both of them will bring severe contamination to the shallow groundwater in regional areas.[150] Recent studies have shown elevated levels of chloride and potassium in water wells around extensive natural gas operations in Pavilion, Wyoming[151] [152].

Oil and gas contamination in the subsurface has been studied for years but there are relatively few research studies that use mathematical transport models combined with real-time data collection. In our

study, contaminant transport models together with real time water quality data is used to understand the practical application of subsurface contamination characterization.

7.2 Methods

Darcy's law is the fundamental principle illustrating movement of groundwater in subsurface porous media.[153] Since most oil and gas related contaminants are soluble under high pressure, the transport is dominated by groundwater movement. In our study, the groundwater modeling refers to the mathematical representation of the Darcy flow system with specific hydrogeological conditions. In general, the groundwater flow and contaminant transport in the porous medium domain are three-dimensional[154]. However, groundwater flow in the saturated thickness of an unconfined aquifer is practically horizontal. In this context, all the models are built on the assumption that the aquifer flow is essentially horizontal, i.e. 2-dimensional.

To describe the groundwater flow through porous medium, the Darcy problem is used in a bounded polygonal area as below[155],

$$\begin{cases} \nabla \cdot (-K\nabla p) \equiv \nabla \cdot u = f, \ x \in \Omega \\ p = p_D, \ x \in \Gamma^N, \ u \cdot n = u_N, \ x \in \Gamma^N \end{cases} \quad (1)$$

where $\Omega \in R^2$ is the polygonal domain, K is the horizontal hydraulic conductivity, f is the specific discharge, p is an unknown pressure, p_D is a Dirichlet boundary condition, u_N is the Neumann boundary condition and n is a unit outward normal vector on $\partial\Omega = \Gamma^D \cup \Gamma^N$.

The transport process can be prototyped by the convection-diffusion equation,

$$\begin{cases} \partial_t c + \nabla \cdot (vc - D\nabla c) = f(x,y,t), \ (x,y) \in \Omega, \ t \in (0,T), \\ c(x,y,t) = 0, \ (x,y) \in \partial\Omega, \ t \in (0,T), \\ c(x,y,0) = c_0(x,y), \ (x,y) \in \Omega \end{cases} \quad (2)$$

where $c(x,y,t)$ is the unknown contaminant concentration to be solved, v is the fluid velocity, $D > 0$ is the diffusion coefficient of specified pollutant and f is the source term.

Generally speaking, the mechanisms of transport include convection, diffusion and reaction. When there is no reaction, and the diffusion can be safely ignored, we have a pure convection problem which takes the form: $\partial_t c + \nabla \cdot vc = f(x,y,t)$ (3)

7.2.1 Finite Difference Method (FDM) for Darcy Velocity

To solve the Darcy equation (1) and obtain Darcy velocity u, FDM can be applied if the domain is rectangular and discretized. As is known, the Darcy velocity is calculated based on the equation,

$u = -K\nabla p$ (4)

where $\nabla p = \left(\frac{\Delta h_x}{\Delta l_x}, \frac{\Delta h_y}{\Delta l_y}\right)$ is the gradient of water level in 2-dim, h hydraulic head (unit m) and l_x, l_y flow path along x, y directions, as shown in Figure 39.

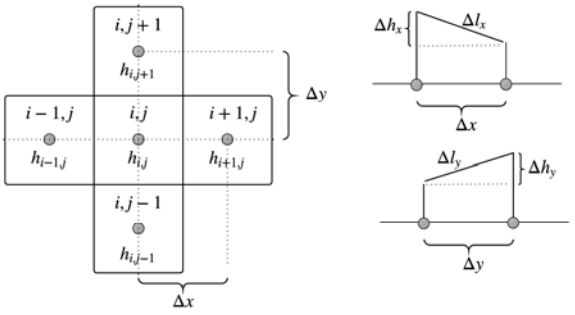

Figure 39. Schematic diagram of finite difference scheme for solving Darcy equation

The hydraulic conductivity K is defined by the following tensor:

$$K = \begin{bmatrix} K_{xx} & K_{xy} \\ K_{yx} & K_{yy} \end{bmatrix} \quad (5)$$

It is a common practice to assume that the principal directions of anisotropy can be aligned with the x, y coordinate axes such that $K_{xy} = K_{yx}\ and\ K_x = K_{xx}, K_y = K_{yy}$ (Galluzzo 2011). Therefore, Darcy velocity equation 4 takes the form

$$u = \left(-K_x \frac{\partial h_x}{\partial l_x}, -K_y \frac{\partial h_y}{\partial l_y}\right) \quad (6)$$

If the hydraulic conductivity is homogenous in the grid cell, then $K_x = K_y = K$. The derivative $\frac{\partial h_x}{\partial l_x}$ and $\frac{\partial h_y}{\partial l_y}$ can be obtained in three different ways: forward difference $\frac{\partial h}{\partial l} = \frac{h_{k+1} - h_k}{2\Delta l}$, backward difference $\frac{\partial h}{\partial l} = \frac{h_k - h_{k-1}}{\Delta l}$ and central difference $\frac{\partial h}{\partial l} = \frac{h_{k+1} - h_{k-1}}{2\Delta l}$. At the boundary of the domain, forward or backward

difference at cells might be the choice, the inner cells can take any of them, but central difference is adopted in this study.

7.2.2 Upwind Finite Difference Method for Transport Simulation

With the Darcy velocity u, we can solve the convection-diffusion equation for contaminant transport through the discretized area by using a FDM approach:

$$\frac{\partial c(x,y)}{\partial t} + v(x,y)\nabla \cdot c(x,y) + c(x,y)\nabla \cdot v(x,y) - D\nabla \cdot \nabla c(x,y) = f(x,y,t) \quad (7)$$

We apply the 1st order upstream scheme to the convection problem with flow $v(x,y) = (v_x, v_y)$. If $v_x > 0$ in x direction and $v_y > 0$ in y direction, then the scheme will be:

$$\frac{c_{i,j}^{(n+1)} - c_{i,j}^{(n)}}{\Delta t} + \left(v_x \frac{c_{i,j}^{(n)} - c_{i-1,j}^{(n)}}{\Delta x} + v_y \frac{c_{i,j}^{(n)} - c_{i,j-1}^{(n)}}{\Delta y} \right) + \left(c_{i,j} \frac{v_{x_i,j}^{(n)} - v_{x_i-1,j}^{(n)}}{\Delta x} + c_{i,j} \frac{v_{y_i,j}^{(n)} - v_{y_i-1,j}^{(n)}}{\Delta y} \right) +$$

$$D\left(\frac{C_{i+1,j}^{(n)} - 2c_{i,j}^{(n)} + c_{i-1,j}^{(n)}}{(\Delta x)^2} + \frac{C_{i+1,j}^{(n)} - 2c_{i,j}^{(n)} + c_{i-1,j}^{(n)}}{(\Delta y)^2} \right) = f_{i,j}^{(n)} \quad (8)$$

The resulting scheme takes the form:

$$c_{i,j}^{(n+1)} = c_{i,j}^{(n)} - \Delta t \left(v_x \frac{c_{i,j}^{(n)} - c_{i-1,j}^{(n)}}{\Delta x} + v_y \frac{c_{i,j}^{(n)} - c_{i,j-1}^{(n)}}{\Delta y} \right) - \Delta t \left(c_{i,j} \frac{v_{x_i,j}^{(n)} - v_{x_i-1,j}^{(n)}}{\Delta x} + c_{i,j} \frac{v_{y_i,j}^{(n)} - v_{y_i-1,j}^{(n)}}{\Delta y} \right) +$$

$$D\Delta t \left(\frac{C_{i+1,j}^{(n)} - 2c_{i,j}^{(n)} + c_{i-1,j}^{(n)}}{(\Delta x)^2} + \frac{C_{i+1,j}^{(n)} - 2c_{i,j}^{(n)} + c_{i-1,j}^{(n)}}{(\Delta y)^2} \right) + f_{i,j}^{(n)} \quad (9)$$

If $v_x < 0$ in x direction and $v_y < 0$ in y direction, then the resulting scheme will be:

$$c_{i,j}^{(n+1)} = c_{i,j}^{(n)} - \Delta t \left(v_x \frac{c_{i+1,j}^{(n)} - c_{i,j}^{(n)}}{\Delta x} + v_y \frac{c_{i,j+1}^{(n)} - c_{i,j}^{(n)}}{\Delta y} \right) - \Delta t \left(c_{i,j} \frac{v_{x_i+1,j}^{(n)} - v_{x_i,j}^{(n)}}{\Delta x} + c_{i,j} \frac{v_{y_i,j+1}^{(n)} - v_{y_i,j}^{(n)}}{\Delta y} \right) +$$

$$D\Delta t \left(\frac{C_{i+1,j}^{(n)} - 2c_{i,j}^{(n)} + c_{i-1,j}^{(n)}}{(\Delta x)^2} + \frac{C_{i,j+1}^{(n)} - 2c_{i,j}^{(n)} + c_{i,j-1}^{(n)}}{(\Delta y)^2} \right) + f_{i,j}^{(n)} \quad (10)$$

Similarly, we can get the combination equations when $v_x > 0$, $v_y < 0$ and $v_x < 0, v_y > 0$. To solve this partial differential equation, the Courant-Friedrichs-Lewy (CFL) condition is necessary for stability, that is,

$$\Delta t \leq \frac{\min(\Delta x, \Delta y)}{\| v \|_{max}} \quad (11)$$

7.3 Study Area and Dataset

To simulate contaminant transport in the subsurface, we selected a study area with sufficient hydraulic and geologic data, shown in Figure 40, located in the south rural area of Greeley, CO. This area is one part of the Wattenberg filed with intensive oil and gas production operations and covered by the groundwater monitoring system – CWW [156]. Therefore, we can couple the transport simulation with real-time groundwater monitoring.

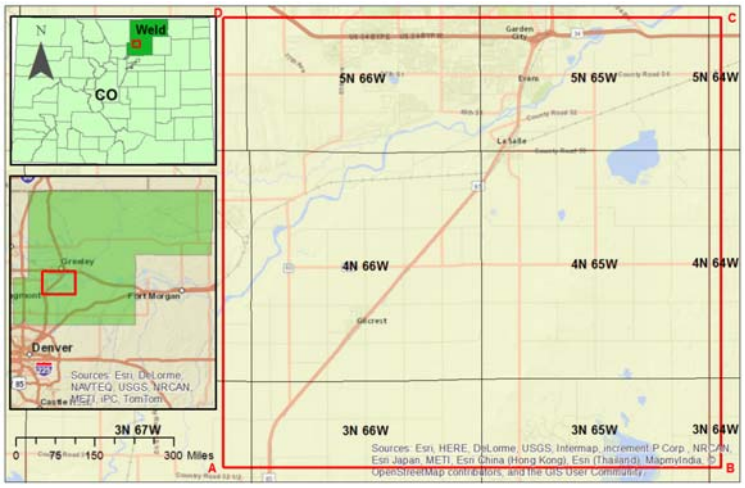

Figure 40. The rectangular area for study, 21,000 meters (13.0 miles) from A to B and 19,000 meters (11.8 miles) from A to D

A, B, C and D are the vertices of the rectangular area in this study. The coordinates of A, B, C and D are listed below in Table 10.

Table 10. The boundary coordinates of the study area

Corner	Longitude	Latitude	X (meters)	Y (meters)
A	-104.844	40.228	513296.815	4453116.455
B	-104.597	40.228	534296.815	4453116.455
C	-104.597	40.399	534296.815	4472116.455
D	-104.844	40.399	513296.815	4472116.455

Projected coordinate system: NAD_1983_UTM_Zone_13N

According to Colorado Oil & Gas Conservation Commission (COGCC), nearly 3500 producing wells were built in the study area by 2014. Two monitoring wells, Gilcrest and Platteville, in the Colorado Water Watch groundwater monitoring network were located in this area surrounded with lots of producing oil and gas wells (Figure 41).

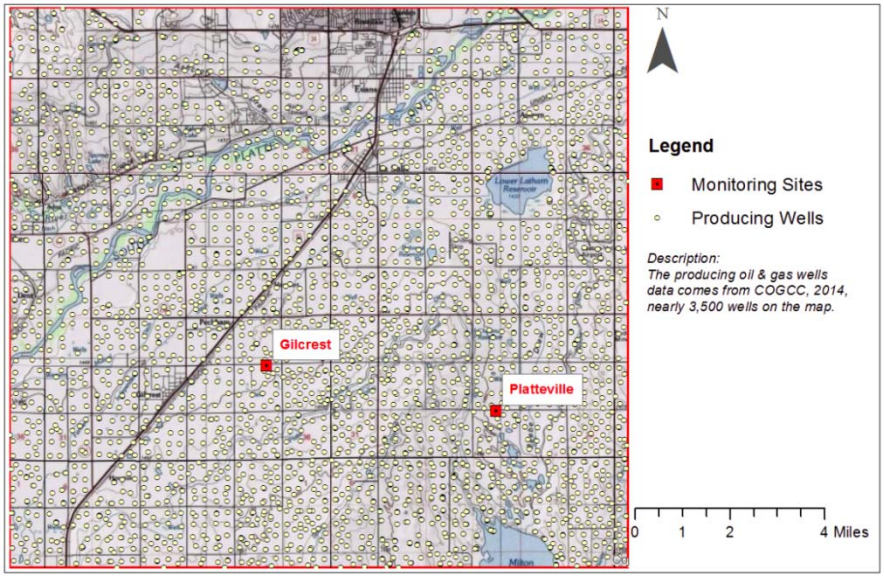

Figure 41. Map of oil and gas producing wells and two monitoring wells in the study area

To calculate Darcy velocity, groundwater surface elevation from Colorado Geological Survey and the horizontal hydraulic conductivity from the SPDSS (http://cdss.state.co.us/GIS/Pages/Division1SouthPlatte.aspx) are discretized by 19×21 cells (19 rows $\times$ 21 columns), each cell is $1000m \times 1000m$, as shown in Figure 41.

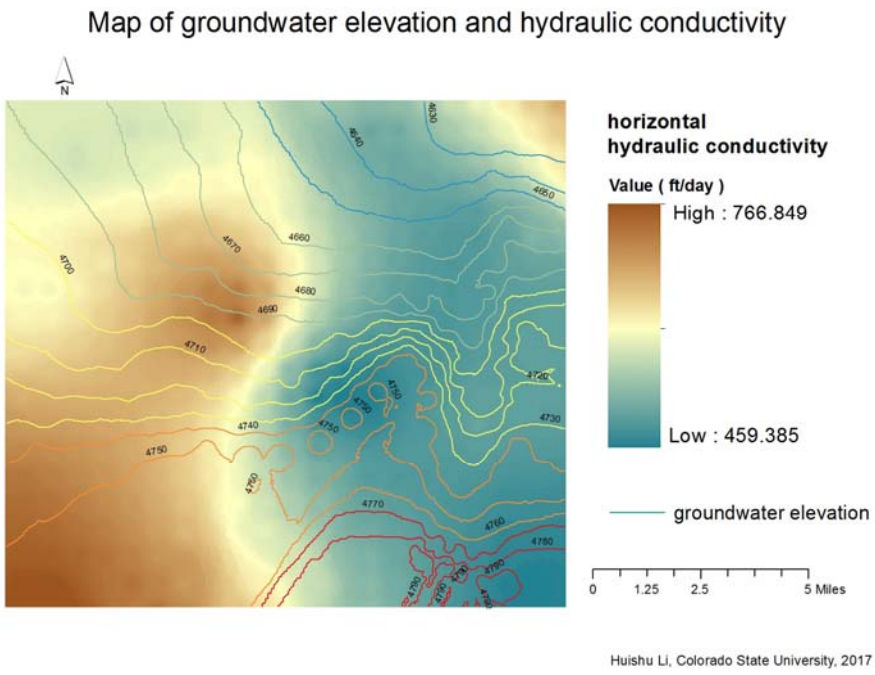

Figure 42. Map of groundwater elevation and horizontal hydraulic conductivity in the study area. (Groundwater elevation, unit: ft*,* $1m = 3.281\ ft$*; horizontal hydraulic conductivity, unit:* ft/day*.)*

As shown in Figure 43, the highest surface elevation of groundwater occurs in the southeast (4790 ft above sea level) and decreases to the northeast, therefore laterally the groundwater flow direction in this study area is from southeast to northeast. Since Laramie-Fox Hills aquifer is a confined aquifer, the vertical upgrade transport of the contaminant as well the diffusion could be ignored compared with the horizontal transport and advection. Therefore, 3-dimesion transport could be degraded to 2-dimension. The formation rocks on the west part of the study area have relative high horizontal hydraulic conductivity than on the east side,

7.4 Result

Based on groundwater elevation and horizontal hydraulic conductivity data, we can calculate Darcy velocity $u = \left(-K\frac{\partial h_x}{\partial l_x}, -K\frac{\partial h_y}{\partial l_y}\right)$ which has a close relationship with the fluid velocity v, i.e., $v = \frac{u}{\rho}$, where ρ is the effective porosity of the medium.

In this area, the contaminant transport porous media (Laramie-Fox Hills aquifer) has the porosity range in [0.21, 0.44] with the mean of 0.32 according to the USGS[157]. We assume that the porosity in this relatively small area is homogenous and we use the mean value $\rho = 0.32$ to calculate Darcy velocity and fluid velocity, which are shown in Figure 43 below.

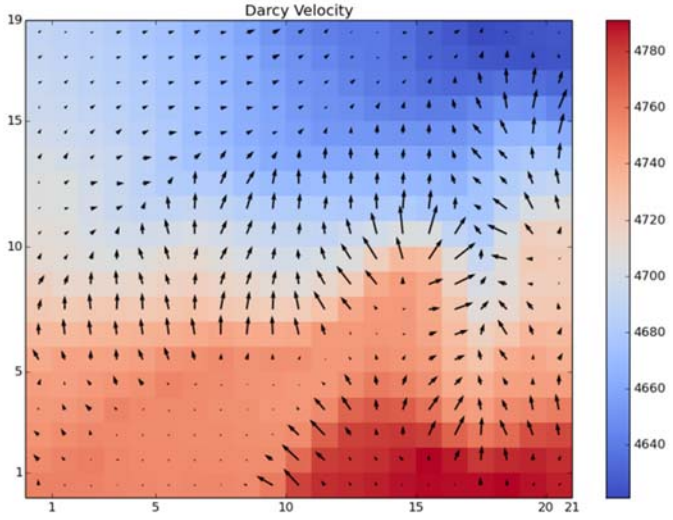

Figure 43. Interpolation map of Darcy velocity

In Figure 43, the background color map is rendered based on the groundwater elevation, where red color represents high levels and the blue represents low levels. The interpolation map shows the direction of the groundwater flow represented by the orientation of the arrows and the length of the arrows represent the magnitude of the velocity, according to equation (5). The absence of velocity arrows is due to the insufficient data resulting in interpolation of zero for the area on the left bottom of Figure 43.

To understand the transport of contaminants in the groundwater, we use chloride as an indicator of deep formation water intrusion and simulate the real-time event. Since according to the CWW study (Li et al 2016), salinity of the deep formation water (produced water) is 100-1000 times of the salinity of shallow drinking water and chloride is a major component of the salinity in groundwater and also is conservative with groundwater movement, the transport of chloride should be representative of the transport of the other

solute pollutants from deep formation or leakage from an oil and gas site. The fluid velocity we get from the previous steps can be input into the convection equation to simulate the chloride transport.

Given two contamination sources at time t_0, and the concentrations of chloride respectively are $c_0^1(7,7) = 20{,}000\, mg/L$, $c_0^2(18,4) = 20{,}000\, mg/L$. Compared with advection, the diffusion effect of chloride could be ignored, i.e.$D = 0$. Also, set $f = 0$, and time step $\Delta t = 3600s$ (1 hour). Based on these initial conditions, we simulate the chloride's transport process within some certain periods of time. The results are shown in Figure 44 below.

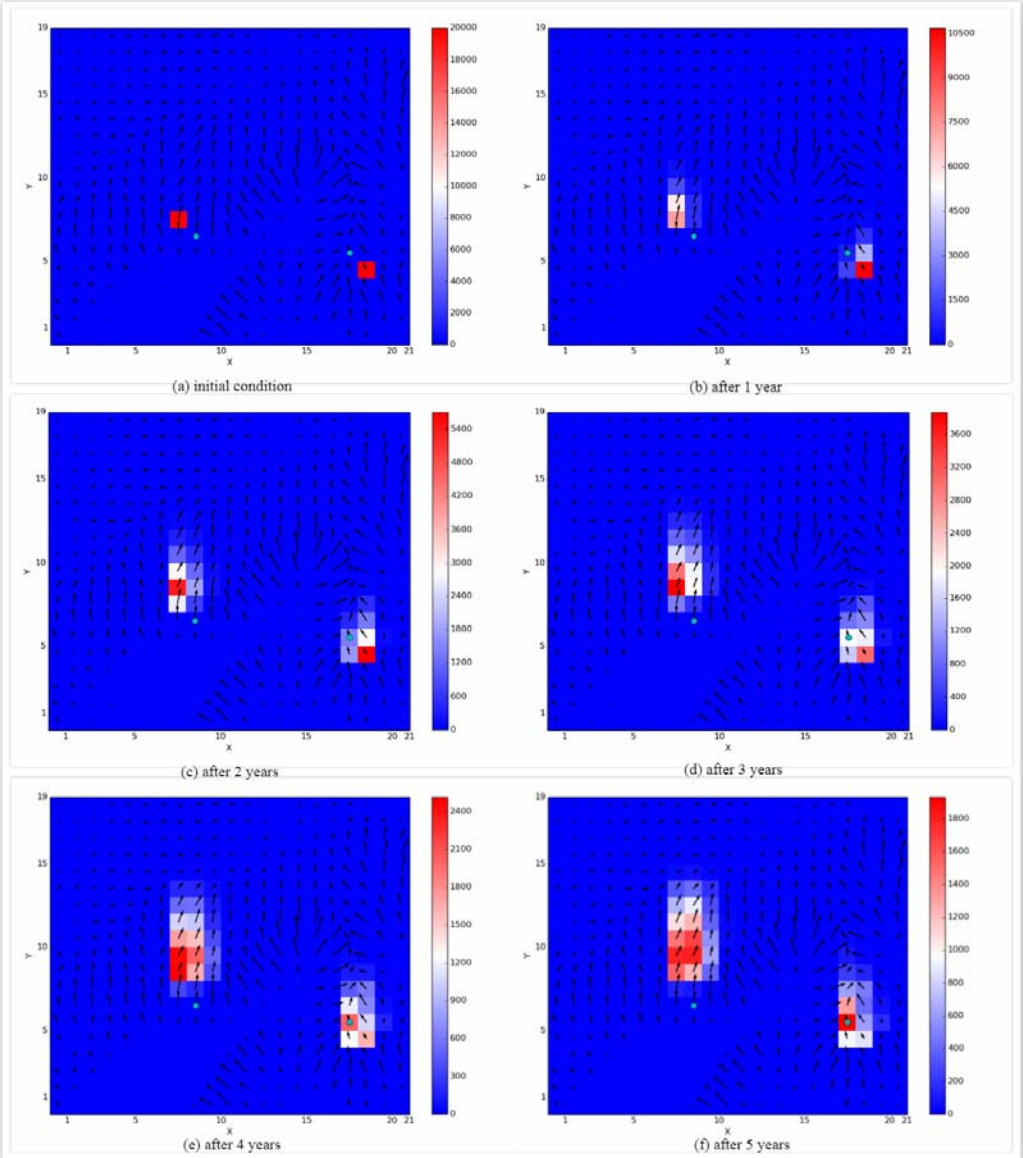

Figure 44. The change of contamination concentration with time.Red color represents high concentration, and blue represents low concentration. Two green points represent the location of monitoring stations. (a) – (f) represent the concentration of chloride in different time periods.

Figure 44 illustrates the chloride transport and migration at different time points. Figure 44 (a) is the initial condition that the maximum concentration of chloride occurs near the monitoring sites. Gilcrest, the green dots on the left, located parallel to the location where the contamination starts, while Platteville is in the downstream of this simulated contamination. After 1 year with groundwater movement, the chloride concentration near Gilcrest began to decrease since some chloride has been transported with groundwater and 5 years later, the chloride has been expanded to a larger area including an estimated 17 cells (1000m * 1000m). For the chloride contamination near Platteville, the pollution has not extended to the areas as large as the contamination near Gilcrest has, due to the low velocity in this region.

This simulation could help us understand the pollution transport with time, and also could help us to estimate the scope of the contaminant and the time when the maximum contaminant could reach at a certain point. As a result of Figure 7, Platteville could detect the pollution event since the contamination occurred upstream of the monitoring site of the groundwater flow. While for the Gilcrest site, the contaminant plum moves away from the site since the event occurred downstream of the monitoring site.

7.5 Conclusion

The case study simulation was based on the Darcy equation and the convection-diffusion equation. The finite difference method (FDM) was used to solve these two partial differential equations and to study the rectangular study area. Even though there are some shortcomings in this model (for example a cell size of 1000m x 1000m), the case study indicates the importance of the number and site selection of monitoring stations. The physical modeling presented here can be a powerful tool when interpreting real-time water quality modeling data, both as a predictor of where the contamination is going but perhaps more importantly, possible source areas that may correlate with oil and gas or other industrial activity.

Chapter 8 Paper 5- Site selection and performance evaluation for Colorado Water Watch groundwater monitoring network[5]

Overview

With the increased development of oil and gas activities in northern Colorado, public concerns over the environmental impacts associated with well drilling and fracturing has continued to rise. Issues such as oil and gas leakage to the subsurface environment and groundwater contamination have led to community interest and state regulations related to the establishment of groundwater quality monitoring sites in oil and gas activity areas, particularly those adjacent to urban development. The Colorado Water Watch was a groundwater monitoring network comprised of seven existing monitoring wells in the Wattenberg field to monitor shallow and deep groundwater quality and detect abnormal environmental events. In this study, the hydraulic and geologic data are used for site selection targeted to understand the groundwater quality and changes over time in the oil and gas active area. Water quality data over 2 years from five monitoring wells enable us to do performance evaluation and comparisons using entropy information and PCA methods. As a result, CHILL is the top information giving monitoring well, Gilcrest and LaSalle are the least informative and least important stations because of data efficiency.

8.1 Introduction

Groundwater quality issues related to the development of unconventional oil and natural gas exploration and production has received a lot of attention in recent years. To extract the natural gas and oil buried thousands of feet underground, wells are drilled vertically and then transitioned to a horizontal direction at the target formation (called horizontal drilling), and industrial fracture fluid is then injected to create "cracks" in the source rocks allowing the gas and oil to flow out of the low permeability and porosity rocks (such as tight sands and shale), known as "hydraulic fractu[5]ring"[158 159]. Additionally, a large amount of wastewater is generated during the exploration and production of oil and natural gas[160], and the majority of this

[5] Authors: Huishu Li*, Jianli Gu, Ken Carlson
Department of Civil and Environmental Engineering, Colorado State University, Fort Collins, CO, USA
Email: * huishu@rams.colostate.edu

wastewater is re-injected into the subsurface through class 2 disposal and enhanced oil recovery (EOR) wells[161]. Although drinking water aquifers are protected by several layers of well bore casing, natural gas, petroleum products or the wastewater has leaked into the environment when casing failures occurred[162]. There have been a few fatal events in Colorado due to natural gas leakage from pipelines or well bores[163] [164]. Areas with intense oil and gas activities, such as the Wattenberg field in northeast Colorado, also overlap with urban development or rural areas where the primary source of drinking water comes from groundwater aquifers. This colocation of oil and gas development with rural and urban populations has led to concerns regarding the health and safety of these activities. The Colorado Oil and Gas Conservation Commission has recently implemented Rule 609 requiring all new oil and gas wells to be accompanied by ground water wells within 0.5 miles to collect grab sample baseline data.[165]

Designing a groundwater monitoring network requires an understanding of hydrology, geology and geography at regional scale.[166] At the same time, it is necessary and important to quantify the effectiveness of a groundwater monitoring network to optimize the network design and give some valuable information to the well selection. An effective groundwater monitoring network should have a minimum numbers of monitoring sites but could still detect the contamination events from surrounding oil and gas wells at a high rate. Since a groundwater quality monitoring network is complicated, difficult and costly to establish, optimizing the monitoring locations is essential. Setting up a monitoring well is not easy and the network must be changed from time to time in concert with the changing data objectives and requirements. Importantly, a groundwater monitoring network is not only to collect data, but also to give information. The precision of decision-making with site selection in a groundwater quality monitoring network depends on how much regional and hydrogeological information is known. In addition, the increasing concerns for groundwater quality associated with unconventional oil and gas drilling and fracking has placed greater importance on groundwater management and monitoring.

The purpose of the groundwater monitoring network is to efficiently gather quality data. This goal can be achieved through the following procedures,

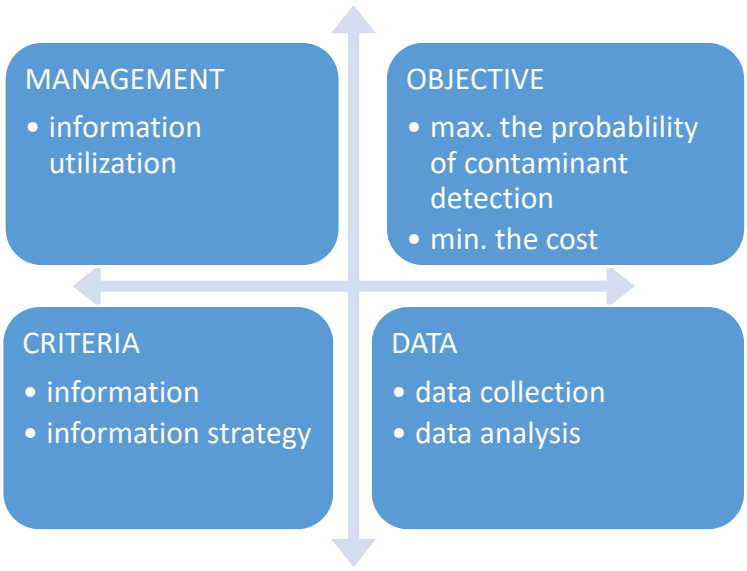

Figure 45. Diagram of the groundwater monitoring network design procedure

As shown in Figure 45, the first step is to define the major objectives of the project, which are groundwater quality monitoring and event detection in our study. The second step is to collect the requisite information and develop design strategies for the efficient collection of sufficient data. For the background information, we need to know the groundwater hydrology (such as groundwater level and groundwater flow direction), geology (such as the aquifer porosity, permeability), surface vegetation and elevation as well as current information about the oil and gas wells (such as locations, age and capacity) in the Wattenberg field. Based on this information, important criteria are determined and used to evaluate the candidate sites for monitoring wells. Finally based on the evaluation scores of each alternative location and the costs, the highest priority sites for monitoring can be determined. Besides the background knowledge discussed above, it is also important to determine the parameters that need to be measured, which not only provide the basic information about real-time water quality, but also can detect unusual changes or anomalies.

8.2 Methodology

8.2.1 Study area

The Colorado Water Watch[167] was developed initially to monitor the groundwater for areas in the Denver-Julesburg (DJ) Basin located in northern Colorado to detect statistically valid changes in groundwater quality that may be due to oil and gas industry activity. The Wattenberg field is located within the DJ Basin in northeast Colorado including the towns of Windsor, Greely, Johnstown, Longmont, Platteville, Fort Lupton and Brighton.[168] The Wattenberg field covers approximately 1,896 sections, a $1\ mile \times 1\ mile$ square area used in PLSS (the Public Land Survey System[169]), south to north ranges from 3S to 8N and west to east ranges from 68W to 61W.

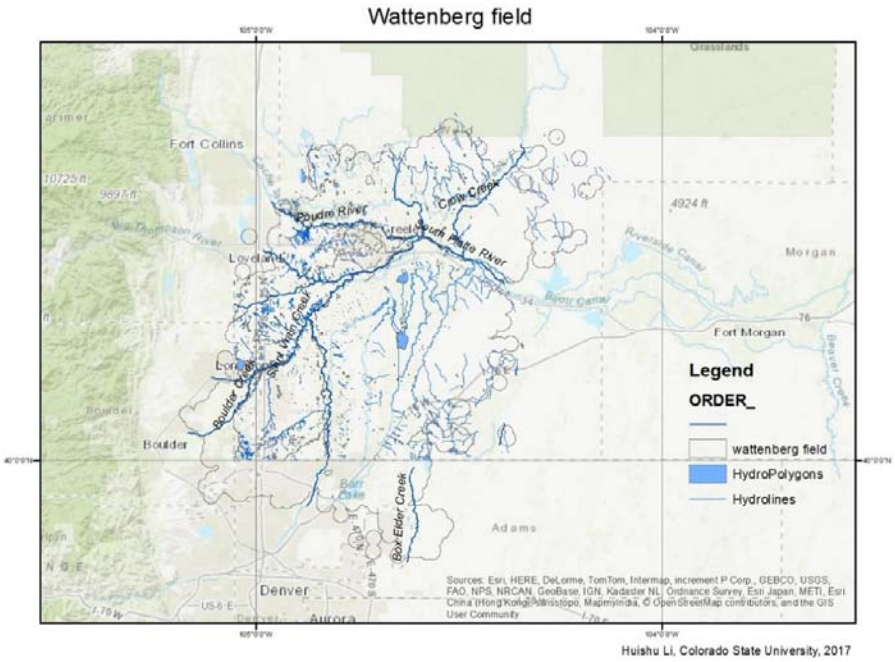

Figure 46. Map of study area, Wattenberg field

There are five major rivers that flow through the Wattenberg field; Cache la Poudre River, South Platte River, Boulder Creek, Crow Creek and Saint Vrain Creek.

8.2.2 Site selection criteria

The purpose of the monitoring wells is to monitor groundwater quality in oil and gas development regions and detect changes that could be related to any surface or sub-surface activity. Because it is of larger

probability that more "suspect contamination events" related to oil and gas activity would be caused by more oil and gas wells activity such as drilling and fracturing, we chose densities of oil and gas wells as one criteria for monitoring site selection. Also, since the overall aim of this project is to protect drinking water aquifers, it is important to have a monitoring well which is near to a groundwater well or surrounded by a few groundwater wells. Another essential factor when designing a groundwater monitoring network is the groundwater flow direction.

Therefore, the key criteria for selecting monitoring sites are:

I. Proximity: 1) proximity to existing oil and gas operations to monitor closely any potential adverse effects on groundwater aquifers; 2) proximity to future permitted oil and gas operations to be able to monitor before and after drilling and fracking in a particular area, and 3) proximity to municipal or domestic groundwater wells to monitor any potential effects of oil and gas development on these users and protect them through continuous monitoring.

II. Density: 1) groundwater well density; 2) oil/gas well density.

III. Groundwater flow direction and accumulation.

The data for existing and permitted oil and gas well locations in Colorado were obtained from GIS data provided by the COGCC (http://cogcc.state.co.us/data2.html#/downloads) and the data for active groundwater well locations in Colorado were obtained from the Colorado Division of Water Resources (DWR) database (http://water.state.co.us/DataMaps/DataSearch/Pages/DataSearch.aspx). An MCSDA was then conducted on the geo-processed data by weighting the criteria using the weighted overlay tool in ArcGIS to obtain the potential site recommendations. In order to compare and combine criteria II and criteria III, the Wattenberg field is subdivided into $1\ mile \times 1\ mile$ sections which is also a PLSS section. The densities are the numbers of groundwater wells or oil and gas wells in one section, and groundwater accumulation is also qualified as the sum of flows in one section.

8.2.3 Site performance evaluation

8.2.3.1 Entropy information

According to our previous research[170], the rapid change of conductivity, ORP and DO, would be closely related to oil and gas contamination. Also, multi-probe sensors are economically practical, pH, temperature, EC, ORP, DO and water depth were selected to be monitored by a multi-parameter in-situ probe (Hach Hydrolab, USA).

The entropy information based monitoring network design approach has been applied to evaluate and redesign regional groundwater monitoring networks since the 1990s.[171]

Entropy (H) -- The value of p(x) was calculated based on the frequency analysis of the available water quality parameter data of each well.

$$H(X) = \sum_{i=1}^{n} p_{x_i} \times log\left(p_{x_i}\right)$$

$$H(Y) = \sum_{i=1}^{n} p_{y_i} \times log\left(p_{y_i}\right)$$

$$H(X,Y) = -\sum_{j=1}^{m} \sum_{i=1}^{n} p(x_i, y_i) \times \log p(x_i, y_i)$$

$$T(X,Y) = H(X) + H(Y) - H(X,Y)$$

Pi is the discrete probability of occurrence for a single variable. *T* is the trans-information which is the difference between the sum of entropies and the joint entropy. A well which has a high entropy and low trans-information, gives the highest redundant information; the area or the zone which has the low entropy (information) value should, therefore, be the first priority for collecting more information.

8.2.3.2 Principle Component Analysis evaluation

PCA is another method we used to compare the performance of five monitoring sites.[172] For each year from 2014 to 2016, PCA analysis is performed to calculate the loadings of each monitoring station. The larger the loading is, the greater the contributions from this station. Water quality data for all the five monitoring wells is skewed and therefore we used the annual median value of each parameter to run the

PCA (principle component analysis). Each component of the PCA analysis is comprised of different combinations of the values for five stations.

8.3 Results and Discussion

8.3.1 Site selection

The number of groundwater wells and producing oil/gas wells were calculated for each PLSS section and the results are shown in Figure 47. The Wattenberg field covers 1,896 sections and 902 sections (47.6%) have no groundwater wells, 852 sections (44.9%) have 1-7 groundwater wells and 142 sections (7.5%) have more than 7 groundwater wells. As a result, there are 19 sections (1%) which have more than 7 groundwater wells and more than 20 oil and gas wells. The project called for installing 5 wells in the first year including a control site outside of the Wattenberg field. The 19 sections with more than 7 groundwater wells and more than 20 oil and gas wells are filtered out first and tagged as “high density PLSSs”.

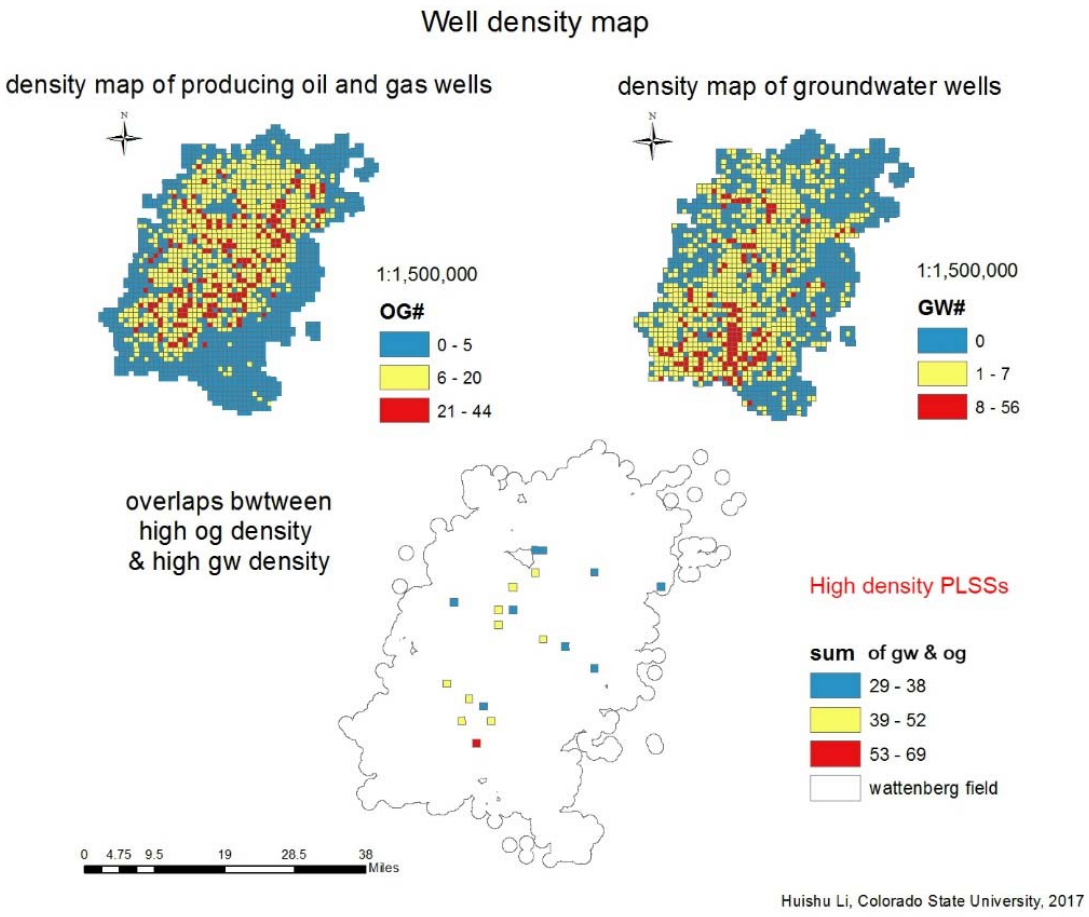

Figure 47. Density map of groundwater well and producing oil/gas well

Water well elevation data was collected from a U.S.G.S groundwater survey online database[19] including 3,125 wells in the Wattenberg field. The contour map of the groundwater table level (Figure 49 left) was interpolated from the groundwater table level and flow direction (Figure 49 right) and was determined by the hydraulic gradients which were represented as flow direction numbers in ArcGIS (the flow direction numbers are accumulated summation of inflows from adjacent cells). Most of the flow accumulation points are located near a water body, such as along the rivers, or near lakes.

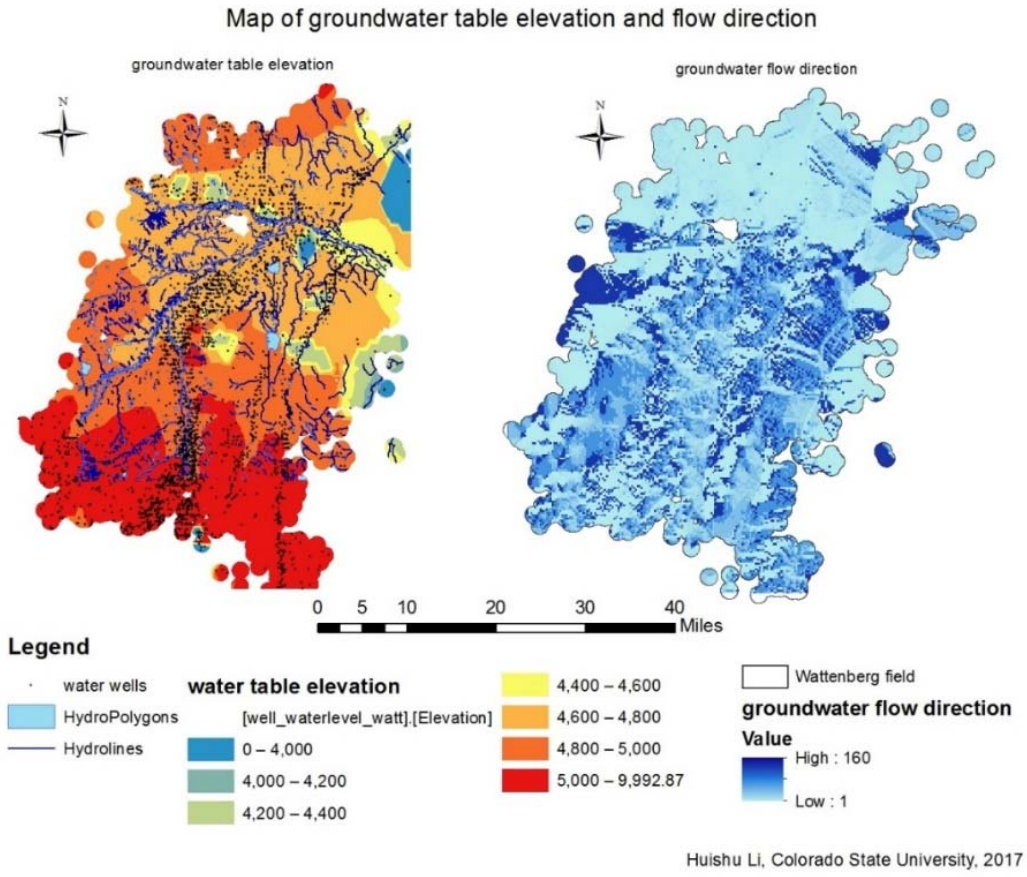

Figure 48. Contour map of groundwater table elevation and flow direction and flow accumulation Wattenberg field

The number of flow accumulations for each PLSS are calculated (Figure 48 left) and the overlap areas between high flow areas and high-density areas (Figure 49 right). Flow accumulation and flow direction are primarily based on the groundwater elevation file, calculating the differences in elevation (hydraulic head) and distances and as a result, groundwater flow along the "hydraulic slope" (slope equals to the ratio of elevation difference over distance difference between two points). Since the formation is confined, we assume lateral advection will be the major movement of the groundwater.

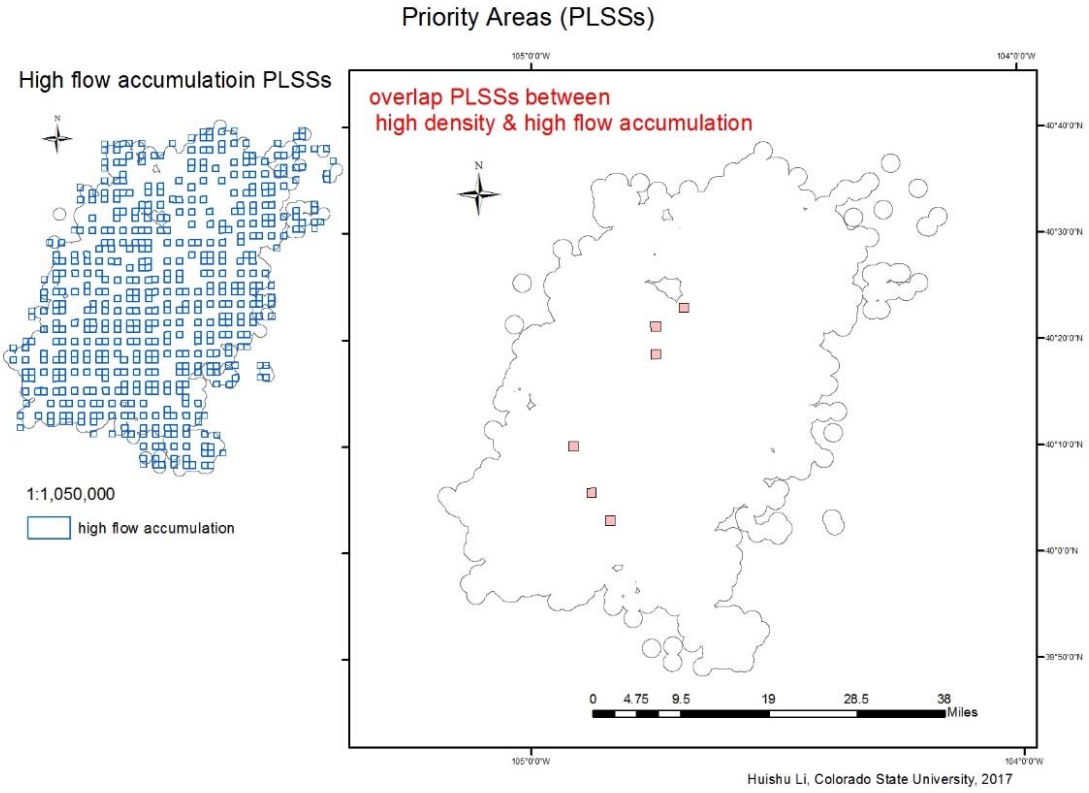

Figure 49. Map of priority areas to install monitoring well

Overall, 533 sections have accumulated flow ranked as the top 30% of all the sections. (Figure 49) Fortunately, there are six sections which are the overlaps between the 19 sections as the "high density sections" and the high flow accumulation sections. These 6 sections could be used as the potential sections for monitoring sites.

But due to the data unavailability at the beginning of this project design, criteria I is the major consideration to choose the site locations, and 5 monitoring sites were approved including 4 sites in the active oil and gas E&P area of the Wattenberg Field and one in Fort Collins as the control site (Figure 50). The earliest well ARDEC (the control site) was installed in March 2013 and the latest monitoring well was installed in November 2014.

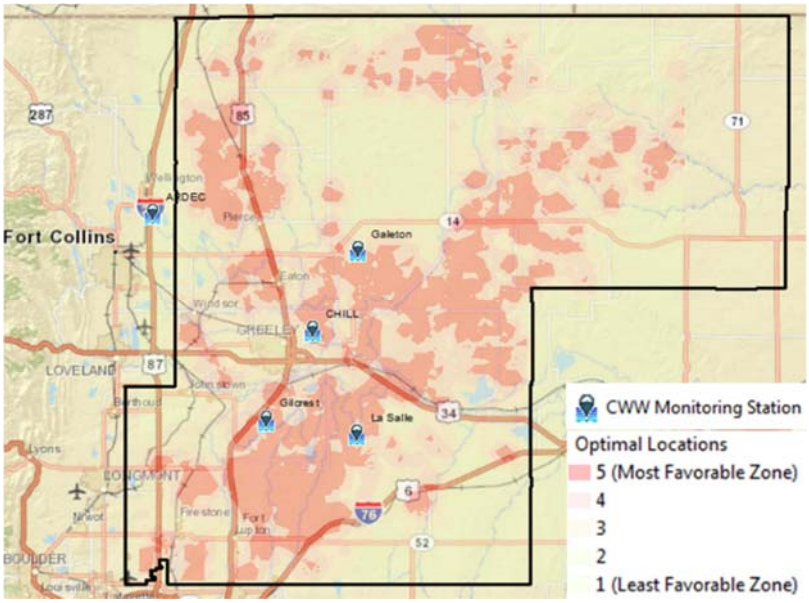

Figure 50. Map of favorable sites for the CWW monitoring stations based on multi-criteria spatial decision analysis

The control site was located in the DJ Basin in Northern Colorado, outside of the Wattenberg Field without any oil and gas wells within a 2-mile radius, surrounded by an agricultural area. Comparisons could be done between data from the control site and other monitoring stations.

8.3.2 Evaluation of monitoring stations' performance

Pearson's chi-square test is used to test the dependency between difference variables in our study (no data or NAs were removed for this test). As a result, all of the five variables are dependent ($p<<0.05$) which agrees with our assumption since except for temperature, the other four parameters are based on different combinations of the same anions and cations in water.

Therefore, we use the value of joint entropy to represent the data efficiency. For the dependent variables which have significant correlations with each other, "joint entropy" would be used and P_i becomes the joint probability. In this case, the joint entropy of the five dependent variables. $A_{1,\ldots,}$ A_5 are the five parameters we monitored.

$$H(A_1, A_2, A_3, A_4, A_5) = K \cdot \sum_{n=1}^{5} \sum_{n=1}^{5} p(A_1, A_2, A_3, A_4, A_5) \times \log\left(\frac{1}{p(A_1, A_2, A_3, A_4, A_5)}\right)$$

and the denotation of joint probability $p(A_1, A_2, A_3, A_4, A_5)$ should be,

$$p(A_1, A_2, A_3, A_4, A_5) = p(A_1/A_2, A_3, A_4, A_5) \cdot p(A_2/A_3, A_4, A_5) \cdot p(A_3/A_4, A_5) \cdot p(A_4/A_5) \cdot p(A_5)$$

The time frame of the water quality data is from the installation date to Sep 2016. Since the oldest well (ARDEC) was installed in Feb 2014 and the last well (LaSalle) was in Nov 2014, the longest water quality dataset contains the data for 137 weeks and the shortest observation period is about 81 weeks. We use the occurrence of the data to represent the probability. Since the default interval for the monitoring is every hour, there should be 24 data points per day for each parameter. Due to sporadic equipment failures or other factors, some data points were not collected. For example, if we got 20 data points for one day for a parameter, the probability will be 0.83 (20/24) which represents the frequency of the collected data. A plot of the trans-information vs time lag (weeks) is shown in Figure 51.

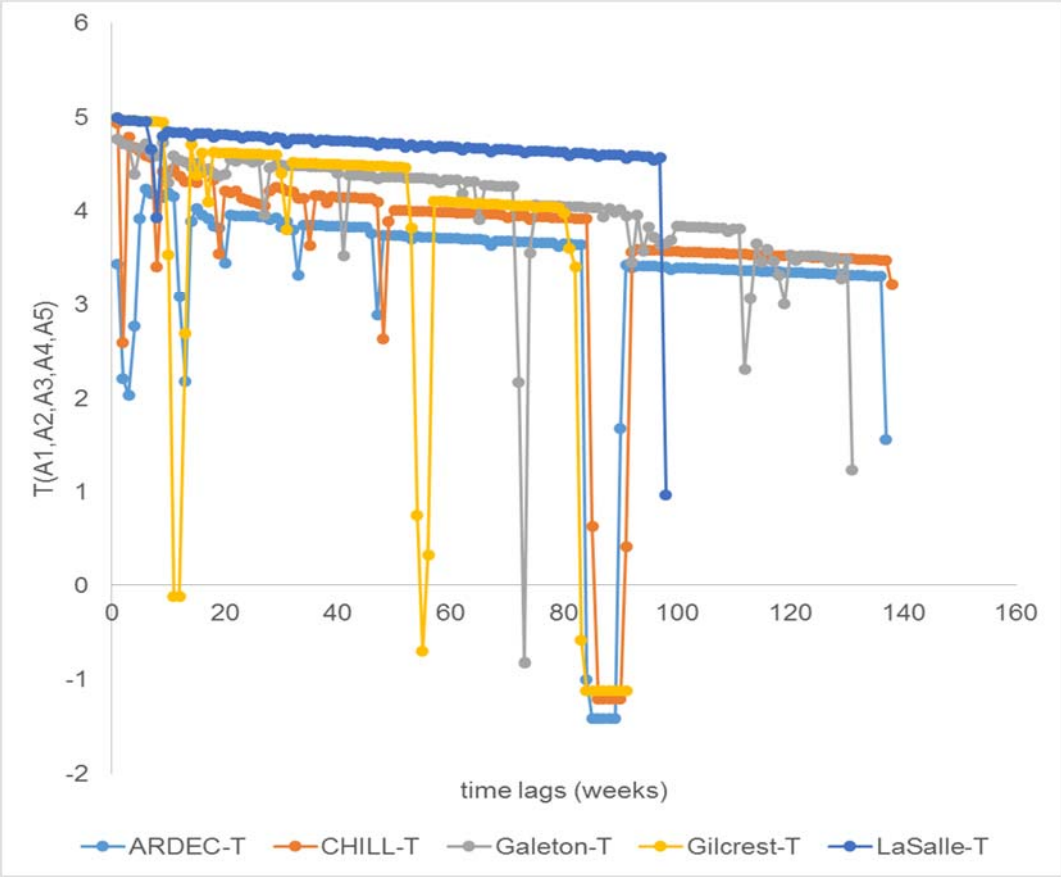

Figure 51. Plots of trans-information of five monitoring stations by week

The largest trans-information (T) is given by CHILL at 3.22, followed by ARDEC, Galeton and LaSalle, the lowest T is given by Gilcrest as -1.12 due to the data absence for over 8 weeks. Because CHILL is the oldest well and contributes the most data, the largest trans-information provided by CHILL indicates it is performing "perfect" among the five monitoring wells since the larger the T is, the more information and the less information redundancy the well provides. While the most redundant information is given by Gilcrest since there is 10 weeks out of the whole 91 weeks (11% of the monitoring period) that the data is invalid or is null.

Table 11. List of annual median values of five monitoring parameters for each well from 2014 to 2016

	2014	ARDEC	CHILL	Galeton	Gilcrest	LaSalle
Temperature		12.30	11.8	16.19	10.679	12.44
pH		7.23	7.87	8.53	7.55	7.38
conductivity		1.295	2.4	1.265	2.26	3.91
ORP		517	506	-198	105.082	90
DO		4.29	7.42	0	2.242	0
	2015	ARDEC	CHILL	Galeton	Gilcrest	LaSalle
Temperature		12.35	11.97	15.99	10.77	12.20
pH		7.23	7.34	8.63	7.20	7.51
conductivity		1.35	2.51	1.08	2.36	4.10
ORP		525	510	-230	364.50	183.00
DO		2.97	7.62	0	2.96	0
	2016	ARDEC	CHILL	Galeton	Gilcrest	LaSalle
Temperature		12.30	11.87	15.91	11.60	12.21
pH		7.34	5.38	8.69	7.15	7.25
conductivity		1.43	2.53	1.07	2.35	4.17
ORP		529	589	-307	507	116
DO		2.76	7.96	0	2.62	0

The summary of groundwater quality for each monitoring site is listed in table 11. Median values are chosen to represent the general groundwater quality. Temperature and pH for all the sites do not vary a lot indicating the groundwater quality as well as the sensors are stable. At the control site, ORP and DO of ARDEC have not changed significantly for the 3-year period. According to the data, the DO sensor is more stable than ORP sensor.

To understand which monitoring site is more important than the others, we use the PCA (principle component analysis) method to quantify the weightings of each site in the whole monitoring network. Considering the whole monitoring network is a matrix comprised of five elements (five monitoring sites), loadings of each site will represent the importance of the site. Higher loading of the site corresponds to a more important role of this site than the sites with lower loadings.

For 2014, 2015 and 2016 data, all the PC1s (first component of principle components usually accounts for the most variability in the database) accounts for over 90% of the total variance, 99.92% for the year 2014, 99.95% for the year 2015 and 99.96% for the year 2016, therefore our focus will be on the first

principle components (PC1). Comparison of the PC1 loadings of each site annually and the percentage for each site taken over the summation of all the loadings by year are plotted in Figure 52.

$$2014: PC1 = 0.5970350 \times ARDEC + 0.6137111 \times CHILL - 0.2971110 \times Galeton + 0.3971286 \times Gilcrest + 0.1446440 \times LaSalle$$

$$2015: PC1 = 0.6042439 \times ARDEC + 0.5851380 \times CHILL - -0.2749790 \times Galeton + 0.4175819 \times Gilcrest + 0.2061911 \times LaSalle$$

$$2016: PC1 = 0.5300739 \times ARDEC + 0.5898578 \times CHILL - 0.3174440 \times Galeton + 0.5077965 \times Gilcrest + 0.1116304 \times LaSalle$$

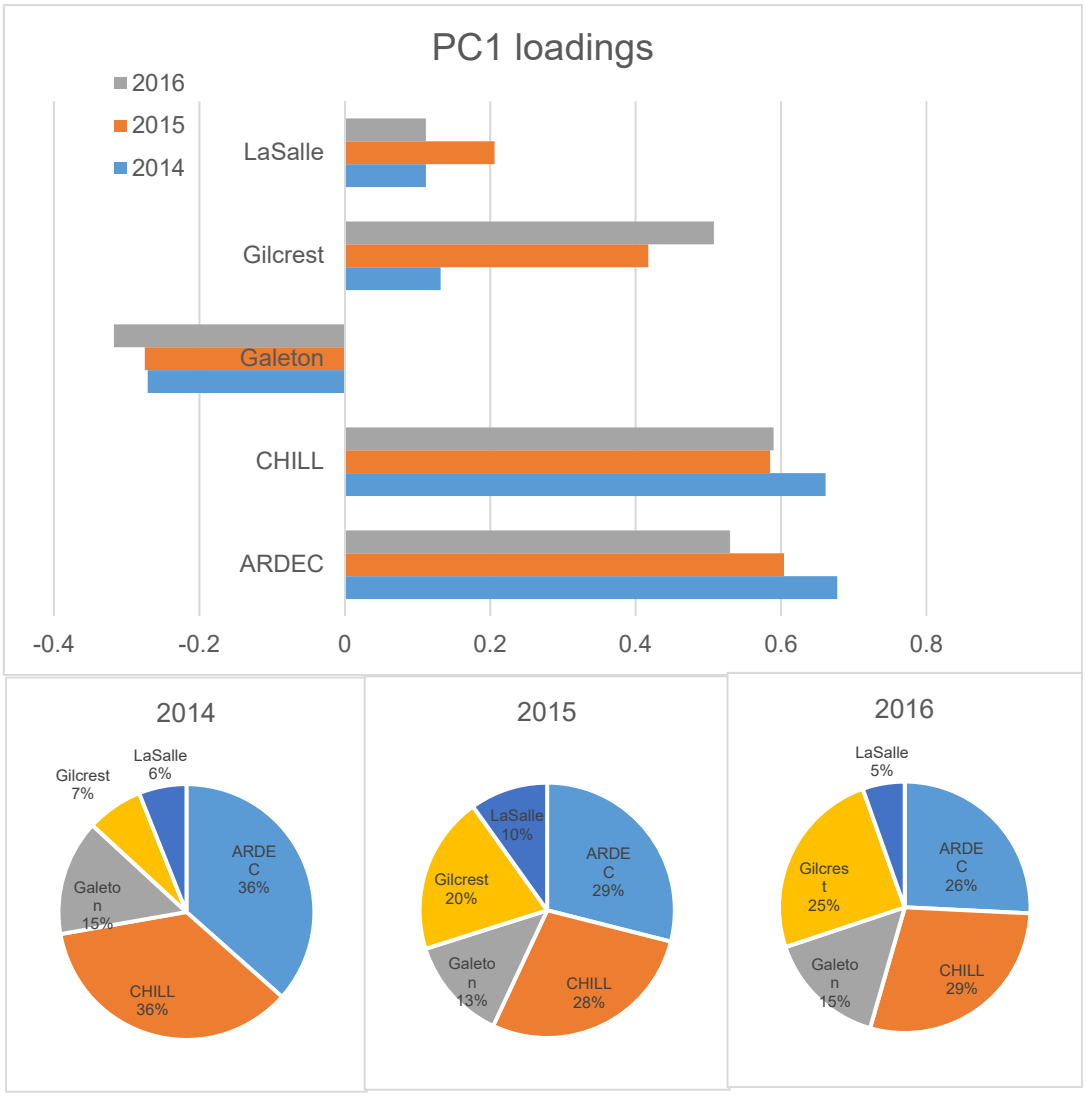

Figure 52. Annual PC1 loadings for each monitoring site

For each year, PC1 loadings of ARDEC and CHILL took over 50% of the total summation of the absolute values of every loading (figure 52). This result agrees with our expectation because ARDEC is the only control site; CHILL is located in a most dense oil/gas active area and also among the oldest wells thus contributing the second most data to the database.

For both PCA analysis and the entropy method, CHILL is the top information giving monitoring well, Gilcrest and LaSalle are the least informative stations in terms of data efficiency and the importance among all of the five monitoring stations.

8.4 Conclusions

Groundwater monitoring network design is usually limited by budget and the availability of data. Accordingly, site selection can be a crucial aspect of network design allowing for the most efficient use of resources. In our study, both geography information (geographic location, density information) and geology information (such as groundwater surface elevation, groundwater flow) are used as the criteria to choose the monitor sites. Additionally, this study has examined methods for utilizing the data while extracting useful information, such as monitoring site performance applying an entropy method and PCA.

Chapter 9 Conclusion and Future Work

As unconventional oil and gas development continues to boom in Colorado and nationally, extracting oil and natural gas from shale formations is a controversial topic due to the uncertain consequences especially caused by hydraulic fracturing. To extract oil and natural gas from a shale formation, it requires vast amount of water to hydraulically fracture the formation to allow hydrocarbons escape from low permeability and low porosity rocks. As oil and natural gas is produced from a well, high volumes of water will also flow to the surface and this produced water is extremely saline and high in oil and grease and other chemicals used in drilling and fracking fluids. The footprint of water in shale oil and gas activity, groundwater protection, and air pollution have been studied by several institutes and universities nation-wide. But due to the disparate geology settings of shale formations, environmental impacts of oil and gas operations and groundwater protection associated with oil and gas development will likely be different.

The produced water cycle involves water demand for hydraulic fracturing, flowback and produced water handling and treatment, deep formation water leakage to shallow groundwater aquifers and other mechanisms. The research discussed in this dissertation was a comprehensive attempt to understand several aspects of the produced water cycle and further to develop methods for monitoring of contamination. This included the characteristics of produced water in the Wattenberg field, dissolved methane distribution in the Wattenberg field, characteristics of "contaminated" groundwater and the differences between produced water and produced water in Wattenberg field, aqueous phase contamination transport in the Wattenberg field, and development of a regional groundwater monitoring network - Colorado Water Watch.

Other environmental issues including monitoring for methane and volatile organic compounds in the atmosphere, water stress and the relationship between oil and gas development and climate change in the Wattenberg field, will be the subject of future research which will help us to further understand the interactions between the environment and oil and gas operations.

References

1. BP statistical review of world energy, June 2017. https://www.bp.com/content/dam/bp/en/corporate/pdf/energy-economics/statistical-review-2017/bp-statistical-review-of-world-energy-2017-full-report.pdf

2. H. Johnson and A. G. Dore, January 2010, Unconventional oil and gas resources and the geological storage of carbon dioxide: overview, Geological Society, London, Petroleum Geology Conference, Vol. 7:1061-1063

3. U.S. Crude oil, natural gas, and natural gas liquids reserves, November 2010, U.S. Energy Information Administration, available online at http://205.254.135.7/pub/oil_gas/natural_gas/data_publications/crude_oil_natural_gas_reserves/current/pdf/table14.pdf

4. Rigzone Staff, December 2010. Shale Gas Development Drives U.S. Reserves to New High. Available online at: https://www.rigzone.com/news/oil_gas/a/101780/shale_gas_development_drives_us_reserves_to_new_high/

5. Colorado School of Mines, Potential Gas Committee reports unprecedented increase in magnitude of U.S. natural gas resource base, June 18, 2009, available online at http://www.mines.edu/Potential-Gas-Committee-reports-unprecedented-increase-inmagnitude-of-U.S.-natural-gas-resource-base

6. Annual Energy Outlook 2017 with projections to 2050, January 2017. U.S. Energy Information Administration. Available online at: https://www.eia.gov/outlooks/aeo/pdf/0383(2017).pdf

7. The SEAB Shale Gas Production Subcommittee Ninety-Day Report, August 11, 2011, available online at http://www.shalegas.energy.gov/resources/081111_90_day_report.pdf

8. J. Daniel Arthur, 2008, Hydraulic Fracturing Considerations for Natural Gas Wells of the Fayetteville Shale, Copyright ©, ALL Consulting, available online at http://www.aogc.state.ar.us/ALL%20FayettevilleFrac%20FINAL.pdf

9. Hubbert, M.K. and Willis, D.G., 1972. Mechanics of hydraulic fracturing.

10. Schein, G. The Application and Technology of Slickwater Fracturing, https://www.onepetro.org/download/general/SPE‐108807‐DL?id=general%2FSPE‐108807‐DL, 2005.

11. Available online at: http://petrowiki.org/Fracturing_fluids_and_additives

12. Luke Geiver, 2014. The slickwater story. North American Shale. Available online at: http://northamericanshalemagazine.com/articles/711/the-slickwater-story

13. E.I.A, 2018. Annual energy outlook 2018. Available online at: https://www.eia.gov/outlooks/aeo/pdf/AEO2018.pdf

14. Matuszczak, R.A., 1973. Wattenberg Field Denver Basin, Colorado. The Mountain Geologist.

15. U.S. Energy Information Administration, March 2015. Top 100 U.S. oil and gas fields. Available online at: https://www.eia.gov/naturalgas/crudeoilreserves/top100/pdf/top100.pdf

16. Clark, C.E and Veil, J. A., 2009. Produced water volumes and management practices in the United States. Available online at: http://www.ipd.anl.gov/anlpubs/2009/07/64622.pdf

17. Available at: https://www.eia.gov/dnav/ng/ng_pri_sum_dcu_nus_m.htm

18. Carr, A.D., 2000. Suppression and retardation of vitrinite reflectance, Part 1. Formation and significance for hydrocarbon generation. Journal of Petroleum Geology, 23(3), 313-343.

19. Available online at: https://www.epa.gov/hfstudy/hydraulic-fracturing-water-cycle

20. Caulton, D.R., Shepson, P.B., Santoro, R.L., Sparks, J.P., Howarth, R.W., Ingraffea, A.R., Cambaliza, M.O., Sweeney, C., Karion, A., Davis, K.J. and Stirm, B.H., 2014. Toward a better understanding and quantification of methane emissions from shale gas development. Proceedings of the National Academy of Sciences, 111(17), pp.6237-6242.

21. Khan, F.I. and Ghoshal, A.K., 2000. Removal of volatile organic compounds from polluted air. Journal of loss prevention in the process industries, 13(6), 527-545.

22. Satterfield, J., M. Mantell, D. Kathol, F. Hiebert, K. Patterson, and R. Lee, September 2008, Chesapeake Energy Corp. Managing Water Resource's Challenges in Select Natural Gas Shale Plays, presented at the GWPC Annual Meeting.

23. Modern Shale Gas Development in the United States: A Primer, pp. 58-59

24. White paper: U.S. Shale Gas -An Unconventional Resource. Unconventional Challenges, Halliburton, 2008. Available online at: http://www.halliburton.com/public/solutions/contents/shale/related_docs/H063771.pdf

25. Veil, J.A., Puder, M.G., Elcock, D. and Redweik Jr, R.J., 2004. A white paper describing produced water from production of crude oil, natural gas, and coal bed methane (No. ANL/EA/RP-112631). Argonne National Lab., IL (US).

26. Veil Environmental LLC, prepared for the groundwater water protection council. U.S. produced water volumes and management practices in 2012.

27. Veil, J., M.G. Puder, D. Elcock, and R.J. Redweik, Jr., 2004, A White Paper Describing Produced Water from Production of Crude Oil, Natural Gas, and Coal Bed Methane. Available at http://www.ead.anl.gov/pub/doc/ProducedWatersWP0401.pdf. Accessed May 5, 2009.

28. Johanna Haggstrom. Toolbox available to treat flowback and produced water.

29. Wachtmeister, H., Lund, L., Aleklett, K. et al, 2017. Production Decline Curves of Tight Oil Wells in Eagle Ford Shale. Natural Resources Research, 26, 365-377. https://doi.org/10.1007/s11053-016-9323-2

30. http://www.cpr.org/news/story/colorado-whats-lifespan-oil-and-gas-well

31. Horn, A.D., 2009. Breakthrough Mobile Water Treatment Converts 75% of Fracturing Flowback Fluid to Fresh Water and Lowers CO2 Emissions, Society of Petroleum Engineers, SPE 121104.

32. Halley L. Brantley, Eben D. Thoma & Adam P. Eisele, 2015. Assessment of volatile organic compound and hazardous air pollutant emissions from oil and natural gas well pads using mobile remote and on-site direct measurements, Journal of the Air & Waste Management Association, 65:9, 1072-1082, DOI: 10.1080/10962247.2015.1056888.

33. Available online at: https://www.epa.gov/ghgemissions/overview-greenhouse-gases

34. J. B. Gilman, B. M. Lerner, W. C. Kuster, and J. A. de Gouw, 2013. Source Signature of Volatile Organic Compounds from Oil and Natural Gas Operations in Northeastern Colorado. Environmental Science & Technology, 47 (3), 1297-1305. DOI: 10.1021/es304119a

35. Argonne national laboratory. Produced water volumes and management practices in the United States. Available online at: http://www.circleofblue.org/wp-content/uploads/2010/09/ANL_EVS__R09_produced_water_volume_report_2437.pdf

36. Arthur, J. D.; et al, 2008. Hydraulic Fracturing Considerations for Natural Gas Wells of the Fayetteville Shale; ALL Consulting: Tulsa. Available online at: http://www.all-llc.com/publicdownloads/ALLFayettevilleFracFINAL.pdf.

37. Kargbo, D. M.; Wilhelm, R. G.; Campbell, D. J. Natural gas plays in the Marcellus shale: Challenges and potential opportunities. Environ. Sci. Technol. 2010, 44, 5679−5684.

38. National Research Council: Hidden costs of energy: unpriced consequences of energy production and use; National Academy of Sciences Press: Washington, DC, 2009.

39. Jiang, M. Life cycle greenhouse gas emissions of Marcellus shale gas. Environ. Res. Lett. 2011, 6 (3), 034014.

40. Rice, D. D.; Claypool, G. E. Generation, accumulation and resource potential of biogenic gas. AAPG Bull. 1981, 65, 5−25.

41. Schoell, M. Multiple origins of methane in the earth. Chem. Geol. 1988, 71, 1−10.

42. Gurevish, A. E.; et al. Gas migration from oil and gas fields and associated hazard. J. Pet. Sci. Eng. 1993, 9, 223−238.

43. COGA. Water Use Fast Facts, 2012; http://www.coga.org/pdfs_facts/WaterUse_Fast_Fact.pdf.

44. Weimer, R. J.; et al. Geology of tight gas reservoirs. In Wattenberg Field, Denver Basin, Colorado: American Association of Petroleum Geologists: Tulsa, 1986; pp 143−164.

45. COGCC-300 series Drilling, Development, Production and Abandonment, Rule 318A.e; http://cogcc.state.co.us/RR_HF2012/Groundwater/FinalRules/FinalGWA_318Ae4_01092013.pdf

46. Wattenberg field. http://www.ci.longmont.co.us/pwwu/oil_gas/documents/2_att1_map1.pdf.

47. United States Environmental Protection Agency. http://water.epa.gov/scitech/drinkingwater/labcert/analyticalmethods.cfm.

48. Kampbell, D. H.; Vandegrift, S. A. Analysis of dissolved methane, ethane, and ethylene in groundwater by a standard gas chromatographic technique. J. Chromatogr. Sci. 1998, 36, 253−256.

49. Aromatic and halogenated volatiles by gas chromatography using photoionization and/or electrolytic conductivity detectors; http://www.epa.gov/osw/hazard/testmethods/sw846/pdfs/8021b.pdf.

50. Chanton, J.; Liptay, K. Seasonal variation in methane oxidation in a landfill cover soil as determined by an in situ stable isotope technique. Global Biogeochem. Cycles 2012, 14 (1), 51−60.

51. Smith, M. R.; Mah, R. A. Acetate as a sole carbon and energy source for growth of Methanosarcina Strain 227. Appl. Environ. Microbiol. 1980, 39 (5), 993−999.

52. Belyaeves, S.; Laurinavichljks, K. S.; Gaytan, V. I. Modem microbiological formation of methane in the quarternary and Pliocene rocks of the Caspanian Sea. Geochem. Int. 1977, 4, 172−l 76.

53. Balabane, M.; Galimov, E.; Hermann, M.; Létolle, R. Hydrogen and carbon isotope fractionation during experimental production of bacterial methane. Org. Geochem. 1987, 11 (2), 115−119.

54. Floodgate, Li; Judd, G. The origins of shallow gas. Cont. Shelf Res. 1992, 12, 1145−1156.

55. Rice, D. D.; Ladwig, L. R. Distinction between in-situ biogenic gas and migrated thermogenic gas in ground water, Denver Basin, Colorado, 1983; http://cogcc.state.co.us/Announcements/1983USGSreport.pdf.

56. Whiticar, M. J.; Faber, E.; Schoell, M. Biogenic methane formation in marine and freshwater environments: CO2 reduction vs. acetate fermentation − Isotope evidence. Geochim. Cosmochim. Acta 1986, 50, 693−709.

57. Rice, D. D.; Claypool, G. E. Generation, accumulation and resource potential of biogenic gas. AAPG Bull. 1981, 65, 5−25.

58. Bowling, D.; et al. Soil, plant, and transport influences on methane in a subalpine forest under high ultraviolet irradiance. Biogeoscience 2009, 6, 1311−1324.

59. Whiticar, M. J.; Muller, V.; Blaut, M. Isotope tracking of methanol disproportionation during methanogenesis – Confirmation of natural isotope effects; USEPA: Washington, DC, 1988; Vol. 195, p 98

60. Mackenzie, A. S.; Quigley, T. M. Principles of geochemical prospect appraisal. Am. Assoc. Pet. Geol. Bull. 1988, 72, 399−415.

61. Collett, T. S.; Dallimore, S. R. Hydrocarbon gases associated with permafrost in the Mackenzie Delta, Northwest Territories, Canada. Appl. Geochem. 1999, 14, 607−620.

62. Jenden, P. D.; Drazan, D. J.; Kaplan, I. R. Mixing of thermogenic natural gases in northern Appalachian basin. Am. Assoc. Pet. Geol. Bull. 1993, 77 (6), 980−998.

63. Lovley, D. R.; Chapelle, F. H. Deep subsurface microbial processes. Geophysics 1995, 33 (3), 365−381.

64. Whiticar, M. J.; Faber, E.; Schoell, M. Biogenic methane formation in marine and freshwater environments: CO2 reduction vs. acetate fermentation-Isotope evidence. Geochim. Cosmochim. Acta 1986, 50, 693−709.

65. Day, M. J.; Reinke, R. F.; Thomoson, J. A. M. Fate and transport of fuel components (including MTBE) below slightly leaking underground storage tanks. Environ. Forensics 2001, 2 (1), 21−28.

66. Poulsen, M.; Lemon, L.; Barker, J. F. Dissolution of monoaromatic hydrocarbons into groundwater from gasoline-oxygenate mixtures. Environ. Sci. Technol. 1992, 26 (12), 2483−2489.

67. Robson, S. G. Geologic Structure, Hydrology, and Water Quality of the Laramie fox Hills Aquifer in the Denver Basin, Colorado. Geological Survey Hydrologic Investigations Atlas HA-650; USGS: Reston, VA, 1981.

68. Robson, S. G.; Banta, E. R. Ground Water Atlas of the United States: Arizona, Colorado, New Mexico, Utah (HA 730-C); U. S. Geological Survey: Reston, VA, 1995.

69. Jackson, R. B.; Vengosh, A.; Darrah, T. H.; Warner, N. R.; Down, A.; Pored, R. J.; Osborn, S. G.; Zhao, K.; Karr, J. D. Increased stray gas abundance in a subset of drinking water wells near Marcellus shale gas extraction. Proc. Natl. Acad. Sci. U.S.A. 2013, 110 (28), 11250−11255.

70. New setback and groundwater rule, Rule 600 series; http://cogcc.state.co.us/announcements/hot_topics/setbacks/Definitions_Zones_Exceptions.pdf.

71. Coplen, T. B. Reporting of stable hydrogen, carbon, and oxygen isotopic abundances. Pure Appl. Chem. 1994, 66, 273−276.

72. Hearne, Glenn A., Wireman, M., Campbell, A., Turner, S., and Ingersoll, G.P., 1995. Vulnerability of the uppermost ground water to contamination in the greater Denver area, Colorado. Water- Resources Investigation Report 92-4143, U. S. Geological Survey.

73. Kharak, Y. K., Thordsen, J.J., Conaway, C.H., and Thomas, R.B., 2013. The energy-water nexus: potential groundwater-quality degradation associated with production of shale gas. Procedia Earth and Planetary Science 7, 417–422.

74. Toril I. Roe Utvik, 1999. Chemical characterization of produced water from four offshore oil production platforms in the North Sea. Chemosphere 39 (15), 2593-2606.

75. McMahon, P.B., Thomas, J.C., and Hunt, A.G., 2013. Chemistry and age of groundwater in Bedrock Aquifers of the Piceance and Yellow Creek Watersheds, Rio Blanco County, Colorado, 2010–12: U.S. Geological Survey Scientific Investigations Report 2013–5132, 89 p., http://pubs.usgs.gov/sir/2013/5132/.

76. Johnson, R. C., and Rice, D. D, 1990. Occurrence and geochemistry of natural gases, Piceance Basin, northwest Colorado. American Association of Petroleum Geologists Bulletin 74, 805–829.

77. Sharma, S., Mulder, M.L., Sack, A., Schroeder, K., and Hammack, R., 2014. Isotope approach to assess hydrologic connections during Marcellus shale drilling. Ground Water 52(3), 424–433.

78. Robson, S. G., 1981. Geologic structure, hydrology, and water quality of the Laramie-Fox Hills aquifer in the Denver Basin, Colorado. U.S. Geological Survey Hydrogeologic Investigations Atlas 650.

79. Knepper, D.H.K., 2002. Planning for the conservation and development of infrastructure resources in urban areas -- Colorado Front Range Urban Corridor. U.S. Geological Survey Circular 1219. U.S. Geological Survey, Denver, CO. http://pubs.usgs.gov/circ/2002/c1219/c1219.pdf.

80. Osborn, S. G., Vengosh, A., Warner, N.R., and Jackson, R.B., 2011. Methane contamination of drinking water accompanying gas-well drilling and hydraulic fracturing. Proceedings of the National Academy of Sciences of the United States of America 108(20), 8172–8176.

81. Stempvoort, D.V., Maathuis H., Jaworski, Ed, Mayer, B., and Rich, K., 2005. Oxidation of fugitive methane in ground water linked to bacterial sulfate reduction. Ground Water 43(2), 187–199

82. Taylor, S.W., Maathuis, H., Jaworski, Ed, Mayer B., and Rich, K., 2000. Bacteriogenic ethane in near-surface aquifers: Implications for leaking hydrocarbon well bores. Environmental Science & Technology 34(22), 4727–4732

83. Entrekin, S., Evans-White, M., Johnson, B., and Hagenbuch, E., 2011. Rapid expansion of natural gas development poses a threat to surface waters. Front. Ecol. Environ 9, 503-511.

84. API Guidance Document HF1 First Edition, 2009. Hydraulic fracturing operations—well construction and integrity guidelines. American Petroleum Institute: Washington, DC. http://www.shalegas.energy.gov/resources/HF1.pdf.

85. Colorado 2014 -- State profiles and energy estimates; http://www.eia.gov/state/?sid=CO#tabs-3 (Accessed on January 7, 2014).

86. Colorado Oil and Gas Commission Website, Colorado Oil and Gas Information System (COGIS) Production Data Inquiry; http://cogcc.state.co.us (Accessed on January 8, 2014).

87. Dusseault, M. B. and Gray, M. N, 2000. Why Oil Wells Leak-Cement behavior and Long Term Consequences, SPE64733. http://dx.doi.org/10.2118/64733-MS.

88. Chafin, D. T, 1994. Sources and migration pathways of natural gas in near-surface ground water beneath the Animas River Valley, Colorado and New Mexico. Water Resources Investigation Report 94-4006. Denver, Colorado: U. S. Geological Survey.

89. Gurevich, A. E., Endres, B.L., Robertson, J.O. and Chilingar, G.V., 1993. Gas migration from oil and gas fields and associated hazards. Journal of Petroleum Science and Engineering 9,223-238.

90. Environmental Protection Agency, 1996. How to effectively recover free product at leaking underground storage tank sites, a guide for state regulators: Chapter 3, Behavior of hydrocarbons in the subsurface. EPA 510-R-96-001.

91. Li, H.S., Carlson, K. H., 2014. Distribution and origin of groundwater methane in the Wattenberg oil and gas field of northern Colorado. Environ. Sci. Technology 48 (3), 1481-1491

92. Land, L. S., Prezbindowski, D. R., 1981. The origin and evolution of saline formation water, lower Cretaceous carbonates, South-Central Texas, U. S. A. Journal of Hydrology 54, 51-74.

93. COGCC- 300 series Drilling, Development, Production and Abandonment, Rule 318A.e, 2015. http://cogcc.state.co.us/RR_HF2012/Groundwater/FinalRules/FinalGWA_318Ae4_01092013.pdf

94. Li, H.S, 2013. Produced water quality characterization and prediction for Wattenberg Field. Colorado State University.

95. Whiticar, M. J, 1999. Carbon and hydrogen isotope systematics of bacterial formation and oxidation of methane. Chemical Geology 161, 291-314.

96. Robson, S. G., Banta, E. R., 1987. Geology and hydrology of deep bedrock aquifers in eastern Colorado. U.S.G.S WRIR 5-4240.

97. Weimer, R. J., 1973. A guide to the uppermost cretaceous stratigraphy, central front range Colorado: deltaic sedimentation, growth faulting and early laramide crustal movements. The Mountain Geologist 10 (3), 53-97.

98. Robson, S. G., Andrew W., 1981. Geologic structure, hydrology and water quality of the Laramie-Fox Hill aquifer in the Denver basin, Colorado. U.S.G.S. 1981.

99. Hem, J. D, 1989. Study and Interpretation of the Chemical Characteristics of Natural Water. U.S.G.S. Water-Supply Paper 2254. US Government Printing Office, Washington.

100. Weimer, R. J., Sonnenberg, S.A., and Young, G.B.C., 1986. Wattenberg field, Denver basin, Colorado. AAPG Studies in Geology of Tight gas reservoirs 24, 143-164.

101. COGA, Water Use Fast Facts, 2012. http://www.coga.org/pdfs_facts/WaterUse_Fast_Fact.pdf.

102. Kinsey, E.W.(III), Sharif, S., and Harry, D.N., 1996. Method of gelling a guar or derivatized guar polymer solution utilized to perform a hydraulic fracturing operation. US 5488083 A.

103. Marandi, A, Karro. E., and Puura, E., 2004. Barium Anomaly in the Cambrian-Vendian Aquifer System in North Estonia. Environmental Geology 47, 132-139.

104. Back, W., 1961. Techniques for mapping of hydrochemical facies. US Geological Survey Professional Paper, 424-D, 380-382.

105. Tibbetts, P. J. C., Buchanan,. I.T., Gawel, L.J., and Large, R., 1992. A comprehensive determination of produced water composition. Produced Water. Environmental Science Research 46, 97-112

106. Chadha, D. K., 1999. A proposed new diagram for geochemical classification of natural waters and interpretation of chemical data. Hydrogeology Journal 7, 431-439.

107. Rich, C. I., 1961. Calcium determination for cation-exchange capacity measurements. Soil Science 92 (4), 226-231.

108. Weimer, R. J., 1973. A guide to the uppermost cretaceous stratigraphy, central front range Colorado: deltaic sedimentation, growth faulting and early laramide crustal movements. The Mountain Geologist 10 (3), 53-97.

109. Drever, J. I., 1997. The geochemistry of natural waters (3rd ed.); New Jersey; Prentice Hall, 436.

110. Lee, R. W., 1981. Geochmistry of water in the fort union formation of the northern powder river basin, southeastern Montana; U. S. G. S.; http://pubs.er.usgs.gov/publication/wsp2076.

111. Richter, B.C., Kreitler, C.W., 1991 Identification of sources of groundwater salinization using geochemical techniques.Robert S. Kerr research laboratory. Ada, OK. EPA/600/2-91/064.

112. Novak, S.A., Eckstein, Y., 1988. Hydrochemical characterization of brine and identification of brine contamination in aquifers. Groundwater, 26 (3), 317-324.

113. Meybeck, M., 1987. Global chemical weathering of surficial rocks estimated from river dissolved loads. American Journal of Science 287, 401-428.

114. Carpenter, A.B., 1978. Origin and chemical evolution of brines in sedimentary basins. SPE Annual Fall Technical Conference and Exhibition, October 1st-3rd, Houston, Texas. Society of Petroleum Engineers

115. Pilz, J., Spöck, G., 2008. Why do we need and how should we implement Bayesian kriging methods. Stochastic Environmental Research and Risk Assessment 22 (5), 621-632.

116. United States Energy Information Agency (2011) Annual Energy Outlook 2011 with Projections to 2035. DOE/EIA-0383, United States Energy Information Agency, Washington DC.

117. United States Energy Information Agency (2012) Annual Energy Outlook 2012 with Projections to 2035. DOE/EIA-0383, United States Energy Information Agency, Washington DC.

118. United States Energy Information Agency (2013) Annual Energy Outlook 2013 with Projections to 2035. DOE/EIA-0383, United States Energy Information Agency, Washington DC.

119. Holditch, S.A. (2012) Getting the Gas out of the Ground. CEP, 41-48. https://www.aiche.org/sites/default/files/cep/20120841.pdf

120. United States Environmental Protection Agency (2004) Evaluation of the Impacts to Underground Sources of Drinking Water by Hydraulic Fracturing of Coalbed Methane Reservoirs. EPA 816-R-04-003. https://fracfocus.org/sites/default/files/publications/evaluation_of_impacts_to_underground_sources_of_drinking_water_by_hydraulic_fracturing_of_coalbed_methane_reservoirs.pdf

121. API Guidance Document HF1 (2009) Hydraulic Fracturing Operations-Well Construction and Integrity Guidelines. http://www.hollandhart.com/pdf/API_Guidance_Document_HF1_1st_Edition_October_2009.pdf

122. Gregory, K.B., Vidic, R.D. and Dzombak, D.A. (2011) Water Management Challenges Associated with the Production of Shale Gas by Hydraulic Fracturing. Elements, 7, 181-186. https://doi.org/10.2113/gselements.7.3.181H. S. Li et al. DOI: 10.4236/jwarp.2017.913104 1679 Journal of Water Resource and Protection

123. United States Department of Energy (2009) Modern Shale Gas Development in the US: A Primer. https://energy.gov/sites/prod/files/2013/03/f0/ShaleGasPrimer_Online_4-2009.pdf

124. United States Environmental Protection Agency (2012) Study of the Potential Impacts of Hydraulic Fracturing on Drinking Water Resources-Progress Report. EPA 601/R-12/011. https://www.epa.gov/sites/production/files/documents/hf-report20121214.pdf

125. Gassiat, C., Gleeson, T., Lefebvre, R. and McKenzie, J. (2013) Hydraulic Fracturing in Faulted Sedimentary Basins: Numerical Simulation of Potential Contamination of Shallow Aquifers over Long Time Scales. Water Resources Research, 49, 8310-8327. https://doi.org/10.1002/2013WR014287

126. Kharaka, Y.K., Thordsen, J.J., Conaway, C.H. and Thomas, R.B. (2013) The Energy-Water Nexus: Potential Groundwater-Quality Degradation Associated with Production of Shale Gas. Procedia Earth and Planetary Science, 7, 417-422. https://doi.org/10.1016/j.proeps.2013.03.132

127. Vengosh, A., Warner, N., Jackson, R. and Darrah, T. (2013) The Effects of Shale Gas Exploration and Hydraulic Fracturing on the Quality of Water Resources in the United States. Procedia Earth and Planetary Science, 7, 863-866. https://doi.org/10.1016/j.proeps.2013.03.213

128. Vidic, R.D., Brantley, S.L., Vandenbossche, J.M., Yoxtheimer, D. and Abad, J.D., 2013. Impact of Shale Gas Development on Regional Water Quality. Science , 340, 826-834. https://doi.org/10.1126/science.1235009

129. Osborn, S.G., Vengosh, A., Warner, N.R. and Jackson, R.B. (2011) Methane Contamination of Drinking Water Accompanying Gas-Well Drilling and Hydraulic Fracturing. PNAS, 109, 8172-8176. https://doi.org/10.1073/pnas.1100682108

130. Li, H. and Carlson, K.H. (2014) Distribution and Origin of Groundwater Methane in the Wattenberg Oil and Gas Field of Northern Colorado. Environmental Science & Technology, 48, 1484-1491. https://doi.org/10.1021/es404668b

131. Haraka, Y.K. and Otton, J.K. (2007) Preface to Special Issue on Environmental Issues Related to Oil and Gas Production. Applied Geochemistry, 22, 2095-2098. https://doi.org/10.1016/j.apgeochem.2007.04.006

132. The Royal Society and the Royal Academy of Engineering (2012) Shale Gas Extraction in the UK: A Review of Hydraulic Fracturing. London, DES2597.

133. Colorado Oil and Gas Conservation Commission (2013) Rule 609: Statewide Groundwater Baseline Sampling and Monitoring. Denver.

134. Higley, D.K. and Cox, D.O. (2007) Oil and Gas Exploration and Development along the Front Range in the Denver Basin of Colorado, Nebraska, and Wyoming. In: Higley, D.K., Ed., Compiler , Petroleum Systems and Assessment of Undiscovered Oil and Gas in the Denver Basin Province , Colorado, Kansas , Nebraska , South Dakota, and Wyoming—USGS Province 39, US Geological Survey Digital Data Series DDS-69-P, United States Geological Survey, Washington DC, 41.

135. US Geological Survey (2002) Planning for the Conservation and Development of Infrastructure Resources in Urban Areas-Colorado Front Range Urban Corridor. Circular 1219. United States Geological Survey, Denver.

136. Colorado Oil and Gas Commission Website. Colorado Oil and Gas Information System (COGIS) Production Data Inquiry.

137. Ground Water Atlas of Colorado (2003) Special Publication 53. Colorado Geologi. S. Li et al. DOI: 10.4236/jwarp.2017.913104 1680 Journal of Water Resource and Protection cal Survey. Golden. http://coloradogeologicalsurvey.org/apps/wateratlas.html

138. Son, J.H. and Carlson, K.H. (2014) Real-Time Surrogate Analysis for Potential Oil and Gas Contamination of Drinking Water Resources. Applied Water Science, 5, 283. https://doi.org/10.1007/s13201-014-0190-x

139. United States Environmental Protection Agency (2010) Water Quality Event Detection Systems for Drinking Water Contamination Warning Systems: Development, Testing, and Application of CANARY. EPA 600/R-010/036, 29.

140. Carol, J.B., James, R.G. and Kevin, A.S. (2010) Arsenic-Related Water Quality with Depth and Water Quality of Well-Head Samples from Production Wells, Oklahoma, 2008. U. S. Geological Survey, Scientific Investigations Report 2010-5047.

141. Richter, B.C. and Kreithler, C.W. (1993) Geochemical Techniques for Identifying Sources of Ground-Water Salinization. CRC Press, Boca Raton.

142. Moore Jr, A.W. and Jorgenson, J.W. (1993) Median Filtering for Removal of Low-Frequency Background Drift. Analytical Chemistry, 65, 188-191. https://doi.org/10.1021/ac00050a018

143. Moore Jr, A.W. and Jorgenson, J.W. (1993) Median Filtering for Removal of Low-Frequency Background Drift. Analytical Chemistry, 65, 188-191. https://doi.org/10.1021/ac00050a018

144. Biemans, H., Haddeland, I., Kabat, P., Ludwig, F., Hutjes, R.W.A., Heinke, J. and Gerten, D. (2011) Impact of Reservoirs on River Discharge and Irrigation Water Supply during the 20th Century. Water Resources Research, 47, W03509. https://doi.org/10.1029/2009WR008929

145. Mahvi, A.H., Nouri, J., Babaei, A.A. and Nabizadeh, R. (2005) Agricultural Activities Impact on Groundwater Nitrate Pollution. International Journal of Environmental Science & Technolog, 2, 41-47. https://doi.org/10.1007/BF03325856

146. Boulton, N.S. (1954) The Drawdown of the Water-Table under Non-Steady Conditions near a Pumped Well in an Unconfined Formation. Proceedings of the Institution of Civil Engineers, 3, 564-579. https://doi.org/10.1680/ipeds.1954.12586

147. Li, H., Son, J.H. and Carlson, K.H. (2016) Concurrence of Aqueous and Gas Phase Contamination of Groundwater in the Wattenberg Oil and Gas Field of Northern Colorado. Water Research, 88, 458-466. https://doi.org/10.1016/j.watres.2015.10.031

148. Son, J. H., & Carlson, K. H. (2015). Real-time surrogate analysis for potential oil and gas contamination of drinking water resources. Applied Water Science, 5(3), 283-289.

149. Li, H., Son, J. H., & Carlson, K. H. (2016). Concurrence of aqueous and gas phase contamination of groundwater in the Wattenberg oil and gas field of northern Colorado. Water research, 88, 458-466

150. Vidic, R. D., Brantley, S. L., Vandenbossche, J. M., Yoxtheimer, D., & Abad, J. D. (2013). Impact of shale gas development on regional water quality. Science, 340(6134), 1235009.

151. DiGiulio, D. C., Wilkin, R. T., Miller, C., & Oberley, G. (2011). Investigation of ground water contamination near Pavillion, Wyoming. Office of Research and Development, National Risk Management Research Laboratory.

152. Vengosh, A., Warner, N., Jackson, R., & Darrah, T. (2013). The effects of shale gas exploration and hydraulic fracturing on the quality of water resources in the United States. Procedia Earth and Planetary Science, 7, 863-866.

153. Schweizer, B. (2015). Darcy's law and groundwater flow modelling

154. Bear, J., Beljin, M. S., & Ross, R. R. (1992). Fundamentals of ground-water modeling. Superfund Technology Support Center for Ground Water, Robert S. Kerr Environmental Research Laboratory.

155. Liu, J., Sadre-Marandi, F., & Wang, Z. (2016). DarcyLite: A matlab toolbox for darcy flow computation. Procedia Computer Science, 80, 1301-1312.

156. Carlson, K.H., Hanif, A., Dhanasekar, A., Li, H. (2014). The Colorado Water Watch, Real-Time Aquifer Monitoring in the Denver Julesburg Basin. Colorado Water Quality Control Division Newsletter, June.

157. Robson, S. G. (1987). Bedrock aquifers in the Denver Basin, Colorado; a quantitative water-resources appraisal (No. 1257). US Geological Survey.

158. Jarvie, Daniel M., et al. "Unconventional shale-gas systems: The Mississippian Barnett Shale of north-central Texas as one model for thermogenic shale-gas assessment." AAPG bulletin 91.4 (2007): 475-499.

159. Orangi, Abdollah, et al. "Unconventional shale oil and gas-condensate reservoir production, impact of rock, fluid, and hydraulic fractures." SPE Hydraulic Fracturing Technology Conference. Society of Petroleum Engineers, 2011.

160. Gregory, Kelvin B., Radisav D. Vidic, and David A. Dzombak. "Water management challenges associated with the production of shale gas by hydraulic fracturing." Elements 7.3 (2011): 181-186.

161. Bernays, Adam, Antoine Le Cotty, and Vincent Alary. "Produced water disposal." U.S. Patent No. 8,540,023. 24 Sep. 2013.

162. Li, Huishu, Ji-Hee Son, and Kenneth H. Carlson. "Concurrence of aqueous and gas phase contamination of groundwater in the Wattenberg oil and gas field of northern Colorado." Water research 88 (2016): 458-466.

163. Leak in Line From Gas Well Blamed in Fatal Colorado Blast, May 2, 2017. Available at https://www.usnews.com/news/best-states/colorado/articles/2017-05-02/firefighters-to-discuss-probe-of-fatal-blast-near-gas-well

164. Gas Leaks Cause Explosions and Other Health Risks. Available at http://www.inspection-perfection.com/gas-leaks-cause-explosions-and-other-health-risks.html#.Wh9DMbNKvIU

165. Rule 609: Statewide Groundwater Baseline Sampling and Monitoring. Available at https://cogcc.state.co.us/COGIS_Help/SampleData.pdf

166. Loaiciga, H. A. "Groundwater monitoring network design." Developments in water science 36 (1988): 371-376.

167. Huishu Li, Ji-hee Son, Asma Hanif, Jianli Gu, Ashwin Dhanasekar, Kenneth Carlson. Colorado Water Watch: Real-Time Groundwater Monitoring for Possible Contamination from Oil and Gas Activities. Journal of Water Resource and Protection (2017), 9, 1660-1687.

168. Li, Huishu, and Kenneth H. Carlson. "Distribution and origin of groundwater methane in the Wattenberg oil and gas field of northern Colorado." Environmental science & technology 48.3 (2014): 1484-1491.

169. Public Land Survey Service. Available at https://nationalmap.gov/small_scale/a_plss.html

170. Son, Ji-Hee, and Kenneth H. Carlson. "Real-time surrogate analysis for potential oil and gas contamination of drinking water resources." Applied Water Science 5.3 (2015): 283-289.

171. Harmancioglu, Nilgun B., and Necdet Alpaslan. "WATER QUALITY MONITORING NETWORK DESIGN: A PROBLEM OF MULTI‐OBJECTIVE DECISION MAKING." JAWRA Journal of the American Water Resources Association 28.1 (1992): 179-192.

172. Bakshi, Bhavik R. "Multiscale PCA with application to multivariate statistical process monitoring." AIChE journal 44.7 (1998): 1596-1610.